STATIC AND DYNAMIC ANALYSIS OF VISCO-ELASTOPLASTIC FIBER REINFORCED COMPOSITE SHELLS IN MISSILE STRUCTURES

T. J. Chung, et al

Alabama University

Prepared for:

Army Missile Command

January 1973

STATIC AND DYNAMIC ANALYSIS OF VISCOELASTOPLASTIC FIBER REINFORCED COMPOSITE SHELLS IN MISSILE STRUCTURES

By

T. J. Chung and R. L. Eidson

Annual Report

This research work was supported by the
U. S. Army Missile Command under
Contract DAAH01-72-C-0281

Department of Engineering Mechanics
The University of Alabama in Huntsville
Huntsville, Alabama

January, 1973

UNCLASSIFIED

Security Classification

DOCUMENT CONTROL DATA – R & D

(Security classification of title, body of abstract and indexing annotation must be entered when the overall report is classified)

1. ORIGINATING ACTIVITY (Corporate author) The University of Alabama in Huntsville P. O. Box 1247 Huntsville AL 35807	2a. REPORT SECURITY CLASSIFICATION None 2b. GROUP None

3. REPORT TITLE

STATIC AND DYNAMIC ANALYSIS OF VISCOELASTOPLASTIC FIBER REINFORCED COMPOSITE SHELLS IN MISSILE STRUCTURES

4. DESCRIPTIVE NOTES *(Type of report and inclusive dates)*

Annual report (1 Jan – 31 Dec 72)

5. AUTHOR(S) *(First name, middle initial, last name)*

T. J. Chung

Robert L. Eidson

6. REPORT DATE January 1973	7a. TOTAL NO. OF PAGES ~~196~~ 203	7b. NO. OF REFS 25
8a. CONTRACT OR GRANT NO. DAAH01-72-C-0281 b. PROJECT NO. c. d.	9a. ORIGINATOR'S REPORT NUMBER(S) 9b. OTHER REPORT NO(S) *(Any other numbers that may be assigned this report)*	

10. DISTRIBUTION STATEMENT

Approved for public release; distribution unlimited

11. SUPPLEMENTARY NOTES	12. SPONSORING MILITARY ACTIVITY Commanding General U. S. Army Missile Command Redstone Arsenal AL 35809 At: AMSMI-RLA

13. ABSTRACT

This report is concerned with theories, formulations, and computer programs for the analysis of shell structures in general and fiber reinforced rocket motor cases in particular. Arisymmetric isothermal deformations subjected to either static or dynamic loading are included in the present study. All possible material properties such as elastic, viscoelastic, elastoplastic, and visco-elastoplastic are explored. Analyses are carried out with the structure regarded either as a thin shell or as a thick shell. It has been found that the thin shell theory is inadequate for yielding of many layers of fibers through the shell thickness. The finite element method is used in handling unusual geometry and boundary conditions, and various modern numerical schemes are employed in domains of space and time.

DD FORM 1473

UNCLASSIFIED

Security Classification

STATIC AND DYNAMIC ANALYSIS OF VISCOELASTOPLASTIC FIBER REINFORCED COMPOSITE SHELLS IN MISSILE STRUCTURES

By

T. J. Chung and R. L. Eidson

Annual Report

This research work was supported by the
U. S. Army Missile Command under
Contract DAAH01-72-C-0281

Department of Engineering Mechanics
The University of Alabama in Huntsville
Huntsville, Alabama

January, 1973

PREFACE

This study was conducted during the period November 3, 1971, through December 31, 1972, under Contract DAAH01-72-C-0281, "Static and Dynamic Analysis of Viscoelastoplastic Fiber-Reinforced Composite Shells in Missile Structures", technically monitored by Mr. Charles M. Eldridge, GE&M Directorate, U. S. Army Missile Command, Redstone Arsenal, Alabama.

Mr. R. L. Eidson was responsible for coding of entire computer programs. Mr. J. K. Lee and Dr. G. Yagawa assisted in a certain portion of the research project.

TABLE OF CONTENTS

TABLE OF CONTENTS (cont.)

TABLE OF CONTENTS (cont.)

SECTION 1

INTRODUCTION

This report is concerned with theories, formulations, and computer programs for the analysis of shell structures in general and fiber reinforced rocket motor cases in particular. Such analysis is intended for use in efficient design of missile structures consisting of complex structural components subjected to various loading conditions. Only the isothermal problems are reported herein.

Various material properties such as elasticity, plasticity, viscoelasticity, and viscoelastoplasticity are considered in the present study. Schapery [19,13], among others, confirmed that glass fiber-reinforced structures embedded in epoxy exhibit significant rate-dependent elastoplastic or viscoelastoplastic behavior.

The response of such structures depends greatly on types of loading, static or dynamic. Perzyna [18] presented the thermodynamic foundations of the theory of viscoplasticity. Experimental evidences in his study necessitated the simultaneous consideration of viscoelastic and plastic properties of a material. Both static and dynamic loadings will be studied in detail in the present study.

Yielding of the fiber-reinforced structure in the context of present state of art still remains a controversial matter. Studies of plastically anisotropic materials were initiated by Hill [8] who postulated the form of yield condition based on the von Mises criterion for isotropic plastic material. Hu [10], on the other hand, generalized the Tresca shear-stress

yield criterion in a similar manner. These theories, however, are incapable of taking into account the presence of fibers in a ductile matrix. Mulhern, Rogers and Spencer [14] proposed a general continuum theory of the mechanical behavior of fibers which are considered plastically inextensible. Lance and Robinson [12] more recently presented a theory of ductile behavior of composite materials based on physical ideas related to those contained in the maximum shear stress theory of isotropic materials. It is evident that this later theory removes shortcomings of all other theories but successful application to a shell structure with fiber angle plys appears to be doubtful. In view of these developments, the most promising approach is to modify Hill's theory to incorporate strain-hardening of fibers in similar context of the work of Lance and Robinson. Jensen [11] and Whang [23] applied this idea to orthotropic material. In the present study a further extension is made to account for layers of fiber angle plys.

Thin and thick shells are considered. A treatment as a thin shell requires plane stress approximation of the finite element model in which anisotropic parameters for each axisymmetric layer of angle plys through the shell thickness must be characterized. Detailed study on this subject which has not appeared in the literature will be elaborated in the present report. The results of a thin shell approximation are compared with three dimensional thick shell theory in which imposition of axisymmetry permits use of a plane strain isoparametric finite element. This comparison points to a distinct superiority of three dimensional theory in dealing with filament wound fibers. The computer program is capable of analyzing a body composed of a combination of several monolithic materials and composite materials.

Based on these ideas and the theoretical background, details of formulation of governing equations are presented in the following sections. A thin shell is discussed in Section 2 and a thick shell in Section 3 with specialized topics included in Appendices A.1 through A.12. Computer programs are written with maximum utilization of currently available numerical methods. Demonstrative problems are solved and results presented in Section 4. Conclusions and recommendations are given in Section 5. Documentation of the computer programs is included in Appendices B.1 through B.6.

SECTION 2

THIN SHELL ANALYSIS

2.1 GENERAL

Since an extensive review of developments of thin shell theory is beyond the scope of the present study we simply begin with Novozhilov's theory [15,16] which is relatively widely accepted among the engineers. Modifications are then introduced to account for anisotropy, fiber-reinforced composites, plasticity, viscoelasticity, and viscoelastoplasticity. Axisymmetric shells under static and dynamic loadings will be considered.

2.2 CONSTITUTIVE EQUATIONS FOR ELASTIC AND PLASTIC BEHAVIOR

Based on the Love-Kirchhoff hypothesis, small strains, large displacements, and moderate rotations, the membrane strain tensor $e_{\alpha\beta}$ and the bending strain tensor $\chi_{\gamma\beta}$ are given below:

$$e_{\alpha\beta} = \frac{1}{2}\{u_{\alpha|\beta} + u_{\beta|\alpha} - 2u^{\lambda}b_{\alpha\beta} + (u^{3}_{,\alpha} + u^{\lambda}b_{\alpha\lambda})(u^{3}_{,\beta} + u^{\gamma}b_{\beta\gamma})\} \tag{2.1}$$

$$\chi_{\gamma\beta} = -u^{3}_{|\gamma\beta} - u_{\lambda|\beta}\, b^{\lambda}_{\alpha} - u_{\lambda}\, b^{\lambda}_{\alpha|\beta} - u^{\mu}_{\beta}\, u_{\mu|\alpha} + b^{\mu}_{\beta}\, b_{\mu\alpha}\, u^{3} \tag{2.2}$$

Here all Greek letters range from 1 to 2 and u_{α} and u^{3} are the displacements, $b_{\alpha\beta}$ is the second fundamental tensor , the commas and strokes represent, respectively, ordinary and covariant differentiations. It should be noted that all nonlinear terms in the bending

strain are neglected. Derivations of (2.1) and (2.2) and the physical components based on Novozhilov's theory are given in Appendix A.1.

For linear elastic behavior, the stress tensor is given by

$$\sigma^{\alpha\beta} = \sigma^{\alpha\beta}_{(a)} + \sigma^{\alpha\beta}_{(b)} \tag{2.3}$$

where the membrane stress tensor $\sigma^{\alpha\beta}_{(a)}$ and the bending stress tensor $\sigma^{\alpha\beta}_{(b)}$ are, respectively,

$$\sigma^{\alpha\beta}_{(a)} = hD^{\alpha\beta\lambda\mu}e_{\lambda\mu}, \quad \sigma^{\alpha\beta}_{(b)} = \frac{h^3}{12} D^{\alpha\beta\lambda\mu} \gamma_{\lambda\mu} \tag{2.4}$$

in which h is the shell thickness and $D^{\alpha\beta\lambda\mu}$ is the tensor of elastic moduli.

If yielding of the material is considered we must modify (2.4) in order to incorporate plastic behavior. For the isotropic von Mises material the plastic potential function f becomes [8]

$$f = \bar{\sigma}^2 = 3J \tag{2.5}$$

where J is the second deviatoric stress invariant and $\bar{\sigma}$ is the equivalent yield stress. For the anisotropic von Mises material [8], however, we have

$$f = \bar{\sigma}^2 = \frac{1}{2} A_{ijk\ell} S^{ij} S^{k\ell} \tag{2.6}$$

where $A_{ijk\ell}$ is the anisotropic parameters, S^{ij} is the deviatoric

stress tensor, and $i,j,k,\ell = 1,2,3$. For the case of plane stress (2.6) becomes

$$f = \bar{\sigma}^2 = \frac{1}{2} \underset{\sim}{\sigma}^T \underset{\sim}{A} \underset{\sim}{\sigma} \tag{2.7}$$

in which

$$\underset{\sim}{\sigma} = [\, \sigma^{11} \;\; \sigma^{22} \;\; \sigma^{12} \,]$$

and

$$\underset{\sim}{A} = \begin{bmatrix} A_{11} & -A_{12} & 0 \\ -A_{21} & A_{22} & 0 \\ 0 & 0 & 6A_{33} \end{bmatrix}$$

Explicit forms of (2.5) and (2.7) are given in Appendix A.2.

The incremental plastic strain tensor is related by an associated flow rule,

$$d\gamma^{(p)}_{\alpha\beta} = \frac{\partial f}{\partial \sigma^{\alpha\beta}} \, d\lambda \tag{2.8}$$

where $d\lambda$ is the positive constant.

Differentiating (2.5) or (2.7) yields

$$d\bar{\sigma} = \frac{1}{2\bar{\sigma}} \frac{\partial f}{\partial \sigma^{\alpha\beta}} \, d\sigma^{\alpha\beta} = Z_{\alpha\beta} \, d\sigma^{\alpha\beta} \tag{2.9}$$

where

$$Z_{\alpha\beta} = \frac{1}{2\bar{\sigma}} \frac{\partial f}{\partial \sigma^{\alpha\beta}}$$

Let the plastic modulus $E_{(p)}$ be given by

$$E_{(p)} = \frac{d\bar{\sigma}}{d\bar{\gamma}^{(p)}} \tag{2.10}$$

where $d\bar{\gamma}^{(p)}$ is the incremental equivalent yield strain. By equating the incremental plastic work $dW^{(p)}$ done by the current stress and current incremental plastic strain with that done by the equivalent yield stress and incremental equivalent yield strain,

$$dW^{(p)} = \sigma^{\alpha\beta} d\gamma^{(p)}_{\alpha\beta} = \bar{\sigma} d\bar{\gamma}^{(p)} \tag{2.11}$$

and substituting (2.8) into (2.11), we obtain

$$d\lambda = d\bar{\gamma}^{(p)}/2\bar{\sigma} \tag{2.12}$$

Now inserting (2.12) into (2.8) yields

$$d\gamma^{(p)}_{\alpha\beta} = Z_{\alpha\beta} d\bar{\gamma}^{(p)}_{\alpha\beta} \tag{2.13}$$

Since the total incremental strain is the sum of the elastic and plastic strains we can write

$$d\gamma^{(e)}_{\alpha\beta} = d\gamma_{\alpha\beta} - d\gamma^{(p)}_{\alpha\beta} \tag{2.14}$$

where $d\gamma^{(e)}_{\alpha\beta}$ is the elastic strain tensor. This enables us to express the total incremental stress in the form,

$$d\sigma^{\alpha\beta} = D^{\alpha\beta\lambda\mu}(d\gamma_{\lambda\mu} - d\gamma^{(p)}_{\lambda\mu}) \tag{2.15}$$

or

$$d\sigma^{\alpha\beta} = D^{\alpha\beta\lambda\mu}(d\gamma_{\lambda\mu} - Z_{\lambda\mu}d\bar{\gamma}^{(p)}) \tag{2.16}$$

In view of (2.13), (2.16), and (2.9) we solve for $d\bar{\gamma}^{(p)}$,

$$d\bar{\gamma}^{(p)} = H^{-1}Z_{\alpha\beta}D^{\alpha\beta\lambda\mu}\,d\gamma_{\lambda\mu} \tag{2.17}$$

in which

$$H^{-1} = E_{(p)} + Z_{\rho\eta}Z_{\delta\gamma}D^{\rho\eta\delta\gamma}$$

Substituting (2.17) into (2.16) gives

$$d\sigma^{\alpha\beta} = (D^{\alpha\beta\lambda\mu} + \overset{*}{D}{}^{\alpha\beta\lambda\mu})d\gamma_{\alpha\beta} \tag{2.18}$$

where $\overset{*}{D}{}^{\alpha\beta\lambda\mu}$ is the tensor of plastic moduli,

$$\overset{*}{D}{}^{\alpha\beta\lambda\mu} = -H^{-1}D^{\alpha\beta\rho\sigma}Z_{\rho\sigma}Z_{\phi\psi}D^{\phi\psi\lambda\mu} \tag{2.19}$$

The explicit form of $\overset{*}{D}{}^{\alpha\beta\lambda\mu}$ is given in Appendix A.2.

2.3 CONSTITUTIVE EQUATIONS FOR VISCOELASTOPLASTIC BEHAVIOR

The principle of conservation of energy states that the time rates of the kinetic energy k and the internal energy U are equal to the mechanical power R and the heat energy Q. In the absence of the thermal loading this principle may be expressed as

$$\dot{k} + \dot{U} = R \tag{2.20}$$

Here the superposed dot represents the time rate and

$$k = \frac{1}{2}\int_V \rho v_\alpha v_\alpha dV \tag{2.21}$$

$$U = \int_V \rho e dV \tag{2.22}$$

$$R = \int_V \rho F^\beta v_\beta dV + \int_A s^{\alpha\beta} n_\alpha v_\beta \, dA \tag{2.23a}$$

in which ρ is the density; v_α is the velocity component; e is the internal energy density; F^β is the body force; $s^{\alpha\beta}$ is the surface traction; and n_α is the unit normal to the surface. Here the small strain and rectangular cartesian coordinates are used. Using the Green-Gauss theorem, (2.23a) becomes

$$R = \int_V (\rho F^\beta v_\beta + \sigma^{\alpha\beta} v_{\beta,\alpha} + \sigma^{\alpha\beta}_{,\alpha} v_\beta) dV \tag{2.23b}$$

Now, inserting (2.21) and (2.23b) into (2.20) yields

$$\int_V [\sigma^{\alpha\beta}_{,\alpha} + \rho F^\beta - \rho a^\beta) v_\beta - \rho \dot{e} + \sigma^{\alpha\beta} v_{\beta,\alpha}] dV = 0 \tag{2.24}$$

For the principle of linear momentum to hold and for arbitrary volumes we must have

$$\sigma^{\alpha\beta}_{,\alpha} + \rho F^\beta - \rho a^\beta = 0$$

and

$$\rho\dot{\epsilon} = \sigma^{\alpha\beta}v_{\beta,\alpha} = \sigma^{\alpha\beta}\dot{\gamma}_{\alpha\beta} \tag{2.25}$$

Here the commas denote ordinary differentiation and a^{α} is the acceleration.

Our objective here is to propose a form of free energy functions in incremental quantity such that the non-smooth or inelastic strains may be included for a small time interval Δt. For isothermal conditions, the incremental free energy $\phi(\Delta t)$ and stresses $\sigma^{\alpha\beta}(\Delta t)$ are assumed to be functions of incremental strains $\gamma_{\alpha\beta}(\Delta t) = \gamma^{(e)}_{\alpha\beta}(\Delta t) + \gamma^{(p)}_{\alpha\beta}(\Delta t)$ and incremental internal variables (hidden variables) $\overset{(r)}{\alpha}_{ij}(\Delta t) = \overset{(r)(e)}{\alpha}_{ij}(\Delta t) + \overset{(r)(p)}{\alpha}_{ij}(\Delta t)$. This statement may be written as

$$\phi(\Delta t) = \hat{\phi}[\gamma^{(e)}_{ij}(\Delta t),\ \gamma^{(p)}_{ij}(\Delta t),\ \overset{(r)(e)}{\alpha}_{ij}(\Delta t),\ \overset{(r)(p)}{\alpha}_{ij}(\Delta t)] \tag{2.26}$$

$$\sigma^{ij}(\Delta t) = \hat{\sigma}[\gamma^{(e)}_{ij}(\Delta t),\ \gamma^{(p)}_{ij}(\Delta t),\ \overset{(r)(e)}{\alpha}_{ij}(\Delta t),\ \overset{(r)(p)}{\alpha}_{ij}(\Delta t)] \tag{2.27}$$

For isothermal conditions, the free energy is the same as the internal energy so that

$$\rho\dot{\phi} = \rho\dot{\epsilon} = \sigma^{\alpha\beta}\dot{\gamma}_{\alpha\beta}$$

or for the small time interval Δt,

$$\rho\dot{\phi}(\Delta t) = \sigma^{\alpha\beta}(\Delta t)\ \{\dot{\gamma}^{(e)}_{\alpha\beta}(\Delta t) + \dot{\gamma}^{(p)}_{\alpha\beta}(\Delta t)\} \tag{2.28}$$

At this point we introduce here the incremental form of free energy in a truncated Taylor series expansion [5],

$$\begin{aligned}\rho\phi(\Delta t) = {} & \frac{1}{2} D^{\alpha\beta\lambda\mu}\gamma^{(e)}_{\alpha\beta}\gamma^{(e)}_{\lambda\mu} + \frac{1}{2} D^{\alpha\beta\lambda\mu}\gamma^{(p)}_{\alpha\beta}\gamma^{(p)}_{\lambda\mu} \\ & + \frac{1}{2}\sum_{r=1}^{n} g^{\alpha\beta\lambda\mu}_{(r)}\left(q^{(r)(e)}_{\alpha\beta} + q^{(r)(p)}_{\alpha\beta}\right)\left(q^{(r)(e)}_{\lambda\mu} + q^{(r)(p)}_{\lambda\mu}\right) \\ & + \sum_{r=1}^{n} g^{\alpha\beta\lambda\mu}_{(r)}\left(q^{(r)(e)}_{\lambda\mu} + q^{(r)(p)}_{\lambda\mu}\right)\left(\gamma^{(e)}_{\alpha\beta} + \gamma^{(p)}_{\alpha\beta}\right)\end{aligned} \tag{2.29}$$

where $g^{\alpha\beta\lambda\mu}_{(r)}$ are stiffness constants associated with the internal variables. Note that (2.29) has the form of truncated Taylor series expansion only to include quadratic terms. However, the product term of $\gamma^{(e)}_{\alpha\beta}$ and $\gamma^{(p)}_{\alpha\beta}$ is missing. This is because an explicit material kernel relating the product of $\gamma^{(e)}_{\alpha\beta}$ and $\gamma^{(p)}_{\alpha\beta}$ is nonexistent and coupling of elastic and plastic strains can be obtained using any one of the failure theories. Lastly, $q^{(r)}_{\alpha\beta}$ defined here as the internal variables represent time dependent physico-chemical properties or simply a viscous behavior which may be expressed as

$$q^{(r)}_{\alpha\beta} = \int_0^t \exp\ \frac{-(t-\tau)}{T_{(r)}}\ \dot{\gamma}_{\alpha\beta}(\tau)\,d\tau \tag{2.30}$$

where τ is the time variable and $T_{(r)}$ is the relaxation time. In

order to facilitate an explicit integration we assume a linear variation of $\dot{\gamma}_{\alpha\beta}$ within the time interval Δt given by

$$\dot{\gamma}_{\alpha\beta}(s) = \dot{\gamma}_{\alpha\beta}(s-1) + \frac{\tau-(t-\Delta t)}{\Delta t}\left(\dot{\gamma}_{\alpha\beta}(s-1) - \dot{\gamma}_{\alpha\beta}(s)\right) \tag{2.31}$$

where (s) is the current time step. Substituting (2.31) in (2.30) and performing integration we obtain

$$q^{(r)}_{\alpha\beta}(s) = A^{(r)}\, q^{(r)}_{\alpha\beta}(s-1) + B^{(r)}\, \dot{\gamma}_{\alpha\beta}(s-1) + C^{(r)}\, \dot{\gamma}_{\alpha\beta}(s) \tag{2.32}$$

in which

$$A^{(r)} = \exp\left(\frac{-\Delta t}{T_{(r)}}\right), \qquad B^{(r)} = T_{(r)}\left(\phi^{(r)} - A^{(r)}\right)$$

$$C^{(r)} = T_{(r)}\left(1 - \phi^{(r)}\right) \qquad \phi^{(r)} = \frac{T_{(r)}}{\Delta t}\left(1 - A^{(r)}\right)$$

The derivation of these parameters is given in Appendix A.3.

Rewriting (2.28) for the current time step (s) as

$$\Omega\left\{\frac{\partial \Phi^{(\bullet)}(s)}{\partial \dot{\gamma}^{(\bullet)}_{\alpha\beta}(s)}\, \dot{\gamma}^{(\bullet)}_{\alpha\beta}(s) + \frac{\partial \Phi^{(r)}(s)}{\partial \dot{\gamma}^{(r)}_{\alpha\beta}(s)}\, \dot{\gamma}^{(p)}_{\alpha\beta}(s) + \frac{\partial \Phi^{(r)(\bullet)}(s)}{\partial\, q^{(r)(\bullet)}_{\alpha\beta}(s)}\, q^{(r)(\bullet)}_{\alpha\beta}(s) + \frac{\partial \Phi^{(r)(p)}(s)}{\partial\, q^{(r)(p)}_{\alpha\beta}(s)}\, q^{(r)(p)}_{\alpha\beta}(s)\right\}$$

$$- \sigma^{\alpha\beta}(s)\left(\dot{\gamma}^{(\bullet)}_{\alpha\beta}(s) + \dot{\gamma}^{(p)}_{\alpha\beta}(s)\right) = 0 \tag{2.33}$$

and substituting (2.32) and (2.29) into (2.33) yields

$$\Big\{ D^{\alpha\beta\lambda\mu} \gamma^{(e)}_{\lambda\mu}(s) + \sum_{r=1}^{n} \xi^{\alpha\beta\lambda\mu}_{(r)} \big({}^{(r)}A\, {}^{(r)}q_{\lambda\mu}(s-1) + {}^{(r)}B\, {}^{(r)}\dot{\gamma}_{\lambda\mu}(s-1) + {}^{(r)}C\, \dot{\gamma}_{\lambda\mu}(s) \big)$$

$$- \sigma^{\alpha\beta}(s) \Big\} \dot{\gamma}^{(e)}_{\alpha\beta}(s) + \sum_{r=1}^{n} \xi^{\alpha\beta\lambda\mu}_{(r)} \big({}^{(r)}q_{\alpha\beta}(s)\, {}^{(r)}q_{\lambda\mu}(s) + {}^{(r)}q_{\lambda\mu}(s)\, \dot{\gamma}^{(e)}_{\alpha\beta}(s)$$

$$+ {}^{(r)}q_{\lambda\mu}(s)\, \dot{\gamma}_{\alpha\beta}(s) + \gamma_{\alpha\beta}\, {}^{(r)}\dot{q}_{\lambda\mu}(s) \big) - \sigma^{\alpha\beta}(s)\, \dot{\gamma}^{(p)}_{\alpha\beta}(s) + D^{\alpha\beta\lambda\mu} \gamma^{(p)}_{\lambda\mu}(s)\, \dot{\gamma}^{(p)}_{\alpha\beta}(s) = 0$$

Since all variations other than $\dot{\gamma}^{(e)}_{\alpha\beta}$ are not arbitrary we must have the relationship

$$\sigma^{\alpha\beta}(s) = D^{\alpha\beta\lambda\mu} \gamma^{(e)}_{\lambda\mu}(s) + \sum_{r=1}^{n} \xi^{\alpha\beta\lambda\mu}_{(r)} \big({}^{(r)}A\, {}^{(r)}q_{\lambda\mu}(s-1) + {}^{(r)}B\, \dot{\gamma}_{\lambda\mu}(s-1) + {}^{(r)}C\, \dot{\gamma}^{(e)}_{\lambda\mu}(s) \big) \tag{2.34}$$

and

$$\gamma^{(e)}_{\lambda\mu}(s) D^{\alpha\beta\lambda\mu} \dot{\gamma}^{(p)}_{\alpha\beta}(s) - \sigma^{\alpha\beta}(s)\, \dot{\gamma}^{(p)}_{\alpha\beta} + \sum_{r=1}^{n} \xi^{\alpha\beta\lambda\mu}_{(r)} \Big[{}^{(r)}q_{\alpha\beta}(s)\, {}^{(r)}q_{\lambda\mu}(s) + {}^{(r)}q_{\alpha\beta}(s)\, \dot{\gamma}^{(p)}_{\lambda\mu}(s)$$

$$+ {}^{(r)}q_{\alpha\beta}(s)\, \dot{\gamma}_{\lambda\mu}(s) + \gamma_{\alpha\beta}(s)\, \dot{q}_{\lambda\mu}(s) \Big] = 0 \tag{2.35}$$

It should be noted that (2.34) results from

$$\sigma^{\alpha\beta} = \rho \frac{\partial \psi}{\partial \gamma^{(e)}_{\alpha\beta}}$$

which states that the stresses are derivable from the free energy

functions. In our specific problem, however, this stress is due to an elastic strain and a law governing the plastic strain is needed to obtain the stress due to a total strain as already demonstrated in Section 2.2. The relationship (2.35) may be considered as the dissipation which plays a significant role in heat conduction problems. However, for the isothermal problems as considered here these terms of (2.35) are not needed in the analysis.

Now, if the plastic behavior is considered we must calculate the stress incrementally. For static analysis the load is applied in increments. For transient analysis or time dependent problems, the total loads are applied for each time increment. In either case the incremental stresses $d_\sigma{}^{\alpha\beta}$ are calculated iteratively until convergence is achieved. Therefore, we must express (2.34) in incremental form associated with the total strain in order to be combined with (2.18) for iterative cycling upon direct superposition of viscoelastic behavior and plastic behavior. Such superposition is achieved by calculating $\overset{*}{D}{}^{\alpha\beta\lambda\mu}$ initially by viscoelastic stresses. These arguments require that the second term of (2.18) for the current time step (s) be added to the incremental form of (2.34),

$$d_\sigma{}^{\alpha\beta}{}_{(s)} = D^{\alpha\beta\lambda\mu} d\gamma^{(e)}_{\lambda\mu(s)} + \sum_{r=1}^{n} {}_{S(r)}{}^{\alpha\beta\lambda\mu} \left[{}^{(r)}A\, dq^{(r)}_{\lambda\mu(s-1)} + {}^{(r)}B\, d\dot{\gamma}^{(r)}_{\lambda\mu(s-1)} + {}^{(r)}C\, d\dot{\gamma}^{(r)}_{\lambda\mu(s)} \right] + \overset{*}{D}{}^{\alpha\beta\lambda\mu} d\gamma^{(s)}_{\lambda\mu} \qquad (2.36)$$

In earlier studies, the authors obtained a slightly different form

for $d_{\sigma}^{\alpha\beta}(s)$ by means of the generalized Maxwell model [1]. However, a proper choice of the relaxation time would yield identical results.

2.4 THE FINITE ELEMENT EQUATIONS OF MOTION

The use of the finite element method is widespread [17,25]. The advantage is due to its capability in handling complex geometries, boundary and loading conditions.

The generalized coordinates at a node placed in the midsurface of the ring element include the displacements in the meridional, tangential and transverse directions plus the meridional directions.The tangential displacement need not be considered for axisymmetrical deformations. For future use in connection with asymmetrical loadings and for the purpose of generality, we shall include the tangential displacement in our formulation. The element generalized coordinates Θ_i are given by

$$\Theta_i = \psi_{iN}\Theta^N \tag{2.37}$$

where ψ_{iN} is the normalized displacement functions and the superscript ranges from 1 to the total number of generalized coordinates. For the two node element as in the case of the meridional line element used in the present study we have $N = 2i$ for the maximum range.

Appendix A.4 gives the explicit form of ψ_{iN} for linear variations of meridional and tangential displacements, cubic variation of transverse displacement and the corresponding meridional rotation. Such an element has proven to be quite efficient [24].

The general finite element equation of motion is obtained by using (2.3), (2.37), (2.25), (2.22) and (2.33b) in (2.20),

$$M_{NM}\ddot{\Theta}^{M} + \int_{A} \sigma^{\alpha\beta} \frac{\partial \gamma_{\alpha\beta}}{\partial \Theta^{N}} \, dA = P_{N} \tag{2.38a}$$

or

$$M_{NM}\ddot{\Theta}^{M} + \int_{A} \sigma^{\alpha\beta}_{(a)} \frac{\partial e_{\alpha\beta}}{\partial \Theta^{N}} \, dA + \int_{A} \sigma^{\alpha\beta}_{(b)} \frac{\partial \chi_{\alpha\beta}}{\partial \Theta^{N}} \, dA = P_{N} \tag{2.38b}$$

Here M_{NM} is the mass matrix

$$M_{NM} = \int_{V} \rho \psi^{i}_{N} \psi_{iM} \, dV \tag{2.39}$$

and P_{N} is the nodal generalized force derived from (2.23b). It should be noted that (2.38b) is obtained from the relationship

$$\gamma_{\alpha\beta} = e_{\alpha\beta} + \zeta \chi_{\alpha\beta} \tag{2.40a}$$

and the integration through the thickness coordinate ζ is contained in $\sigma^{\alpha\beta}_{(a)}$ and $\sigma^{\alpha\beta}_{(b)}$ of (2.38b). In view of (2.1), (2.2), and (2.37), we have

$$e_{\alpha\beta} = A_{N\alpha\beta}\Theta^{N} + C_{NM\alpha\beta}\Theta^{M}\Theta^{N}$$

$$\chi_{\alpha\beta} = B_{N\alpha\beta}\Theta^{N} \tag{2.40b}$$

and

$$\frac{\partial e_{\alpha\beta}}{\partial \Theta^N} = A_{N\alpha\beta} + C_{NM\alpha\beta}\Theta^M, \quad \frac{\partial \chi_{\alpha\beta}}{\partial \Theta^N} = B_{N\alpha\beta}$$

where $A_{N\alpha\beta}$, $C_{NM\alpha\beta}$, and $B_{N\alpha\beta}$ represent derivatives of the normalized interpolation function in the membrane and bending strains of (2.1) and (2.2).

We now introduce a perturbation or a variation to (2.38b) for an arbitrary time step (s)

$$M_{NM}\,d\ddot{\Theta}^M(s) + \int_A d_{(a)}\sigma^{\alpha\beta}(s)\,(A_{N\alpha\beta} + C_{NM\alpha\beta}\Theta^M(s))\,dA + \int_A \sigma^{\alpha\beta}_{(a)}(s)\,C_{NM\alpha\beta}\,dA\;d\Theta(s)$$

$$+ \int_A d\sigma^{\alpha\beta}_{(b)}(s)\,B_{N\alpha\beta}\,dA = dP_N(s) \qquad (2.41)$$

where $d\sigma^{\alpha\beta}_{(a)}(s)$ and $d\sigma^{\alpha\beta}_{(b)}(s)$ are deduced from (2.36),

$$d\sigma^{\alpha\beta}_{(a)}(s) = h(D^{\alpha\beta\lambda\mu} + \overset{*}{D}{}^{\alpha\beta\lambda\mu})\,de_{\lambda\mu}(s) + h\sum_{r=1}^{n} \xi^{\alpha\beta\lambda\mu}_{(r)}\left[{}^{(r)}C\,d\dot{e}_{\lambda\mu}(s)\right.$$

$$\left. + {}^{(r)}A\,d\,{}^{(r)}q^{(a)}_{\lambda\mu}(s-1) + {}^{(r)}B\,d\dot{e}_{\lambda\mu}(s-1)\right] \qquad (2.42a)$$

and

$$d\sigma^{\alpha\beta}_{(b)}(s) = \frac{h^3}{12}(D^{\alpha\beta\lambda\mu} + \overset{*}{D}{}^{\alpha\beta\lambda\mu})\,d\chi_{\lambda\mu}(s) + \frac{h^3}{12}\sum_{r=1}^{n} \xi^{\alpha\beta\lambda\mu}_{(r)}\left[{}^{(r)}C\,d\dot{\chi}_{\lambda\mu}(s)\right.$$

$$\left. + {}^{(r)}A\,d\,{}^{(r)}q^{(b)}_{\lambda\mu}(s-1) + {}^{(r)}B\,d\dot{\chi}_{\lambda\mu}(s-1)\right] \qquad (2.42b)$$

Substituting (2.42a) and (2.42b) into (2.41) the local finite element equation of motion becomes

$$M_{NM}\ddot{d\Theta}^{M}(s) + J_{NM}\dot{d\Theta}^{M}(s) + K^{(e)}_{NM}\,d\Theta^{M}(s) = dF_N(s) \tag{2.43}$$

in which J_{NM} and $K^{(e)}_{NM}$ are the viscosity matrix and linear elastic stiffness matrix, respectively,

$$J_{NM} = h\int_A \sum_{r=1}^{n} \xi^{\alpha\beta\lambda\mu}_{(r)} C^{(r)} A_{N\alpha\beta} A_{M\lambda\mu}\,dA + \frac{h^3}{12}\int_A \sum_{r=1}^{n} \xi^{\alpha\beta\lambda\mu}_{(r)} C^{(r)} B_{N\alpha\beta} B_{M\lambda\mu}\,dA \tag{2.44}$$

$$K^{(e)}_{NM} = h\int_A D^{\alpha\beta\lambda\mu} A_{N\alpha\beta} A_{M\lambda\mu}\,dA + \frac{h^3}{12}\int_A D^{\alpha\beta\lambda\mu} B_{N\alpha\beta} B_{M\lambda\mu}\,dA \tag{2.45}$$

The nodal vector $dF_N(s)$ contains not only the external load but also the pseudo loads of various sources,

$$dF_N(s) = dP_N(s) + dF^{(v)}_N(s) + dF^{(q)}_N(s) + dF^{(p)}_N(s) + dF^{(N)}_N(s)$$

or

$$dF_N(s) = dP_N(s) + dF^{(v)}_N(s) + K^{(q)}_{NM}\,d\Theta^{M}(s-1) + K^{(p)}_{NM}\,d\Theta^{M}(s-1) + dF^{(N)}_N(s) \tag{2.46}$$

in which the pseudo viscosity load vector,

$$dF^{(v)}_N(s) = \Big[\, h\Big\{\int_A \sum_{r=1}^{n} \xi^{\alpha\beta\lambda\mu}_{(r)} A^{(r)}\, dq^{(r)(s)}_{\alpha\beta}(s-1)\, A_{N\lambda\mu}\,dA + \int_A \sum_{r=1}^{n} \xi^{\alpha\beta\lambda\mu}_{(r)} B^{(r)} A_{N\alpha\beta} A_{M\lambda\mu}\,dA\Big\} +$$

$$+\frac{h^3}{12}\int_A \sum_{r=1}^{n} \overset{*}{E}{}^{\alpha\beta\lambda\mu}_{(r)} \overset{(r)}{A}{}^{(b)}_{\alpha\beta}(s-1)\, B_{N\lambda\mu}\, dA + \int \sum_{r=1}^{n} \overset{*}{E}{}^{\alpha\beta\lambda\mu}_{(r)} \overset{(r)}{B}\, B_{N\alpha\beta} B_{M\lambda\mu}\, dA\Big]\, d\dot{\Theta}(s-1) \tag{2.47}$$

The geometric stiffness matrix,

$$K^{(G)}_{NM} = \int_A \sigma^{\alpha\beta}_{(s)}(s)\, C_{NM\alpha\beta}\, dA$$

the plastic tangent stiffness matrix,

$$K^{(P)}_{NM} = h\int_A \overset{*}{D}{}^{\alpha\beta\lambda\mu} A_{N\alpha\beta} A_{M\lambda\mu}\, dA + \frac{h^3}{12}\int_A \overset{*}{D}{}^{\alpha\beta\lambda\mu} B_{N\alpha\beta} B_{M\lambda\mu}\, dA$$

and the nonlinear pseudo load vector $dF^{(N)}_N(s)$ contain all nonlinear terms not included in the above. It should be noted that the geometric and plastic stiffness matrices are combined with the responses lagging behind one time step and used here as pseudo loads.

If the structure is fiber-reinforced, then the suitable transformation matrices are applied to (2.43). The derivation of governing equations is quite complicated for asymmetric loads. Stresses, strains, stiffness, and displacements must be expanded into Fourier series. If loads are applied statically, the mass term in (2.43) drops out. For the absence of viscosity the second term is eliminated. This also requires the pseudo viscosity load $dF^{(V)}_N(s)$ to be dropped. We will discuss these special topics in the following sections.

2.5 FIBER-REINFORCED SHELL

In general, an axisymmetric shell reinforced with fibers would

normally have layers of angle plys with each layer provided with $+\alpha$ ply and $-\alpha$ ply, α being the wrap angle. Such arrangements tend to keep the deformation of the shell still axisymmetric if loads are axisymmetrically applied. A typical one layer element is shown in Figure A.5.1.

Orthotropic properties exist in the directions longitudinal and tangential to a fiber. Coordinate transformations for elasticity properties are then necessary to conform to the standard generalized coordinate system of a shell. A similar transformation is required for the plastic stiffness matrix. These transformations are elaborated in Appendix A.5.

2.6 ASYMMETRIC DEFORMATION

Let g represent all components of displacements, strains, stresses, stress resultants, etc.; then, we have the Fourier series expansion of g for asymmetric deformation of the form,

$$g(s,\theta) = g^{(0)}(s) + \sum_{j=1}^{\infty} g^{(j)}(s)\cos j\theta + \sum_{j=1}^{\infty} \bar{g}^{(j)}(s)\sin j\theta \qquad (2.48)$$

in which s and θ are the meridional and tangential coordinates, respectively, j is the harmonic number, the first term in the left hand side represents harmonically uncoupled part, and the second and third terms denote harmonically coupled parts for even and odd functions, respectively. The Fourier series representation of the strain-displacement

relations and stiffness matrices is given in Appendix A.6. Equivalent nodal load vectors and stresses are discussed in Appendices A.7 and A.8, respectively.

2.7 STATIC LOADING

2.7.1 ELASTOPLASTIC ANALYSIS

There are in general two methods to perform an elastoplastic analysis: (1) the tangent stiffness method and (2) the initial stiffness method. The former recalculates or updates the stiffness matrix during the iterative solution cycles whereas the latter takes advantage of the inverse of the original linear elastic stiffness being kept constant on which all subsequent iterative cycles are based. Obviously, this latter approach is simpler in procedure but requires a greater number of cycles for convergence. In both cases, the load is applied in small increments. The present study is based on the tangent stiffness matrix approach. Both of these methods are elaborated in Appendix A.9.

2.7.2 VISCOELASTOPLASTIC ANALYSIS

Problems of creep and stress relaxation are time dependent phenomena. The procedure for analysis is identical to that in the elastoplastic analysis except that the increments in loads are replaced by the increments in time and the total load is applied at each time increment during the numerical integration of the governing equations.

The equations of equilibrium are solved by a recurrence formula derived from a suitable difference operator. Such a formula may

be derived by assuming a linear variation of either displacements or displacement rates. Explicit forms of various difference operators are given in Appendix A.10.

For each time increment the viscoelastic analysis is performed initially; then the plastic matrices are calculated from the viscoelastic stresses. A standard iterative cycle is subsequently repeated until acceptable convergence is achieved.

2.8 DYNAMIC LOADING

2.8.1 ELASTOPLASTIC ANALYSIS

Effects of inertia are added to the governing equation for a dynamically loaded shell. We construct the mass matrix according to the formula (2.39) elaborated in Appendix A.11. The equations of motion thus obtained are solved once again by a suitable difference operator.. In general, a linear or constant acceleration assumed for a small time increment is used for deriving a recurrence formula (Appendix A.10). Various schemes of numerical integration have been investigated and are available in the literature [20].

For all time-dependent problems as indicated in the previous section the increments in loads are replaced by the increments in time to handle nonlinear plastic behavior. This would require the total dynamic load to be applied at each time increment during the numerical integration process [2,3,4].

2.8.2 VISCOELASTOPLASTIC ANALYSIS

The dynamic analysis of a viscoelastoplastic fiber-reinforced shell is our ultimate goal in the present study. Because of this generality we will summarize and itemize the analysis procedure.

(a) During the first time increment, the generalized displacements are calculated from the recurrence formula with initial and boundary conditions.

(b) Examine the current viscoelastic stresses in (a) above to determine if any layer through thickness of any element has yielded. If so, the plastic tangent stiffness coefficients for that portion are developed.

(c) The plastic tangent stiffness matrix, if non-zero as determined in (b), is incorporated into the recurrence formula to calculate displacements and velocities from which incremental strains and strain rates can be found.

(d) The incremental equivalent stress is calculated and compared with that of the previous cycle.

(e) Steps (b) through (d) are repeated until convergence or a certain accuracy is obtained for the incremental equivalent yield stress.

(f) For a yielded element (or layer of the element) the maximum equivalent stress which was originally set equal to the input yield stress is now updated by adding the incremental equivalent yield stress to account for strain hardening. For the yielded portion the anisotropic parameters of plasticity

must be updated.

(g) If no yielding occurred anywhere in the shell the steps (b) through (f) are omitted.

(h) A new time increment is initiated and the above steps are repeated until desired time increments have been completed.

SECTION 3

THICK SHELL ANALYSIS

3.1 GENERAL

It is generally known [15] that a shell with the thickness-radius of curvature ratio of approximately 1/20 or larger is regarded as a thick shell in which transverse shears become significant. Traditionally, a thick shell is analyzed similarly to a thin shell with transverse shears incorporated. Chung and Bandy [6] studied finite element applications to an axisymmetric thick shell considering transverse shears in the planes of meridional and transverse directions and tangential and transverse directions. In their formulation, rates of these transverse shears with respect to meridional coordinate are added to the bending strains of respective directions. For fiber-reinforced shells with several layers of angle plys through the thickness, however, the three dimensional shell theory is more convenient. In fact, it will be shown in Section 4 that even for a thin shell if layers of fiber angle plys exist through the thickness direction the three dimensional theory appears to be more satisfactory, particularly when inelastic yielding is considered.

For the reasons stated above the present study will employ the three dimensional shell theory and be specialized for axisymmetric geometry and deformations.

3.2 INTERPOLATION FUNCTION

Although the three dimensional theory is used only radial and axial displacement fields may be considered because of axisymmetric conditions, thus eliminating shears in the planes of axial and tangential directions and radial and tangential directions. This permits use of a plane element subject to integration around the circumference. Such a plane element as used here is the isoparametric element with four corner nodes which represents a linear variation of axial and radial displacements within the element. This element was originally developed by Ergatoudis and Zienkiewicz [25]. Detailed descriptions of this element are given in Appendix A.12.

The strain components considered here include normal strains in axial, radial and tangential directions plus shear strains in the plane of axial and radial directions because of axisymmetry. Development of governing equations follows closely the procedure presented in Section 2. The isoparametric element is based on the local coordinates with origin at the center of the element and four corner nodes having coordinate values of 1 and -1. This permits use of Gaussian quadrature integration in the plane together with integration around the circumference. Consequently, to conform to global coordinates a transformation by means of Jacobian matrix is needed for stresses and strains. Such transformation is in addition to fiber transformation as elaborated in Appendix A.5.

The generalized displacement field Θ_i ($\Theta_1 = u$, $\Theta_2 = v$) is given by

$$\Theta_i = \psi_{iN}\Theta^N \tag{3.1}$$

where $i=1,2$ and $N=1,2,\ldots 6$ and ψ_{iN} is the normalized interpolation function (isoparametric). Alternatively, Θ_i may be expressed as

$$\Theta_i = \psi_r \Theta_i^r \tag{3.2}$$

where $r=1,2,3,4$ and ψ_r is simply the interpolation function (isoparametric) given by

$$\begin{aligned}
\psi_1 &= \tfrac{1}{4}(1-\xi)(1-\eta) \\
\psi_2 &= \tfrac{1}{4}(1+\xi)(1-\eta) \\
\psi_3 &= \tfrac{1}{4}(1+\xi)(1+\eta) \\
\psi_4 &= \tfrac{1}{4}(1-\xi)(1+\eta)
\end{aligned} \tag{3.3}$$

in which ξ and η are isoparametric coordinates. See Appendix A.12 for derivation of (3.3). The difference between ψ_{iN} and ψ_N is associated with arrangements of the nodal displacement vector.

3.3 LINEAR ELASTIC CONSTITUTIVE EQUATIONS

Because of the isoparametric coordinates which require transformation to the global cartesian coordinates, derivatives of any variable with respect to isoparametric coordinate are given by

$$\begin{bmatrix} \dfrac{\partial}{\partial \xi} \\ \\ \dfrac{\partial}{\partial \eta} \end{bmatrix} = \underline{J} \begin{bmatrix} \dfrac{\partial}{\partial r} \\ \\ \dfrac{\partial}{\partial z} \end{bmatrix} \tag{3.4}$$

where the Jacobian $\underline{J}$ is

$$\underset{\sim}{J} = \begin{bmatrix} \frac{\partial r}{\partial \xi} & \frac{\partial z}{\partial \xi} \\ \frac{\partial r}{\partial \eta} & \frac{\partial z}{\partial \eta} \end{bmatrix} \tag{3.5}$$

Therefore,

$$\begin{bmatrix} \frac{\partial}{\partial r} \\ \frac{\partial}{\partial z} \end{bmatrix} = \underset{\sim}{J}^{-1} \begin{bmatrix} \frac{\partial}{\partial \xi} \\ \frac{\partial}{\partial \eta} \end{bmatrix} \tag{3.6}$$

The linear elastic stress-strain relation for axisymmetric solid is given by

$$\sigma^{ij} = E^{ijkl}\, \gamma_{kl} \tag{3.7}$$

where $i,j = 1,2,3,4$.

The corresponding strain-displacement relations for small displacement using (3.1) through (3.6) may be expressed as

$$\gamma_{11} = \gamma_r = \frac{\partial u}{\partial r} = \sum_{n=1}^{4} \Omega(A_{rn} + B_{rn}\xi + C_{rn}\eta)u_n \tag{3.8a}$$

$$\gamma_{22} = \gamma_z = \frac{\partial v}{\partial z} = \sum_{n=1}^{4} \Omega(A_{zn} + B_{zn}\xi + C_{zn}\eta)v_n \tag{3.8b}$$

$$\gamma_{33} = \gamma_\theta = \frac{u}{r} = \frac{1}{4r}\sum_{n=1}^{4} (1 + B_n\xi + C_n\eta + D_n\xi\eta)u_n \tag{3.8c}$$

$$\gamma_{12} = \gamma_{rz} = \frac{\partial u}{\partial z} + \frac{\partial v}{\partial r} = \sum_{n=1}^{4} \{\Omega(A_{rn} + B_{rn}\xi + C_{rn}\eta)u_n + \Omega(A_{zn} + B_{zn}\xi + C_{zn}\eta)v_n\} \tag{3.8d}$$

in which the values of all constants are defined in Appendix A.12.

3.4 CONSTITUTIVE EQUATIONS FOR FIBER-REINFORCED VISCOELASTOPLASTIC SOLID(AXISYMMETRIC THICK SHELL APPROXIMATION)

The explicit form of the three-dimensional yield function given in (2.6) is elaborated in Appendix A.2. The tensor of plastic moduli $\overset{*}{E}^{ijk\ell}$ generally referred to as plastic matrix is derived in Appendix A.2.

Our purpose here is to derive first of all the orthotropic viscoelastoplastic stress-strain relation of the type (2.36) specialized for axisymmetric three dimensional shell.A detailed procedure achieving this goal has already been presented in Section 2 for a thin shell. The final form requires change of indices from α,β,λ,μ to i,j,k,ℓ so that

$$d\sigma^{ij}(s) = D^{ijk\ell}\, d\gamma_{k\ell}(s) + \sum_{r=1}^{n} F^{ijk\ell}\left[\overset{(r)}{A}\, d\, q_{k\ell}(s-1)\right.$$

$$\left. + \overset{(r)}{B}\, d\dot{\gamma}_{k\ell}(s-1) + \overset{(r)}{C}\, d\dot{\gamma}_{k\ell}(s)\right] + \overset{*}{D}^{ijk\ell}\, d\gamma_{k\ell}(s) \qquad (3.9)$$

3.5 FINITE ELEMENT EQUATIONS OF MOTION

In the case of a thin shell, integration through thickness was required. Such integration here, however, is combined with axial direction over the area of isoparametric plane element by means of Gaussian quadrature. This bypasses distinction between membrane and bending stresses. Effects of these stresses are combined in the present procedure. The final form of equation of motion following the same operations described for a thin shell in Section 2.4 may be

derived in the form

$$M_{NM}d\ddot{\Theta}^{M}(s) + J_{NM}d\dot{\Theta}(s) + K_{NM}^{(e)}d\Theta(s) = dF_N(s)$$

in which

$$J_{NM} = 2\pi\int_{-1}^{1}\int_{-1}^{1}\sum_{r=1}^{n}\xi_{(r)}^{ijk\ell(r)}C\,A_{Nk\ell}A_{Mij}\,r\,|J|d\xi d\eta$$

$$K_{NM}^{(e)} = 2\pi\int_{-1}^{1}\int_{-1}^{1}D^{ijk\ell}\,A_{Nk\ell}A_{Mij}\,r|J|d\xi d\eta$$

$$dF_N(s) = dF_N^{(a)}(s) + dF_N^{(v)}(s) + dF_N^{(p)}$$

$$dF_N^{(v)}(s) = [2\pi\int_{-1}^{1}\int_{-1}^{1}(\sum_{r=1}^{n}\xi_{(r)}^{ijk\ell\,(r)}A\,dq_{k\ell}(s-1)A_{Nij}$$

$$+ \xi_{r}^{ijk\ell\,(r)}B\,A_{Mk\ell}\,A_{Nij})r|J|d\xi d\eta]d\dot{\Theta}^{M}(s-1)$$

$$dF_N^{(p)} = [2\pi\int_{-1}^{1}\int_{-1}^{1}\overset{*}{D}^{ijk\ell}\,A_{Nij}A_{Mk\ell}\,r|J|d\xi d\eta]d\Theta(s-1)$$

It should be noted that $A_{Nk\ell}$ can easily be identified in the expressions (3.8a) through (3.8d). The product term is also shown in expressions such as F_{aa}, G_{aa}, etc. in Appendix A.12.

3.6 ANALYSIS PROCEDURE

Various cases of analysis including elastoplastic and viscoelastoplastic analyses under static and dynamic loadings for a thin shell are described in Sections 2.7 and 2.8. Other than three dimensional yield criteria for the thick shell as shown in Appendix A.2, we follow the

identical procedure as in a thin shell. Therefore, no further comments are required for the case of a thick shell.

SECTION 4

APPLICATIONS

4.1 GENERAL

Based on the theory and procedure described earlier various versions of computer programs have been written. Detailed descriptions of these programs are given in Appendix B and its subappendices.

Some demonstrative problems are solved and the results discussed in the following subsections.

4.2 GEOMETRIC CONFIGURATIONS AND MATERIAL PROPERTIES

Three types of geometry are considered for example problems: (1) cylindrical shell, (2) combined cylinder and spherical dome, and (3) the structure same as (2) with a portion of the dome section built up with increased thickness.

The geometries shown in Figures 1 and 2 are analyzed as thin shells whereas those shown in Figures 3, 4 and 5 are treated as thick shells.

The fiber wrap angle α is measured from the circumferential direction rather than from the longitudinal axis. Analytical results for isotropic solids and fiber angles $\alpha = 0^{\circ}$, 50°, 90° are compared. Determination of isotensoid dome surfaces and corresponding fiber angles based on netting theory is inadequate if bending is significant. The analytical means of determining isotensoid surfaces by bending theory, however, appears to be impractical. Furthermore, wrapping of fibers dictated by bending analysis in general may not be possible. For these

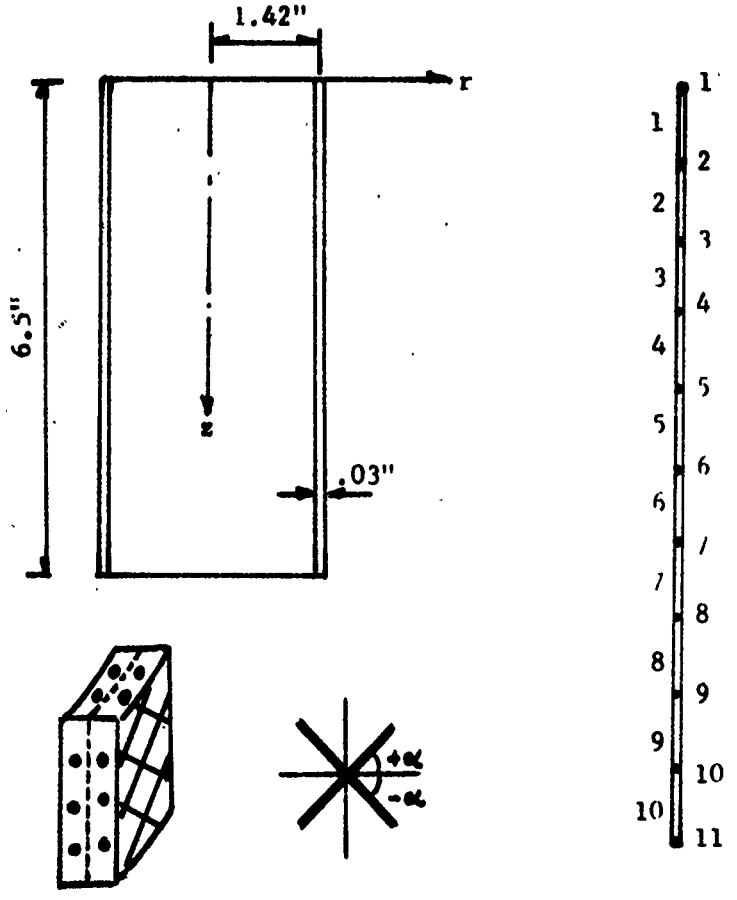

Figure 1. Geometry Case 1 (Thin Shell Cylinder)

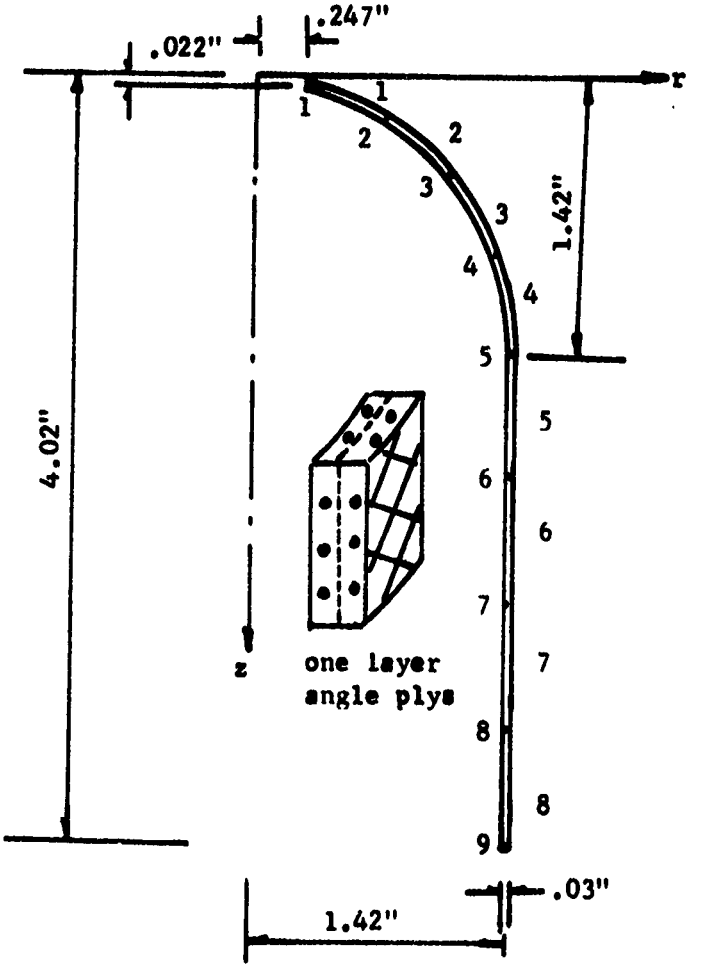

Figure 2. Geometry Case 2 (Thin Shell Cylinder-dome)

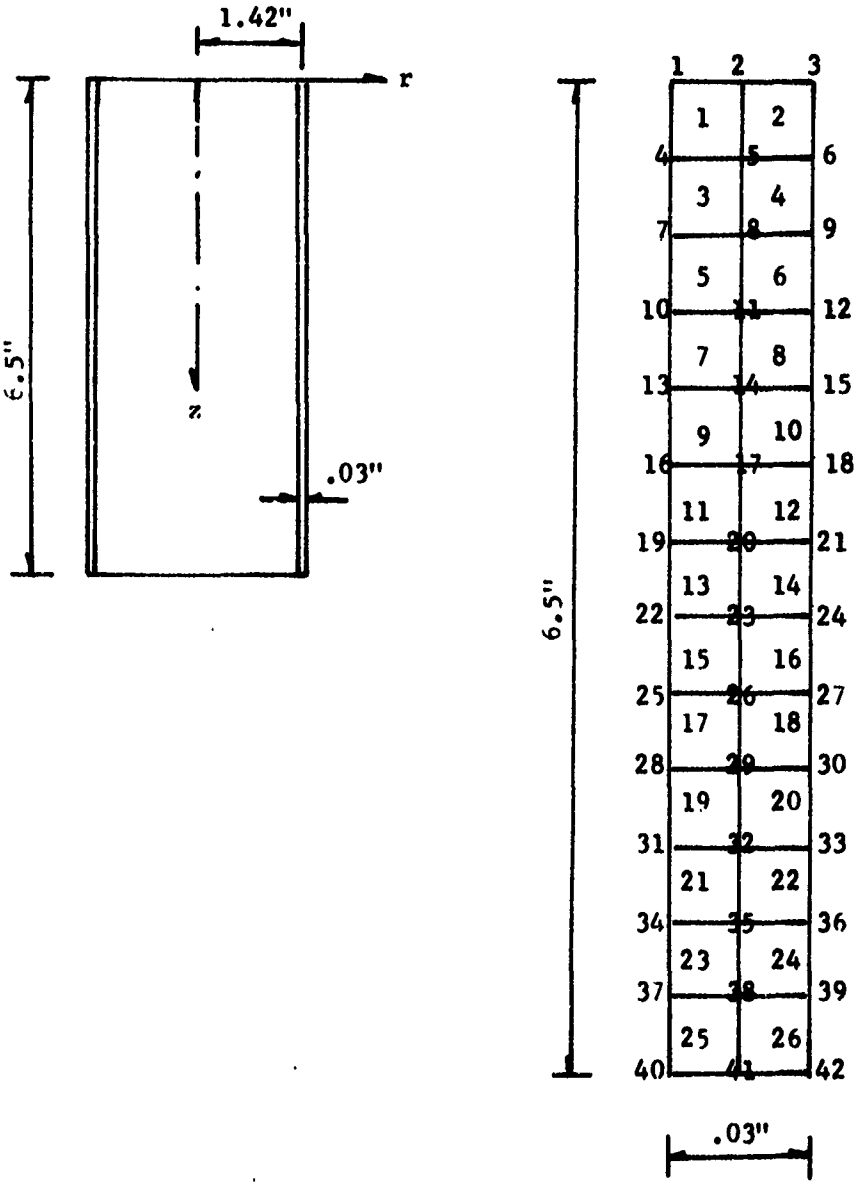

Figure 3. Geometry Case 3 (Thick Shell Cylinder, Same as Geometry Case 1)

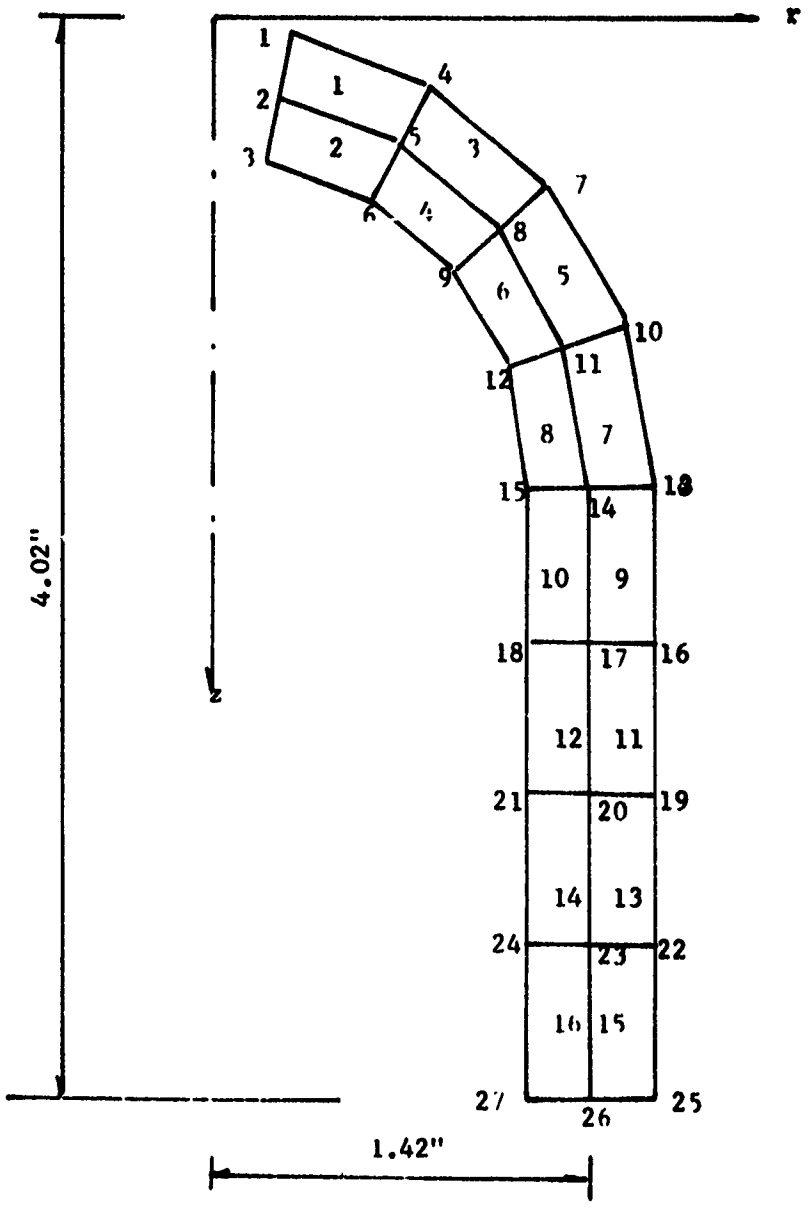

Figure 4. Geometry Case 4 (Thick Shell Cylinder-dome, same as Geometry Case 2)

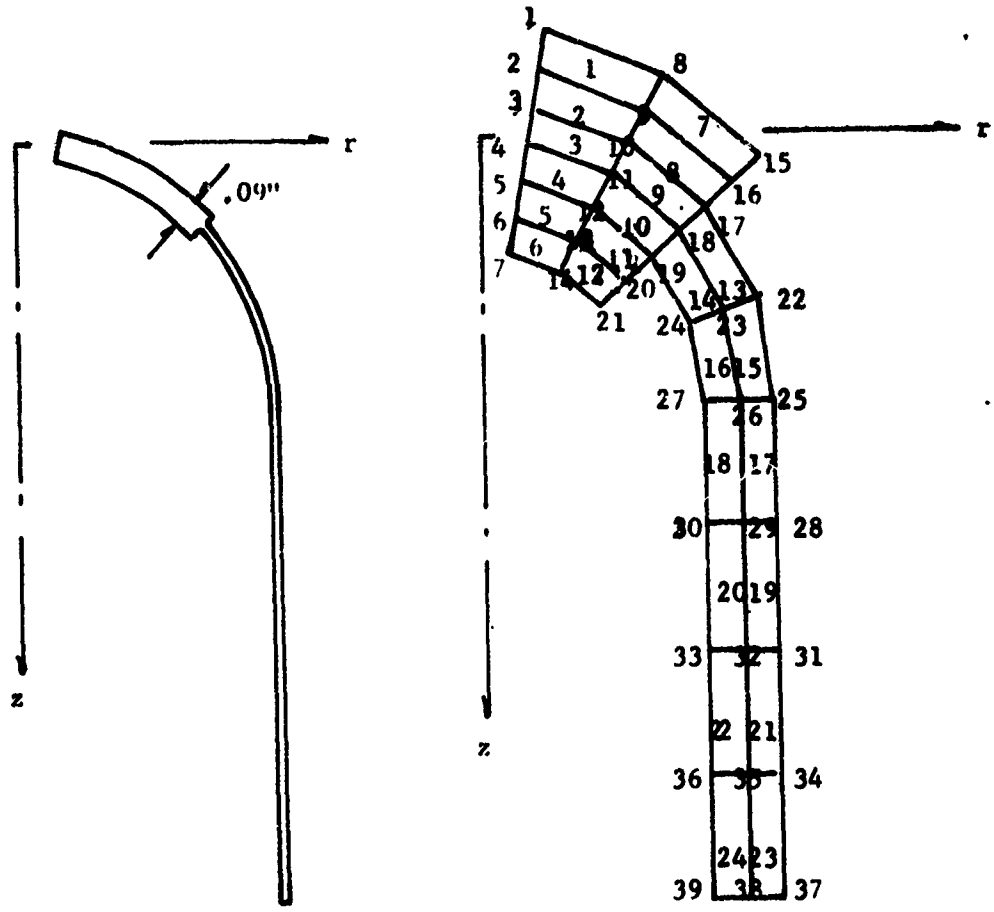

Figure 5. Geometry Case 5 (Connection with Built-up Section, Same as Case 4 Except for Upper Half of Dome with Thickness Increased to 3 Times)

reasons the present program performs stress analysis for given trial geometries and fiber angles to determine efficiency of performance or load carrying capacity.

In our examples to be presented in the following subsections two fiber layers are used. Each layer consists of angle or cross plys wrapped with $+\alpha$ and $-\alpha$ fibers which lead to axisymmetric deformations under axisymmetric loads. Material properties used for all example problems are the same and they are listed in Tables 1 and 2. For the analysis as isotropic solid the material properties corresponding to transverse direction are used.

4.3 STATIC LOADING

4.3.1 THIN SHELL

The computer programs SP1 and SVP1 are used for analysis of the structures as a thin shell.

The elastoplastic deformations of a cylinder (Geometry Case 1, Figure 1) subjected to internal pressures are shown in Figure 6. The only experimental data available for comparison is plotted also in this figure. The elastic load limit for analytical solution is slightly lower than that for the experimental value for $\alpha=50^{\circ}$. It is interesting to note that for $\alpha=90^{\circ}$, which represents fibers oriented in the axial direction, yielding occurs at much smaller strain and no strain-hardening is exhibited.

The viscoelastic response of this cylinder with $\alpha=50^{\circ}$ subjected to an internal pressure of 250 psi is shown in Figure 7. A relaxation time $T(_r) = .005$ sec. with $r = 1,2,3$ and the integration time increment Δt

TABLE 1

MATERIAL CONSTANTS FOR THIN SHELL

Modulus of Elasticity	$E_L = 8.5 \times 10^6$ psi $E_I = 2.8 \times 10^6$ psi
Shear Modulus	$G_{LI} = 1.3 \times 10^6$ psi
Poisson's Ratio	$\nu_{IL} = .4$ $\nu_{LI} = .131$
Plastic Modulus	$E_{(p)L} = 8.5 \times 10^3$ psi $E_{(p)I} = 2.8 \times 10^3$ psi $E_{(p)45^\circ} = 3 \times 10^3$ psi
Plastic Shear Modulus	$G_{(p)IL}$ $G_{(p)II} = 1.3 \times 10^3$ psi
Yield Stress	$\sigma_{(o)L} = 3.05 \times 10^5$ psi $\sigma_{(o)I} = 3 \times 10^3$ psi $\sigma_{(o)45^\circ} = 2 \times 10^4$ psi $\sigma_{(o)IL} = \sigma_{(o)II} = 5 \times 10^3$ psi
Density	.0388548 pci

TABLE 2

MATERIAL CONSTANTS FOR THICK SHELL

Modulus of Elasticity	$E_L = 8.5 \times 10^6$ psi $E_I = 2.8 \times 10^6$ psi
Shear Modulus	$G_{II} = 1 \times 10^6$ psi $G_{LI} = 1.3 \times 10^6$ psi
Poisson's Ratio	$\nu_{LI} = .262$ $\nu_{IL} = .4$
Plastic Modulus	$E_{(p)L} = 8.5 \times 10^3$ psi $E_{(p)I} = 2.8 \times 10^3$ psi
Plastic shear modulus	$G_{(p)L} = 1.3 \times 10^3$ psi $G_{(p)I} = 1 \times 10^3$ psi
Yield Stress	$\sigma_{(o)L} = 3.05 \times 10^5$ psi $\sigma_{(o)I} = 3 \times 10^3$ psi $\sigma_{(o)IL} = 5 \times 10^3$ psi $\sigma_{(o)II} = 2 \times 10^3$ psi
Density	.0388548 pci

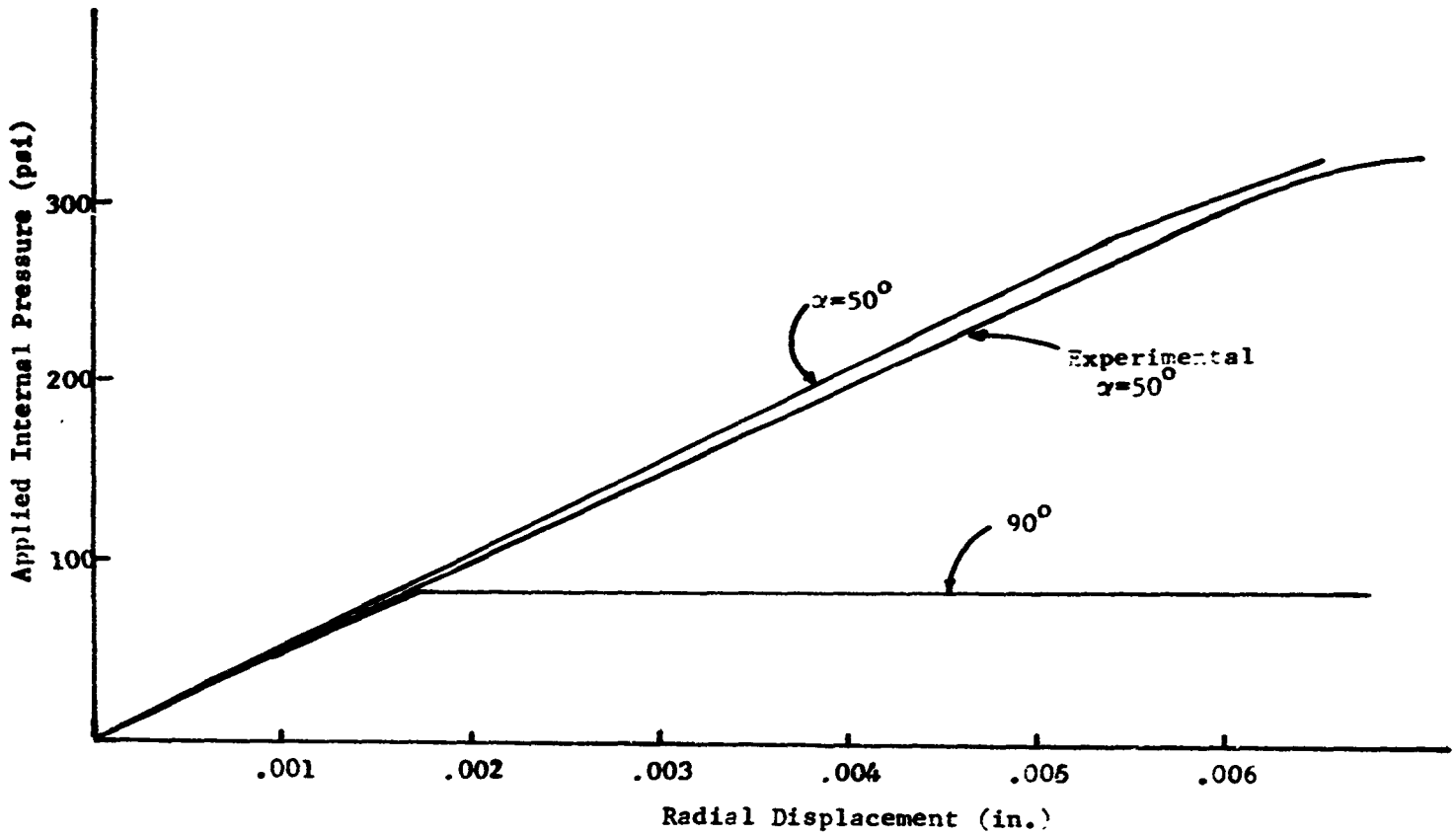

Figure 6. Static Internal Pressure vs. Radial Displacement of Node 1 (Elastoplastic) - Geometry Case 1

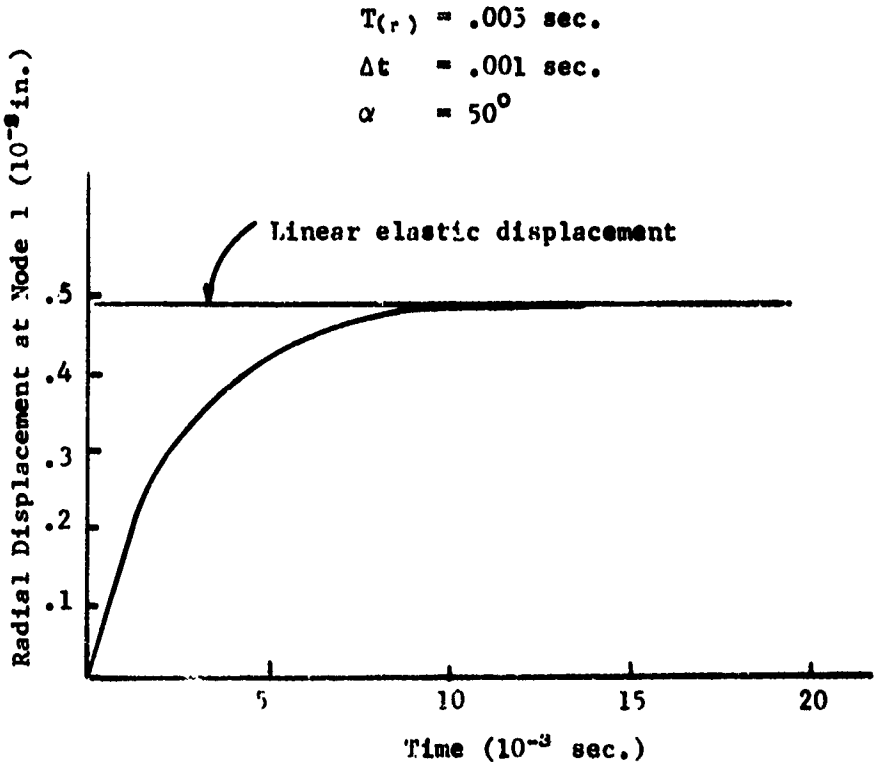

Figure 7. Viscoelastic Response of Thin Cylinder Subjected to Static Internal Pressure of 250 psi - Geometry Case 1

= .001 sec. are used in this case. It is seen that the viscoelastic displacement gradually increases and reaches the linear elastic displacement at approximately .012 sec. More discussions of this subject are given later for a thick shell.

Effects of various fiber angles for a dome-cylinder are shown in Figure 8. The fiber angles for the dome part of the structure are arbitrarily designated as α=5°, 15°, 25°, 35° for elements 1, 2, 3 and 4, respectively. With this dome the fiber angles for the cylinder are taken as α= 0°, 50°, and 90° for 3 separate analyses. In one case α= 90° is used throughout the structure. Displaced shapes of these 4 different cases under 100 psi are compared in Figure 8. For α=0° for the cylinder the displacement is largest at the dome but smallest at the cylinder. In contrast to this, α=90° everywhere gives the least displacement at the dome but considerably larger displacement at the cylinder. For α=50° for the cylinder with variable fiber angles at the dome the displacement is about medium throughout the structure. These results appear to be quite reasonable.

Some serious difficulties remain, however, in the elastoplastic analysis of a fiber-reinforced thin shell. These difficulties stem from our plane stress approximation of three dimensional shell, which in turn effects a unique definition of anisotropic yield parameters as proposed in Appendix A.2. Specifically, the parameter A_{12} lacks uniqueness as the fiber rotates between 0° and 90°. This leads A_{12} to take on large values which consequently cause the equivalent stress $\bar{\sigma}$ to assume a negative value. This situation arises for $\gamma \leq 45°$ in static analysis but such range increases in dynamic analysis. As pointed out in earlier sections, the plane stress approximation for a thin shell is

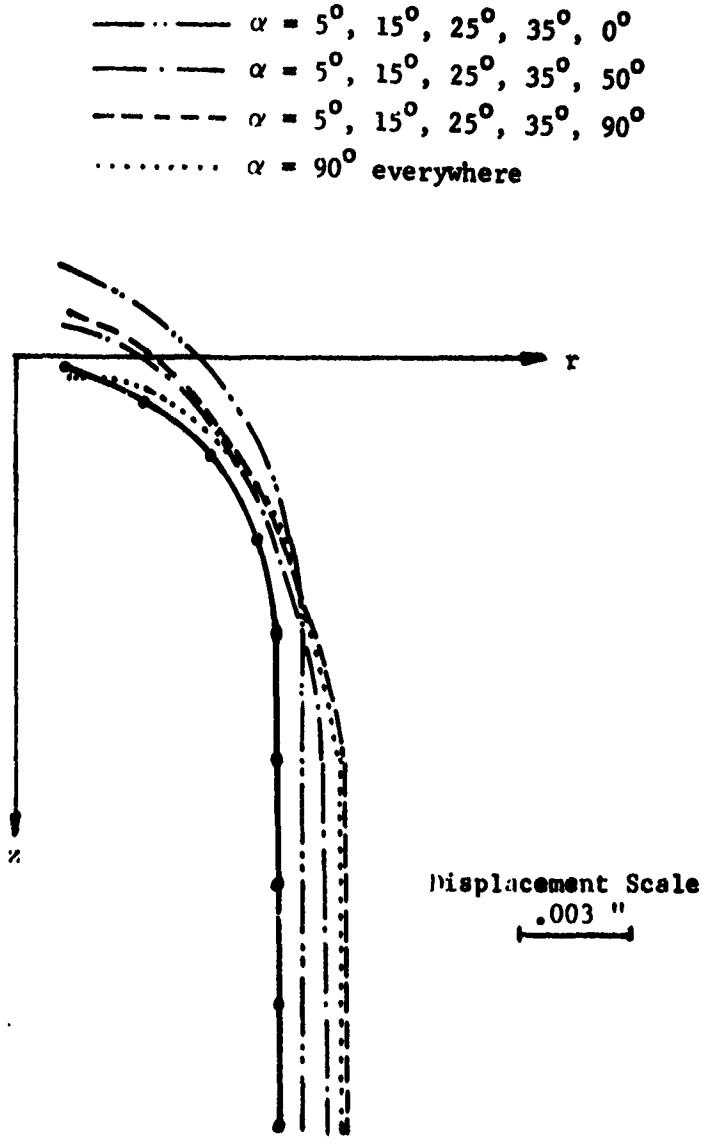

Figure 8. Displaced Shapes under Internal Pressure of 100 psi, Variable Fiber Angles at Dome and Constant Fiber Angle at Cylinder, Static Linear Elastic Analysis - Geometry Case 2

simply a device to avoid treating a shell as a three dimensional structure. It is too simple an approximation to afford checking the yield phenomena of fiber-reinforced shell through the thickness uniquely. Such discrepancy exists also in dynamic loading.

4.3.2 THICK SHELL

The computer programs SP2 and SVP2 are used for analysis of the structure as a thick shell.

Figure 9 shows plots of internal pressure vs. radial displacement for a cylinder (Geometry Case 3, Figure 3). For all wrap angles other than $\alpha=0^{o}$ the elastic limit pressure occurs much smaller than the experimental value for $\alpha=50^{o}$. The shapes of the curves are quite sensitive to wrap angles as noted in the analysis as a thin shell. The results for $\alpha=90^{o}$ are identical in both analyses as either a thin shell or as a thick shell, although the elastic limit for $\alpha=50^{o}$ in the thin shell is larger than that for $\alpha=50^{o}$ in the thick shell. This is attributed to most probably the non-uniqueness of the anisotropic parameter A_{12}, as discussed in the previous Section.

Displaced shapes of cylinder for various wrap angles subjected to the internal pressure of 2.27 psi are shown in Figure 10. The least displacement in both radial and axial directions is caused for $\alpha=0^{o}$ whereas $\alpha=90^{o}$ gives the largest radial displacement but very small axial displacement. For the case of $\alpha=50^{o}$ both axial and radial displacements are medium. Of course, the largest displacements occur in isotropic solid.

Effects of integration time increment and relaxation time are significant in viscoelastic analysis. These effects are even more critical in viscoelastoplastic analysis. Figure 11 shows effects of various

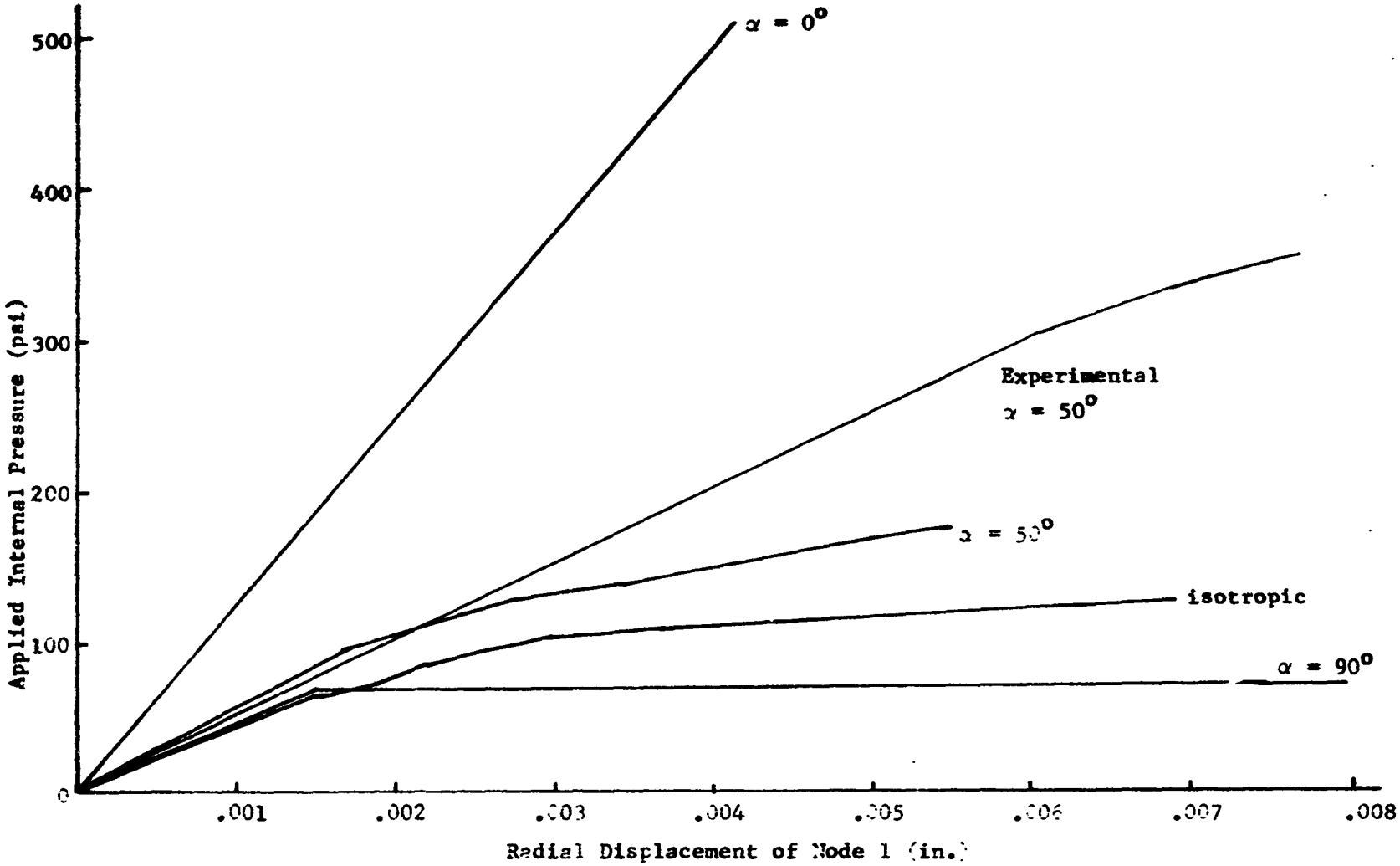

Figure 9. Static Internal Pressure vs. Radial Displacement of Node 1 (Elastoplastic) - Geometry Case 3

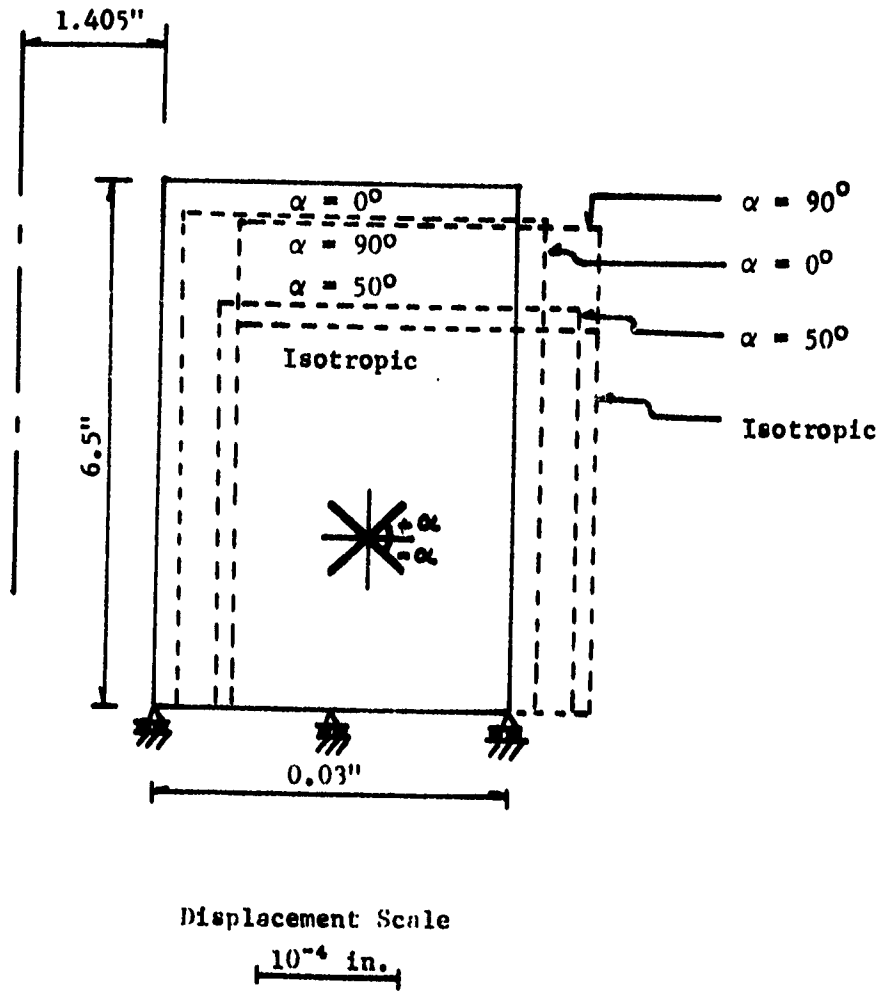

Figure 10. Displaced Shapes of Cylinder (SP2) for Various Wrap Angles (90 - α) Subjected to Static Internal Pressure of 2.24 psi - Geometry Case 3

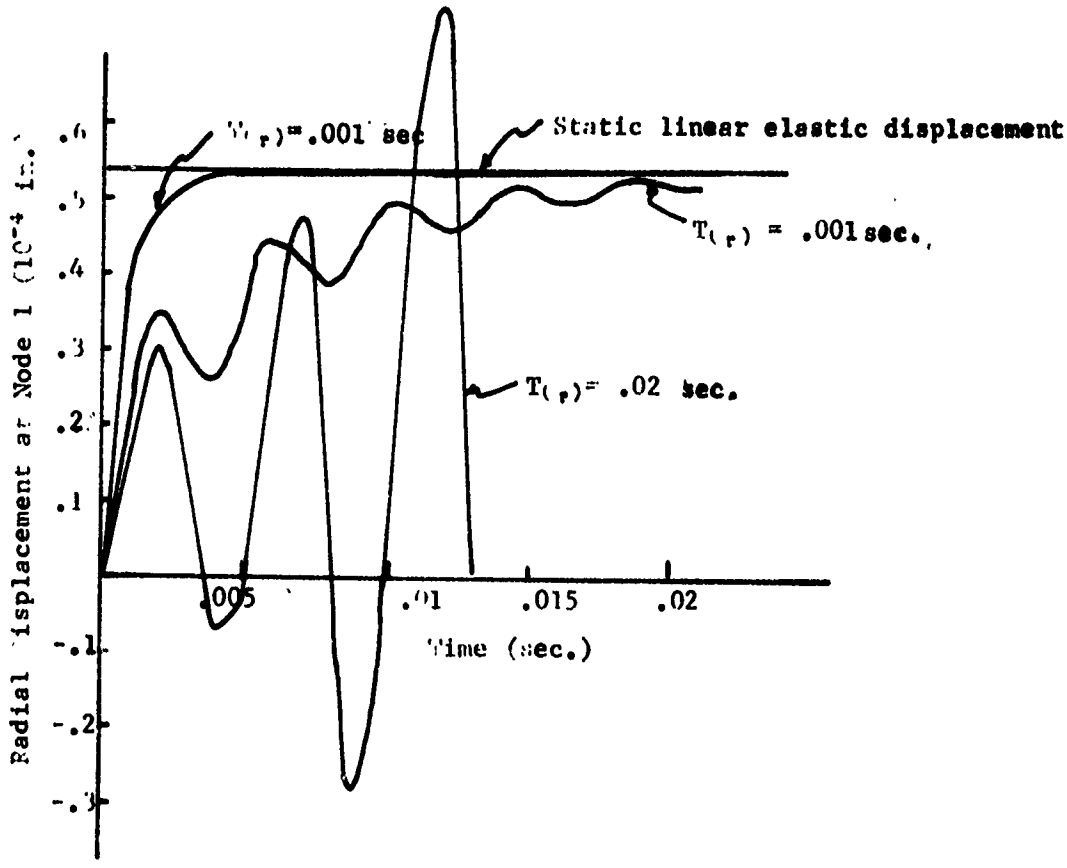

Figure 11. Effects of Relaxation Time on Viscoelastic Response of Isotropic Cylinder Subjected to Internal Pressure of 2.275 psi - Geometry Case 3

values of relaxation time for a constant integration time increment of .001 sec. with an isotropic cylinder subjected to internal pressure of 2.275 psi. For $T_{(r)}$ = .02 sec. the response is extremely erratic. A slight improvement is obtained for $T_{(r)}$ = .001 sec. A stable solution is achieved when the relaxation time is reduced to .0001 sec. at which the ratio of Δt to $T_{(r)}$ is 10. With the relaxation time being the material property in general the integration step size must be adjusted for a given problem. Toward this end Figure 12 shows effects of various integration time increments for $T_{(r)}$ = .0001 sec. For the fiber-reinforced cylinder of $\alpha = 50^{o}$ and isotropic solid subjected to internal pressure of 102.4 psi integration time increments of .0002 sec. and .001 sec. are used. For both material properties Δt = .0002 sec. is unsatisfactory. The smaller increment of Δt = .001 sec. produces a stable solution. In dynamic analysis, however, it is well known that the smaller the time increment the more stable the solution. This is an interesting contrast associated with viscous properties of the material which tend to damp out a motion. Finally, influence of ramp loading is shown in Figure 13. Once again a proper choice of $\Delta t/T_{(r)}$ is needed. This ratio in general larger than 10 appears to be satisfactory, although yield properties may require even larger ratio, say 100 or larger.

Stresses are of fundamental importance to the designer. In Figure 15, viscoelastic stresses in directions longitudinal and transverse to the fiber are plotted. This particular analysis corresponds to $\alpha = 50^{o}$, $T_{(r)}$ = .0001 sec., and Δt = .001 sec. in Figure 12, although these stresses are calculated for the element 1 which contains the node 1 for which Fig. 12 is drawn. It is interesting to note that the viscoelastic

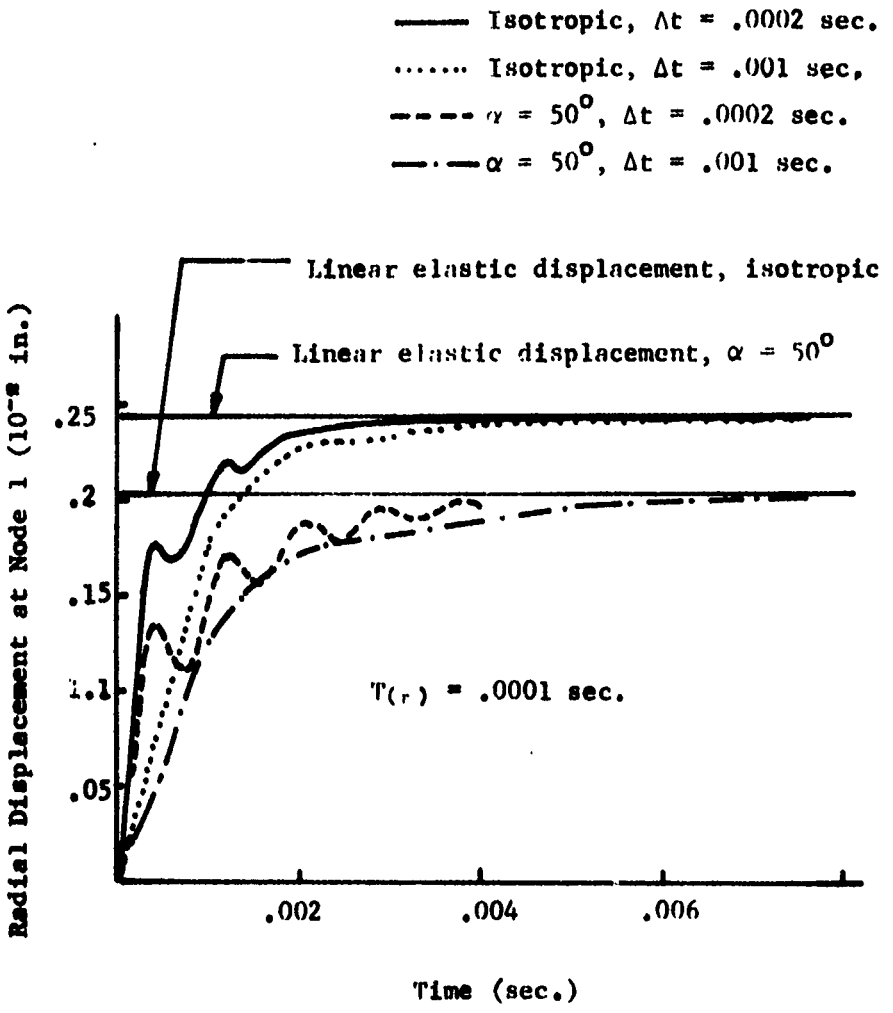

Figure 12. Effects of Integration Time Increments on Viscoelastic Response of Cylinder Subjected to Internal Pressure of 102.4 psi - Geometry Case 3

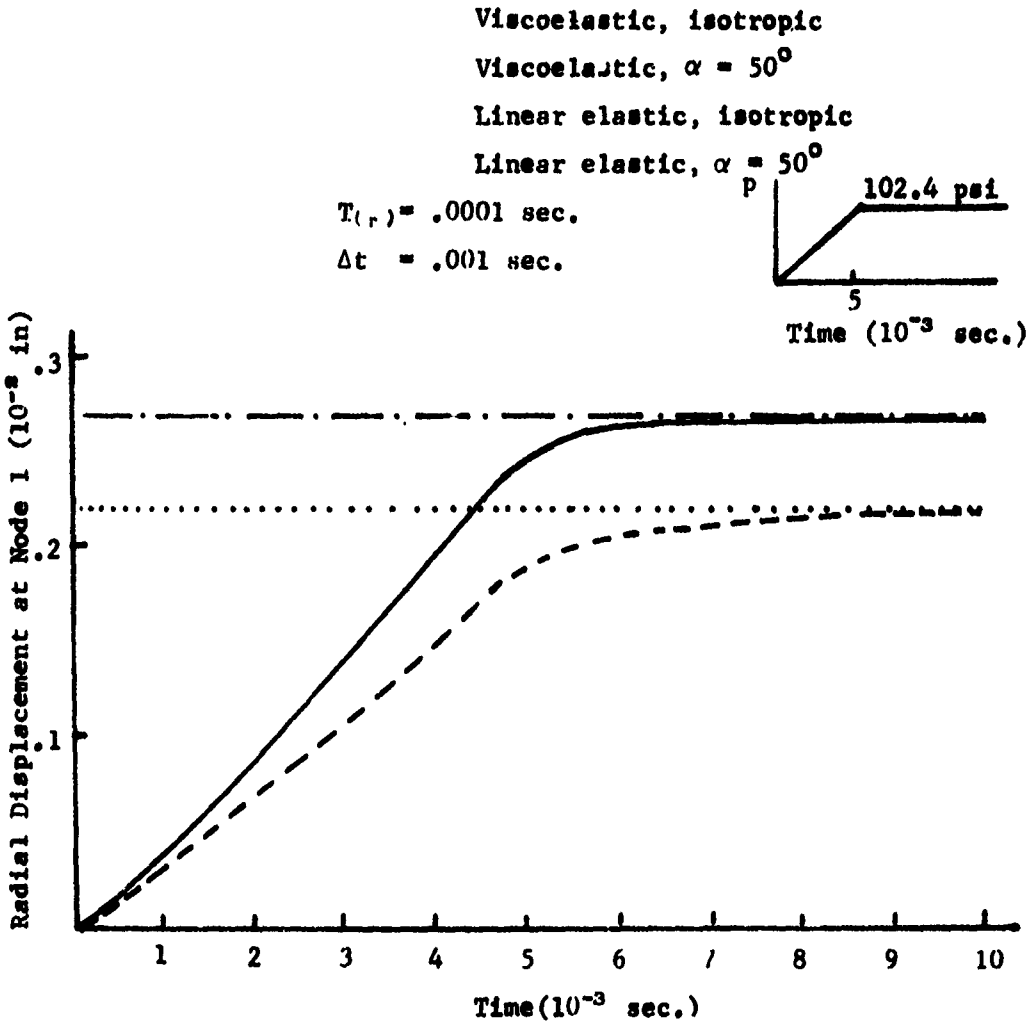

Figure 13. Viscoelastic Response of Thick Cylinder Subjected to Ramp Internal Pressure - Geometry Case 3

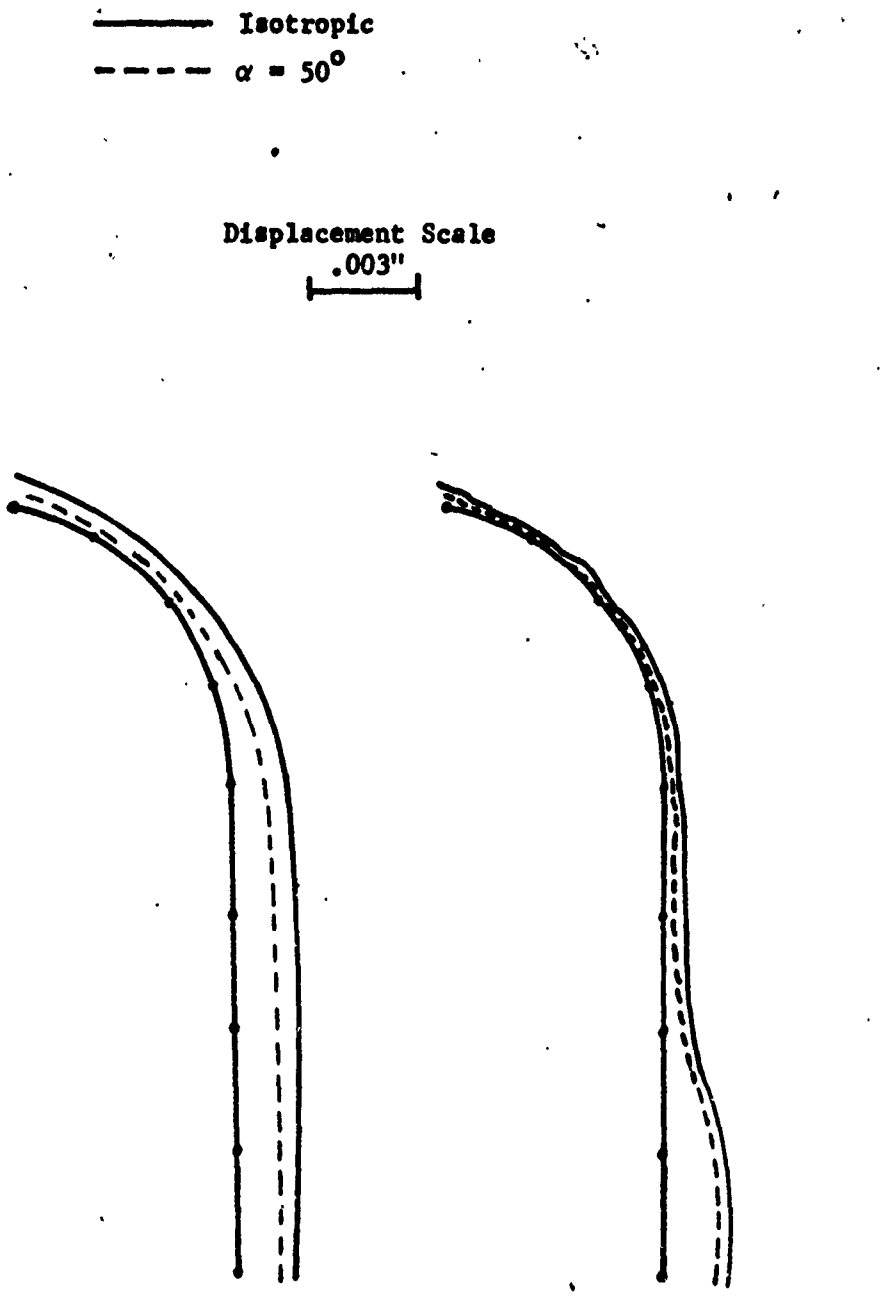

Figure 14. Displaced Shapes of Cylinder-dome with Built-Up Section Subjected to Static Internal Pressure of 100 psi - Geometry Cases 4 and 5

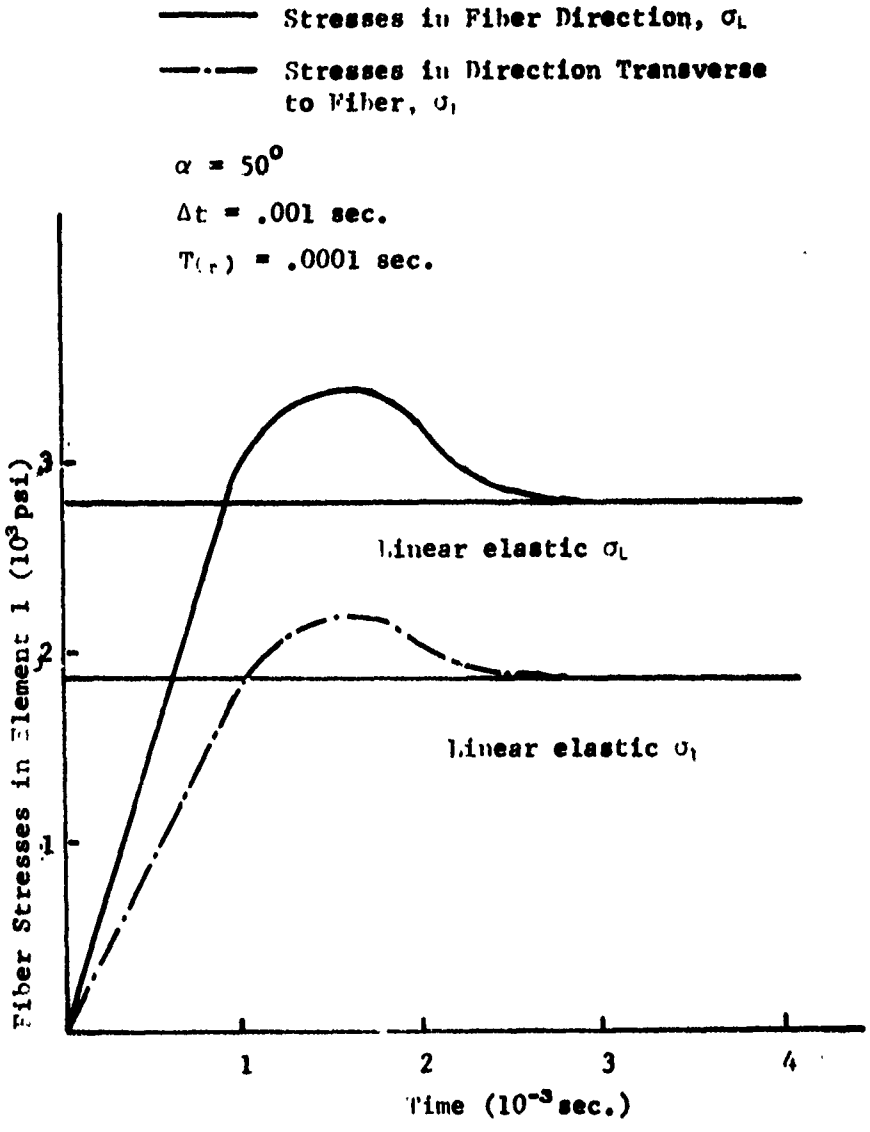

Figure 15. Viscoelastic Fiber Stresses in Element 1 of Cylinder Subjected to Internal Pressure of 102.4 psi - Geometry Case 3

stress increases until $t = 1.5 \times 10^{-3}$ sec. and decays asymptotic to the linear elastic stress at approximately 3×10^{-3} sec. Such decay may not occur for hours, days, months or even years depending on the material property or here the relaxation time. For instance concrete creeps under sustained load and stresses relax over the period of time. The relaxation time could be 100 or 1000 times larger than used in this analysis. Such large value then would require correspondingly large integration time increments to maintain the ratio $\Delta t/T_{(r)}$ for stable solution. In such case the results that might be plotted in Figure 15 would simply require a larger time scale.

Results of analyses of a cylinder-dome (Geometry Case 4) and one with built-up section (Geometry Case 5) are presented in Figure 14. For the cylinder-dome it is shown that $\alpha=50^{o}$ contributes to considerably less displacement than the isotropic solid does. The displacement of the dome with built-up section is very small at the dome portion but very large at the bottom of the cylinder portion (Figure 14b).

4.4 DYNAMIC LOADING

The computer programs DVP1 and DVP2 are used for analysis of the structure as a thin shell and a thick shell, respectively.

In general, displacement of a structure under a load applied dynamically is 60% to 80% more than that under the same magnitude of load applied statically. Consequently, dynamic stresses are larger than static stresses, and design of the structure must depend on accurate or realistic limiting stresses. A need for dynamic analysis is, therefore, apparent when explosive pressure is involved such as in missile structures.

The linear elastic responses of both isotropic and fiber-reinforced cylinders (Geometry Case 1) subjected to internal dynamic pressure of 250 psi are shown in Figure 16. For the case of $\alpha = 50^{o}$ considerably smaller peak response is observed. It is also seen that for both cases the dynamic peak radial displacements are approximately 80% more than the static radial displacements.

The dynamic viscoelastic responses for the cylinder of Geometry Case 3 subjected to dynamic internal pressure of 34.1 psi are shown in Figure 18. Smaller peak responses for viscous behavior are noted. Here the relaxation time of 10^{-4} sec. with integration time increment of 10^{-6} sec. is used. This gives the ratio $\Delta t/T_{(r)}$ of 1. Such ratio would have been too small for stable solution in the case of static loading. For dynamic analysis, however, even $\Delta t/T_{(r)} = 1$ is very large as noticed by significant damping, particularly for $\alpha=50^{o}$. It is expected that the ratio $\Delta t/T_{(r)}$ much smaller than 1 could provide stable solution.

Figure 19 shows the dynamic elastoplastic and viscoelastoplastic responses for the cylinder subjected to internal pressure of 102.5 psi with $T_{(r)} = \Delta t = 10^{-6}$ sec. Once again, effects of viscosity contributed to smaller peak responses. For the case of $\alpha = 50^{o}$ the peak viscoelastoplastic response is considerably smaller than that for the isotropic solid, but such difference is almost absent for elastoplastic response.

Dynamic stresses corresponding to these peak responses are almost twice as high as static stresses. Results of a static analysis, therefore, would lead to unsafe design when such load is to be applied dynamically to the structure in service.

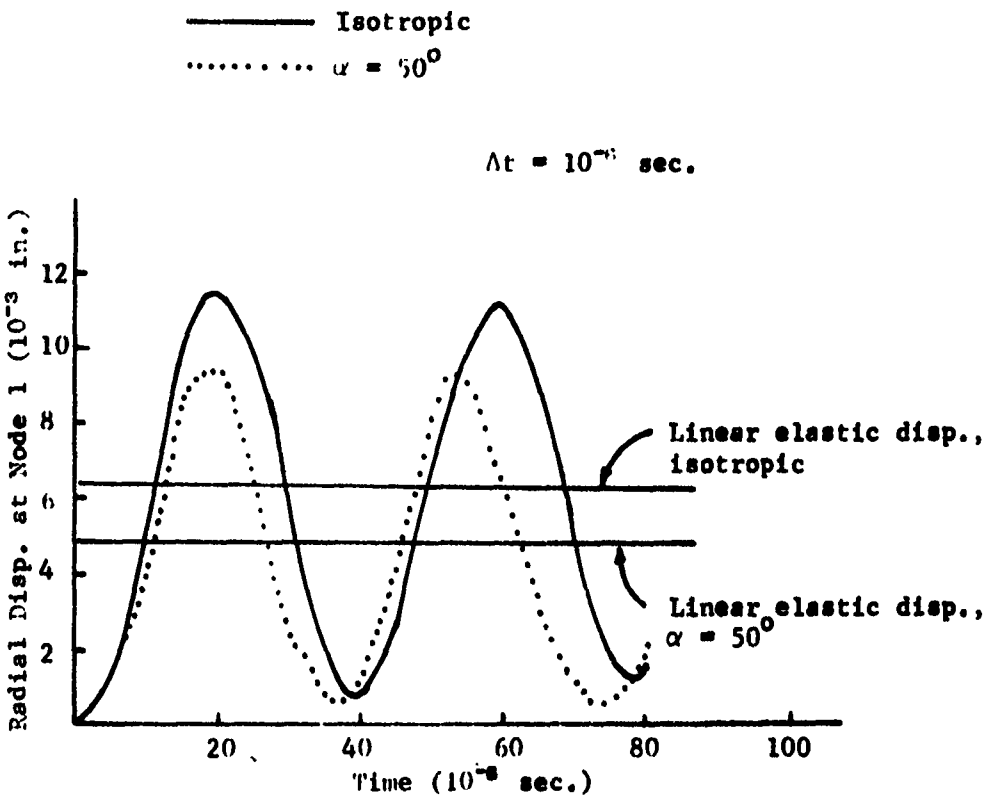

Figure 16. Linear Elastic Response of Isotropic and Fiber Reinforced Cylinder Subjected to Internal Pressure of 250 psi - Geometry Case 1

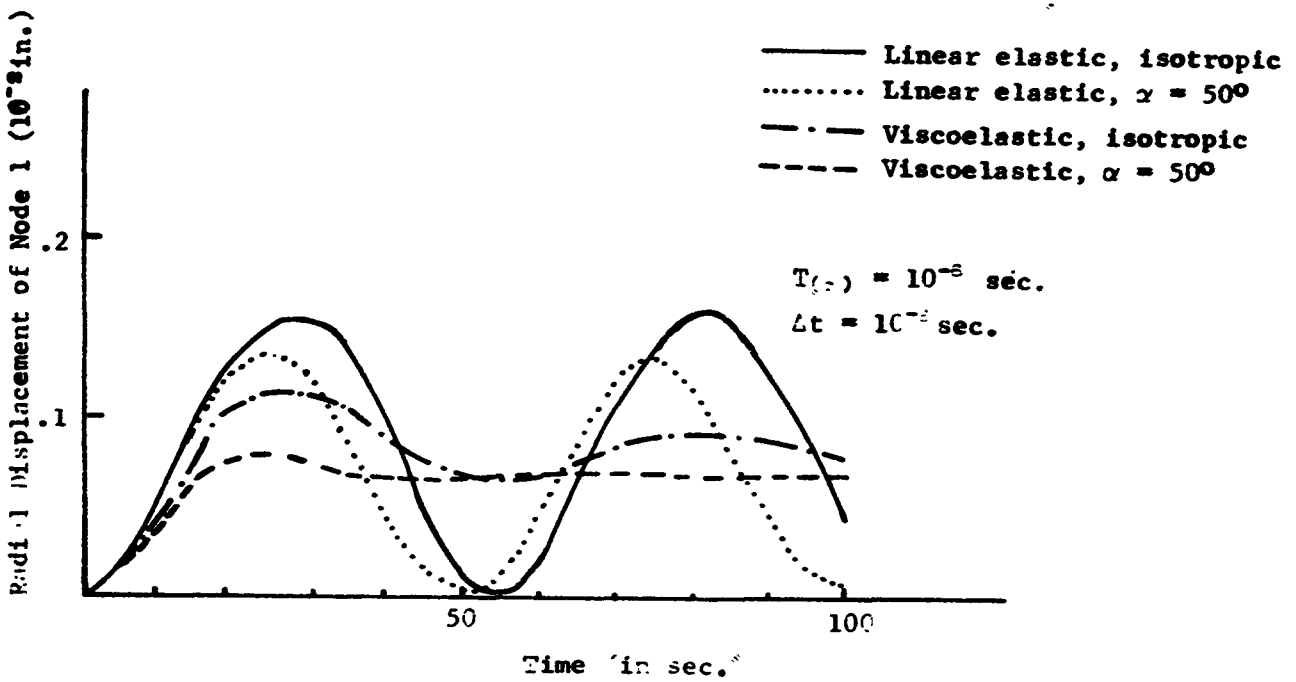

Figure 1[illegible]. Viscoelastic and Linear Elastic Radial Response of Cylinder Subjected to Impulsive Internal Pressure of 34.1 psi psi - Geometry Case 3

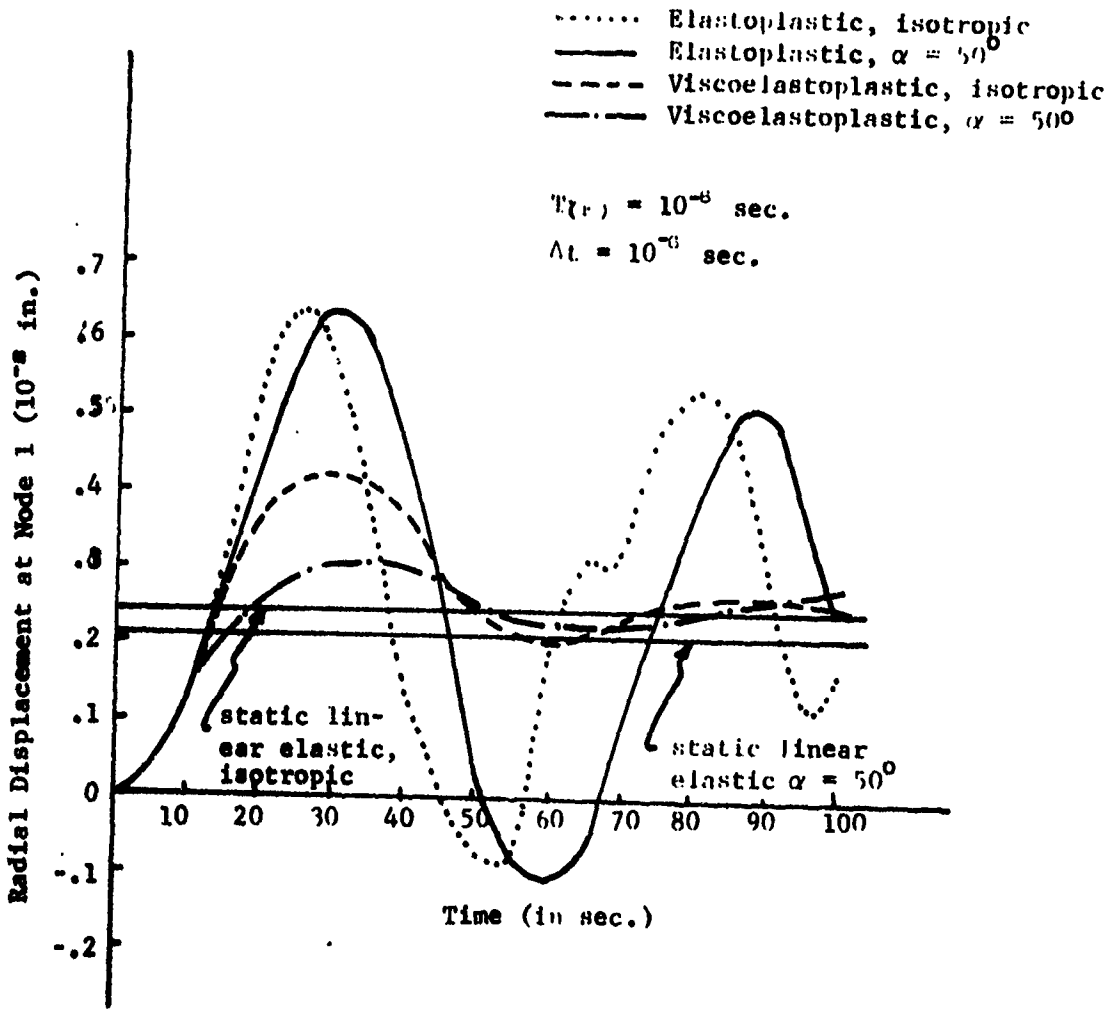

Figure 18. Viscoelastoplastic and Elastoplastic Response of Cylinder Subjected to Impulsive Internal Pressure of 102.5 psi - Geometry Case 3

SECTION 5

CONCLUSIONS

Theoretical formulations and computer programs for the analysis of thin and thick fiber-reinforced arbitrary axisymmetric shells subjected to static and dynamic loadings with diversified material properties such as viscoelasticity, elastoplasticity, and viscoelastoplasticity have been presented.

Adequacy of anisotropic stress-history-dependent yield parameters modified from Hill's yield criteria and internal or hidden variables approach for viscous behavior has been demonstrated. However, the anisotropic parameter corresponding to a plane stress in the fiber-reinforced thin shell is not unique as fibers change in wrap angles. It is, therefore, necessary to analyze the structure as a thick shell in which a three dimensional theory is utilized if yielding of fibers is to be involved.

Dynamic stresses are larger than static stresses. Although design calculations may be carried out with static equivalent load actual dynamic responses for various geometrical and material properties are too complicated to be guessed at from so-called dynamic "load factor".

Viscoelastic stresses are large initially but decay as time elapses. If the structure is under sustained load creep and stress relaxation may be important. However, selection of relaxation time must be made carefully because such viscous behavior may be exhibited for only a few seconds to months or years.

REFERENCES

1. Bland, D. R., The Theory of Linear Viscoelasticity, Pergamon Press,

2. Chung, T. J. and Eidson, R. L., "Incremental Dynamic Plasticity of Shells", Proceedings of 6th Southeastern Theoretical and Applied Mechanics Conference, University of S. Florida, Tampa, March, 1972.

3. Chung, T. J. and Eidson, R. L., "Dynamic Analysis of Viscoelastoplastic Anisotropic Shells", Int. J. of Computers and Structures, in press.

4. Chung, T. J. and Eidson, R. L., "Viscoelastoplastic Axisymmetric Shells Under Impulsive Loadings," AIAA Journal, in press.

5. Chung, T. J. and Yagawa, G., "The Incremental Thermomechanical Theory of Viscoelastoplasticity and its Application to Three Dimensional Solids," Int. J. of Solids and Structures, in review.

6. Chung, T. J. and Bandy, M. A., "Finite Element Analysis of Thick Shell of Revolution," J. of Engineering Mechanics Div., ASCE, Vol. 97, EM4, August, 1971, pp. 1315-1322.

7. Fulton, J. F., "Structural Design and Analysis of Filament Wound Rocket Motor Cases," Technical Report S-267, Rohm and Haas Co., November, 1970.

8. Hill, R., The Mathematical Theory of Plasticity, Oxford at the Clarendon Press, Ely House, London.

9. Hu, L. W., "Modified Trasca's Yield Condition and Associated Flow Rules for Anisotropic Materials and Applications," J. of Franklin Institute, 269, 187, 1958.

10. Hu, L. W.,"Studies on Plastic Flow of Anisotropic Metals,"J. of Applied Mechanics, September, 1956.

11. Jensen, W. R., Falby, W. E. and Prince, N., "Matrix Analysis Methods for Anisotropic Inelastic Structures," AFFDL TR 65-220, 1966.

12. Lance, R. H. and Robinson, D. N., "A Maximum Shear Stress Theory of Plastic Failure of Fiber-Reinforced Materials," J. of Mechanics and Physics of Solids, Vol. 19, 1971.

13. Lou, Y. G. and Schapery, R. A., "Viscoelastic Behavior of a Nonlinear Fiber-Reinforced Plastic," J. of Composite Materials, 5, 208, 1971.

14. Mulhern, J. F., Rogers, T. G., and Spencer, A. J. M., "A Continuum Model for Fiber-Reinforced Plastic Materials," Proceedings of Royal Society, A. 301, 473-492, 1967.

15. Novozhilov, V. V., Thin Shell Theory, P. Noordhoff Ltd., Groningen, The Netherlands.

16. Novozhilov, V. V., Foundations of the Nonlinear Theory of Elasticity, Graylock Press, 1953.

17. Oden, J. T., Finite Elements in Nonlinear Media, McGraw-Hill Book Co., 1972.

18. Perzyna, P., "Fundamental Problems in Viscoplasticity," Archives of Applied Mechanics, 9, 1966.

19. Schapery, R. A., "On the Characterization of Nonlinear Viscoelastic Materials," J. of Poymer Engineering Science, 9, 299, 1969.

20. Stricklin, J. A., Tillerson, J. E., Hong, J. H., and Hasler, W. E., "Nonlinear Dynamic Analysis of Shells of Revolution by Matrix Displacement Method," 11th AIAA/ASME Structures, Structural Dynamics and Materials Conf., Denver, Col., April, 1970.

21. Tsai, S. W. and Wu, E. M., "A General Theory of Strength for Anisotropic Materials," J. of Composite Materials, Vol. 5, January,1971.

22. Tsai, S. W., Adams, D. F., and Doner, D. R., "Analysis of Composite Structures," NASA CR-620, November, 1966.

23. Whang, B., "Elastoplastic Orthotropic Plates and Shells," Proceedings of the Symposium on Applications of Finite Element Methods in Civil Engineering, Vanderbilt University, November, 1969.

24. Witmer, E. A., Pian, T. H. H., Mack, E. W. and Berg, B. A., "An Improved Discrete Element Analysis," ASRL TR 146-4 Part I, March, 1968.

25. Zienkiewicz, O. C., The Finite Element Method in Engineering Science, McGraw-Hill Book Co., 1971.

APPENDIX A.1

STRAIN DISPLACEMENT RELATIONS FOR A THIN SHELL

1. KINEMATICS

Consider the location of a point in the undeformed shell defined by the position vector

$$\underset{\sim}{r} = x_i \, \underset{\sim}{i}_i$$

where

$$x_i = x_i(\xi^1, \xi^2, \xi^3 = z)$$

Thus,

$$\underset{\sim}{r} = \underset{\sim}{r}_0 + z\underset{\sim}{n} \tag{1}$$

where $\underset{\sim}{r}_0$ is the position vector of a point on the undeformed middle surface and $\underset{\sim}{n} = \underset{\sim}{n}(\xi^1, \xi^2)$ is a unit normal vector to the middle surface. The square of the length of the line element is given by

$$(ds_0)^2 = d\underset{\sim}{r} \cdot d\underset{\sim}{r} = g_{\alpha\beta} d\xi^\alpha d\xi^\beta + g_{33} d\xi^3 d\xi^3 \tag{2}$$

where
$$d\underset{\sim}{r} = d\underset{\sim}{r}_0 + d(z\underset{\sim}{n}) = d\underset{\sim}{r}_0 + dz\underset{\sim}{n} + zd\underset{\sim}{n} \tag{3}$$

with $\alpha, \beta = 1, 2$ and $i, j = 1, 2, 3$

Thus,

$$\begin{aligned}(ds_0)^2 = {} & d\underset{\sim}{r}_0 \cdot d\underset{\sim}{r}_0 + 2dz\underset{\sim}{n} \cdot d\underset{\sim}{r}_0 + 2zd\underset{\sim}{n} \cdot d\underset{\sim}{r}_0 \\ & + z^2 \, d\underset{\sim}{n} \cdot d\underset{\sim}{n} + dz^2\end{aligned} \tag{4}$$

Now,

$$d\underset{\sim}{r}_0 \cdot d\underset{\sim}{r}_0 = \underset{\sim}{r}_{0,\alpha} \, d\xi^\alpha \cdot \underset{\sim}{r}_{0,\beta} d\xi^\beta = \underset{\sim}{a}_\alpha \cdot \underset{\sim}{a}_\beta d\xi^\alpha d\xi^\beta = a_{\alpha\beta} d\xi^\alpha d\xi^\beta$$

is the fundamental form of the middle surface where $a_{\alpha\beta}$ = the first fundamental tensor.

$d\underset{\sim}{n} \cdot d\underset{\sim}{r}_0 = \underset{\sim}{n}_{,\alpha} \cdot \underset{\sim}{a}_\beta d\xi^\alpha d\xi^\beta = -b_{\alpha\beta} d\xi^\alpha d\xi^\beta$ is the second fundamental form of

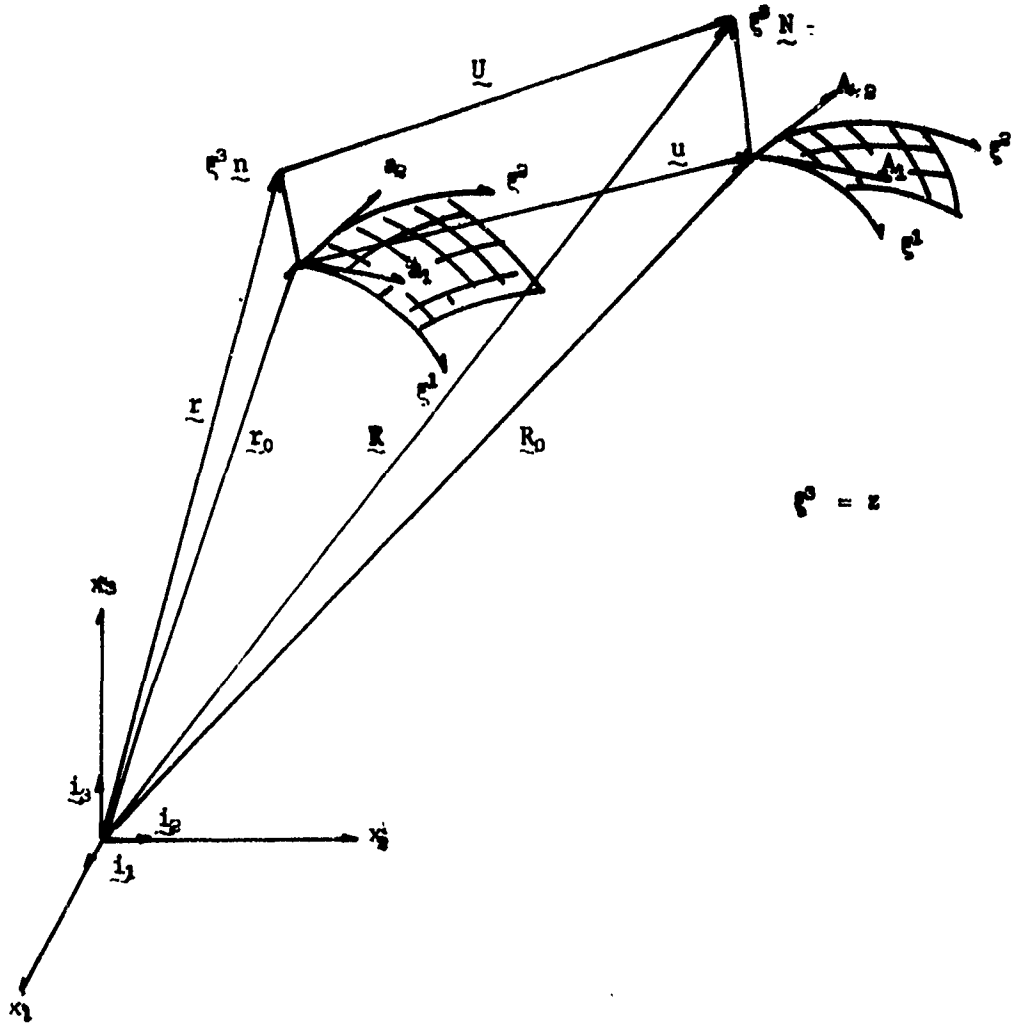

Figure A.1.1: Coordinates for Shell Deformation

the middle surface where $b_{\alpha\beta}$ = the second fundamental tensor,

$dn \cdot dn = \underset{\sim}{n}_{,\alpha} \cdot \underset{\sim}{n}_{,\beta} d\xi^{\alpha} d\xi^{\beta}$ is the third fundamental form of the middle surface where

$$c_{\alpha\beta} = \underset{\sim}{n}_{,\alpha} \cdot \underset{\sim}{n}_{,\beta} = (-b_{\alpha}^{\lambda} \underset{\sim}{a}_{\lambda}) \cdot (-b_{\beta}^{\mu} \underset{\sim}{a}_{\mu})$$

$$= b_{\alpha}^{\lambda} b_{\beta}^{\mu} a_{\lambda\mu} = b_{\alpha}^{\lambda} b_{\beta\lambda}$$

= third fundamental tensor

Substituting these identities into (4) gives

$$(ds_0)^2 = (a_{\alpha\beta} - 2zb_{\alpha\beta} + z^2 c_{\alpha\beta}) d\xi^{\alpha} d\xi^{\beta} + dz^2 \tag{5}$$

Denote that

$$g_{\alpha\beta} = a_{\alpha\beta} - 2zb_{\alpha\beta} + z^2 c_{\alpha\beta}$$

$$g_{\alpha 3} = g_{3\alpha} = 0$$

$$g_{33} = 1$$

Now, after deformation, consider the new position vector

$$\underset{\sim}{R} = \underset{\sim}{R}_0 + z\underset{\sim}{n} \tag{6}$$

and the squared length of the line element on the deformed surface is given by

$$(ds)^2 = dR \cdot dR = G_{ij}\, d\xi^i\, d\xi^j$$

$$= G_{\alpha\beta}\, d\xi^{\alpha} d\xi^{\beta} + G_{\alpha 3} d\xi^{\alpha} d\xi^3 + G_{33} d\xi^3 d\xi^3$$

$$= (\underset{\sim}{A}_{\alpha} + z\underset{\sim}{N}_{,\alpha}) \cdot (\underset{\sim}{A}_{\beta} + z\underset{\sim}{N}_{,\beta}) d\xi^{\alpha}\, d\xi^{\beta}$$

$$+ (\underset{\sim}{A}_{\alpha} + z\underset{\sim}{N}_{,\alpha}) \cdot \underset{\sim}{N}\, d\xi^{\alpha}\, d\xi^3 + dz^2$$

$$= (A_{\alpha\beta} - 2zB_{\alpha\beta} + z^2 C_{\alpha\beta})\, d\xi^{\alpha} d\xi^{\beta} \tag{7}$$

$$+ (\underset{\sim}{A}_{\alpha} + z\underset{\sim}{N}_{,\alpha}) \cdot \underset{\sim}{N}\, d\xi^{\alpha} d\xi^3 + dz^2$$

where

$$G_{\alpha\beta} = A_{\alpha\beta} - 2zB_{\alpha\beta} + z^2 C_{\alpha\beta}$$

$$G_{\alpha 3} = G_{3\alpha} = (\underset{\sim}{A}_\alpha + z\underset{\sim}{N}_{,\alpha}) \cdot \underset{\sim}{N}$$

$$G_{33} = 1$$

and,

$$A_{\alpha\beta} = \underset{\sim}{A}_\alpha \cdot \underset{\sim}{A}_\beta \ , \ \underset{\sim}{A}_\alpha = \underset{\sim}{R}_0{}_{,\alpha} \ , \ \underset{\sim}{A}_\beta = \underset{\sim}{R}_0{}_{,\beta}$$

$$B_{\alpha\beta} = \underset{\sim}{N}_{,\alpha} \cdot \underset{\sim}{A}_\beta$$

$$C_{\alpha\beta} = \underset{\sim}{N}_{,\alpha} \cdot \underset{\sim}{N}_{,\beta} = (-B_\alpha^\lambda \underset{\sim}{A}_\lambda) \cdot (-B_\beta^\mu \underset{\sim}{A}_\mu)$$

$$= B_\alpha^\lambda B_\beta^\mu A_{\lambda\mu} = B_\alpha^\lambda B_{\beta\lambda}$$

The difference between the squared lengths of the line elements on the deformed and undeformed surface is:

$$\begin{aligned} ds^2 - ds_0^2 &= 2\gamma_{ij}\, d\xi^i\, d\xi^j \\ &= 2\gamma_{\alpha\beta}\, d\xi^\alpha d\xi^\beta + 2\gamma_{\alpha 3} d\xi^\alpha d\xi^3 + 2\gamma_{33} dz^2 \\ &= [(A_{\alpha\beta} - a_{\alpha\beta}) - 2z(B_{\alpha\beta} - b_{\alpha\beta}) + z^2(C_{\alpha\beta} - c_{\alpha\beta})]\, d\xi^\alpha d\xi^\beta \\ &\quad + 2(\underset{\sim}{N} \cdot \underset{\sim}{A}_\alpha + z\underset{\sim}{N} \cdot \underset{\sim}{N}_{,\alpha})\, d\xi^\alpha\, d\xi^3 \end{aligned} \tag{8}$$

so that

$$\gamma_{\alpha\beta} = \tfrac{1}{2}[(A_{\alpha\beta} - a_{\alpha\beta}) - 2z(B_{\alpha\beta} - b_{\alpha\beta}) + z^2(C_{\alpha\beta} - c_{\alpha\beta})]$$

$$\gamma_{\alpha 3} = \underset{\sim}{N} \cdot \underset{\sim}{A}_\alpha + z\underset{\sim}{N} \cdot \underset{\sim}{N}_{,\alpha}$$

$$\gamma_{33} = 0$$

Denote the middle surface membrane strain as

$$e_{\alpha\beta} = \tfrac{1}{2}(A_{\alpha\beta} - a_{\alpha\beta}) \tag{9}$$

But,

$$\underset{\sim}{A}_\alpha = \underset{\sim}{R}_0{}_{,\alpha} = (\underset{\sim}{r}_0 + \underset{\sim}{u})_{,\alpha} = \underset{\sim}{r}_0{}_{,\alpha} + \underset{\sim}{u}_{,\alpha} = \underset{\sim}{a}_\alpha + \underset{\sim}{u}_{,\alpha}$$

$$A_{\alpha\beta} = \underset{\sim}{A}_\alpha \cdot \underset{\sim}{A}_\beta = a_{\alpha\beta} + \underset{\sim}{a}_\alpha \cdot \underset{\sim}{u}_{,\beta} + \underset{\sim}{a}_\beta \cdot \underset{\sim}{u}_{,\alpha} + \underset{\sim}{u}_{,\alpha} \cdot \underset{\sim}{u}_{,\beta}$$

Thus,

$$e_{\alpha\beta} = \tfrac{1}{2}(\underset{\sim}{a}_{\alpha}\cdot\underset{\sim}{u}_{,\beta} + \underset{\sim}{a}_{\beta}\cdot\underset{\sim}{u}_{,\alpha} + \underset{\sim}{u}_{,\alpha}\cdot\underset{\sim}{u}_{,\beta}) \tag{10}$$

where

$$\underset{\sim}{u} = u^{\beta}\underset{\sim}{a}_{\beta} + u^{3}\underset{\sim}{n} \tag{11}$$

$$\underset{\sim}{u}_{,\alpha} = (u^{\beta}\underset{\sim}{a}_{\beta})_{,\alpha} + u^{3}_{\ ,\alpha}\underset{\sim}{n} + u^{3}\underset{\sim}{n}_{,\alpha}$$

$$= u^{\beta}_{\ ,\alpha}\underset{\sim}{a}_{\beta} + u^{\beta}\underset{\sim}{a}_{\beta,\alpha} + u^{3}_{\ ,\alpha}\underset{\sim}{n} + u^{3}\underset{\sim}{n}_{,\alpha} \tag{12}$$

in which

$$\underset{\sim}{a}_{\beta,\alpha} = \Gamma^{\mu}_{\beta\gamma}\underset{\sim}{a}_{\mu} + \Gamma^{3}_{\beta\alpha}\underset{\sim}{n} = \Gamma^{\mu}_{\beta\alpha}\underset{\sim}{a}_{\mu} + b_{\beta\alpha}\underset{\sim}{n}$$

where Christoffel symbols,

$$\Gamma^{\mu}_{\beta\alpha} = \underset{\sim}{a}_{\beta,\alpha}\cdot\underset{\sim}{a}^{\mu}\ ,\quad \Gamma^{3}_{\beta\alpha} = \underset{\sim}{a}_{\beta,\alpha}\cdot\underset{\sim}{n} = \underset{\sim}{a}_{\beta}\cdot\underset{\sim}{n}_{,\alpha} = b_{\beta\alpha}$$

Hence,

$$\underset{\sim}{u}_{,\alpha} = (u^{\mu}_{\ ,\alpha} + \Gamma^{\mu}_{\beta\alpha}u^{\beta})\underset{\sim}{a}_{\mu} + u^{\beta}b_{\alpha\beta}\underset{\sim}{n} + u^{3}_{\ ,\alpha}\underset{\sim}{n} - u^{3}b^{\mu}_{\alpha}\underset{\sim}{a}_{\mu}$$

$$= (u^{\mu}_{\ ,\alpha} + \Gamma^{\mu}_{\beta\alpha}u^{\beta} - u^{3}b^{\mu}_{\alpha})\underset{\sim}{a}_{\mu} + (u^{\beta}b_{\alpha\beta} + u^{3}_{\ ,\alpha})\underset{\sim}{n}$$

$$= (u^{\mu}_{\ |\alpha} - u^{3}b^{\mu}_{\alpha})\underset{\sim}{a}_{\mu} + (u^{3}_{\ ,\alpha} + u^{\beta}b_{\alpha\beta})\underset{\sim}{n} \tag{13}$$

where

$$u^{\mu}_{\ |\alpha} = u^{\mu}_{\ ,\alpha} + \Gamma^{\mu}_{\beta\alpha}u^{\beta}$$

and the "|" represents covariant differentiation.

Using (13) in (10) yields:

$$e_{\alpha\beta} = \tfrac{1}{2}\{\underset{\sim}{a}_{\alpha}\cdot[(u^{\mu}_{\ |\beta} - u^{3}b^{\mu}_{\beta})\underset{\sim}{a}_{\mu} + (u^{3}_{\ ,\beta} + u^{\mu}b_{\beta\mu})\underset{\sim}{n}]$$

$$+ \underset{\sim}{a}_{\beta}\cdot[(u^{\mu}_{\ |\alpha} - u^{3}b^{\mu}_{\alpha})\underset{\sim}{a}_{\mu} + (u^{3}_{\ ,\alpha} + u^{\mu}b_{\alpha\mu})\underset{\sim}{n}]$$

$$+[(u^{\mu}_{\ |\alpha} - u^{3}b^{\mu}_{\alpha})\underset{\sim}{a}_{\mu} + (u^{3}_{\ ,\alpha} + u^{\mu}b_{\alpha\mu})\underset{\sim}{n}]\cdot[(u^{\mu}_{\ |\beta} - u^{3}b^{\mu}_{\beta})\underset{\sim}{a}_{\mu}$$

$$+ (u^{3}_{\ ,\beta} + u^{\mu}b_{\beta\mu})\underset{\sim}{n}]\}$$

$$= \tfrac{1}{2}\left[u_{\alpha|\beta} + u_{\beta|\alpha} - 2u^3 b_{\alpha\beta} + (u_{\mu|\alpha} - u^3 b_{\mu\alpha})(u^{\mu}_{|\beta} - u^3 b^{\mu}_{\beta}) \right.$$

$$\left. + (u^3_{,\alpha} + u^{\lambda} b_{\alpha\lambda})(u^3_{,\beta} + u^{\gamma} b_{\beta\gamma})\right] \tag{14}$$

$$\text{Let } \underset{\sim}{m} = \underset{\sim}{N} - \underset{\sim}{n}, \quad \underset{\sim}{N} = \underset{\sim}{m} + \underset{\sim}{n} \tag{15}$$

Denote the change in curvature tensor as

$$\chi_{\alpha\beta} = -(B_{\alpha\beta} - b_{\alpha\beta}) = \underset{\sim}{A}_{\alpha} \cdot \underset{\sim}{N}_{,\beta} - \underset{\sim}{a}_{\alpha} \cdot \underset{\sim}{n}_{,\beta}$$

$$= (\underset{\sim}{a}_{\alpha} + \underset{\sim}{u}_{,\alpha}) \cdot \underset{\sim}{m}_{,\beta} - \underset{\sim}{u}_{,\alpha} \cdot b^{\lambda}_{\beta} \underset{\sim}{a}_{\lambda}$$

Denoting $\underset{\sim}{m} = m^{\alpha} \underset{\sim}{a}_{\alpha} + mn$, then

$$\underset{\sim}{m}_{,\beta} = (m^{\mu}_{|\beta} - m b^{\mu}_{\beta})\underset{\sim}{a}_{\mu} + (m_{,\beta} + m^{\mu} b_{\beta\mu})\underset{\sim}{n}$$

and

$$\chi_{\alpha\beta} = m_{\alpha|\beta} - m b_{\alpha\beta} + (u_{\mu|\alpha} - u^3 b_{\mu\alpha})(m^{\mu}_{|\beta} - m b^{\mu}_{\beta})$$

$$+ (u^3_{,\alpha} + u^{\lambda} b_{\alpha\lambda})(m_{,\beta} + m^{\gamma} b_{\beta\gamma}) - b^{\mu}_{\beta}(u_{\mu|\alpha} - u^3 b_{\mu\alpha})$$

since

$$\underset{\sim}{a}_{\alpha} \cdot \underset{\sim}{a}_{\beta} = \epsilon_{\alpha\beta} \underset{\sim}{n}$$

$$\epsilon^{\alpha\beta} \underset{\sim}{a}_{\alpha} \cdot \underset{\sim}{a}_{\beta} = \epsilon^{\alpha\beta}\epsilon_{\alpha\beta} \underset{\sim}{n} = 2\underset{\sim}{n}$$

$$\underset{\sim}{n} = \tfrac{1}{2} \epsilon^{\alpha\beta} \underset{\sim}{a}_{\alpha} \cdot \underset{\sim}{a}_{\beta}$$

similarly,

$$\underset{\sim}{N} = \tfrac{1}{2} \epsilon^{*\alpha\beta} \underset{\sim}{A}_{\alpha} \cdot \underset{\sim}{A}_{\beta}$$

If the permutation symbols in the deformed and undeformed surfaces are the same (small strain); i.e., $\epsilon^{\alpha\beta} = \epsilon^{*\alpha\beta}$, then

$$\underset{\sim}{m} = \{-u^3_{,\alpha} - u^{\beta} b_{\alpha\beta} - \epsilon^{\lambda\beta} \epsilon_{\alpha\gamma}(u^{\gamma}_{|\lambda} - b^{\gamma}_{\lambda} u^3)(u^3_{,\beta} + b_{\beta n} u^n)\} \underset{\sim}{a}^{\alpha}$$

$$+ \{ u^{\alpha}_{|\alpha} - b^{\alpha}_{\alpha} u^3 + \tfrac{1}{2}\epsilon^{\alpha\beta} \epsilon_{\gamma\lambda} (u^{\gamma}_{|\alpha} - b^{\gamma}_{\alpha} u^3)(u^{\lambda}_{|\beta} - b^{\lambda}_{\beta} u^3) \} \underset{\sim}{n}$$

We define

$$m_{\alpha} = -u^3_{,\alpha} - u^{\beta} b_{\alpha\beta} - \epsilon^{\lambda\beta} \epsilon_{\alpha\gamma} (u^{\gamma}_{|\lambda} - b^{\gamma}_{\lambda} u^3)(u^3_{,\beta} - b_{\beta n} u^n)$$

$$m = u^{\alpha}_{|\alpha} - b^{\alpha}_{\alpha} u^3 + \tfrac{1}{2} \epsilon^{\alpha\beta} \epsilon_{\gamma\lambda} (u^{\gamma}_{|\alpha} - b^{\gamma}_{\alpha} u^3)(u^{\lambda}_{|\beta} - u^3)$$

$$\Lambda_{\alpha\beta} = \tfrac{1}{2}[(m_{\mu|\alpha} - m b_{\mu\alpha})(m^{\mu}_{|\beta} - m b^{\mu}_{\beta}) + (m_{,\alpha} + m^{\mu} b_{\alpha\mu})(m_{,\beta} + m^{\mu} b_{\beta\mu})$$
$$- (m_{\lambda|\alpha} - m b_{\lambda\alpha}) b^{\lambda}_{\beta} - (m_{\lambda|\beta} - m b_{\lambda\beta}) b^{\lambda}_{\alpha}]$$

So finally,

$$\gamma_{\alpha\beta} = e_{\alpha\beta} + z\chi_{\alpha\beta} + z^2 \Lambda_{\alpha\beta}$$

The shear strain is

$$\gamma_{\alpha 3} = \underset{\sim}{N} \cdot \underset{\sim}{A}_{\alpha} + z \underset{\sim}{N} \cdot \underset{\sim}{N}_{,\alpha}$$

$$= m_{\alpha} + m^{\mu} u_{\mu|\alpha} - m^{\mu} u^3 b_{\mu\alpha} + (u^3_{,\alpha} + u^{\mu} b_{\alpha\mu})(m+1)$$

$$+ z m^{\mu} m_{\mu|\alpha} - m^{\mu} m b_{\mu\alpha} + z m (m_{,\alpha} + m^{\mu} b_{\alpha\mu})$$

$$- z m^{\mu} b_{\mu\alpha} + z (m_{,\alpha} + m^{\mu} b_{\alpha\mu})$$

2. SPECIAL APPROXIMATIONS

For large deflections but small rotations

$$b_{\alpha\beta} u^{\beta} \ll u^3_{,\alpha}$$

$$\underset{\sim}{u}_{,\beta} = (u^{\alpha}_{|\beta} - b^{\alpha}_{\beta} u^3) \underset{\sim}{a}_{\alpha} + u^3_{,\beta} \underset{\sim}{n}$$

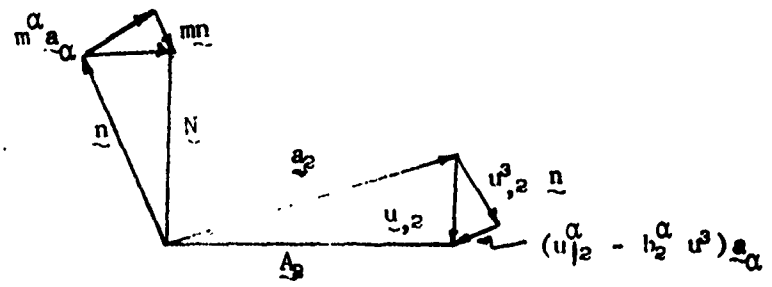

Figure A.1.2: Approximation for Small Rotation

$$\gamma_{\alpha\beta} = \tfrac{1}{2}(u_{\alpha|\beta} + u_{\beta|\alpha} - 2b_{\alpha\beta} u^3 + u^3{}_{,\alpha}\, u^3{}_{,\beta})$$

$$\underset{\sim}{m} = \tfrac{1}{2} \epsilon^{\alpha\beta} (2\underset{\sim}{a}_\alpha + u^3{}_{,\alpha}\, \underset{\sim}{n}) \cdot u^3{}_{,\beta}\, \underset{\sim}{n}$$

$$= \tfrac{1}{2} \epsilon^{\alpha\beta} (-2\epsilon_{\alpha\beta}\, \underset{\sim}{a}^\beta)\, u^3{}_{,\beta} = -u^3{}_{,\beta}\, \underset{\sim}{a}^\beta = -u^3{}_{,\alpha}\, \underset{\sim}{a}^\alpha$$

from which

$$m = 0, \quad m_\alpha = -u^3{}_{,\alpha}$$

Consequently:

$$\underset{\sim}{m}_{,\beta} = -u^3{}_{,\alpha\beta}\, \underset{\sim}{a}^\alpha - u^3{}_{,\alpha}\, (\Gamma^\alpha_{\mu\beta}\, \underset{\sim}{a}^\mu + b^\alpha_\beta\, \underset{\sim}{n})$$

$$= -u^3{}_{|\alpha\beta}\, \underset{\sim}{a}^\alpha - u^3{}_{,\alpha}\, b^\alpha_\beta\, \underset{\sim}{n}$$

$$\chi_{\alpha\beta} = -(\underset{\sim}{a}_\alpha + u^3{}_{,\alpha}\underset{\sim}{n}) \cdot (u^3{}_{|\gamma\beta}\underset{\sim}{a}^\gamma + b^\gamma_\beta\, u^3{}_{,\gamma}\, \underset{\sim}{n}) = -u^3{}_{|\alpha\beta} - b^\gamma_\beta\, u^3{}_{,\gamma}\, u^3{}_{,\alpha}$$

or, neglecting the nonlinear term,

$$\chi_{\alpha\beta} = -u^3{}_{|\alpha\beta}$$

$$\epsilon_{\alpha\beta} = \bar{\epsilon}_{\alpha\beta}\ a\ ,\quad \epsilon^{*}_{\alpha\beta} = \bar{\epsilon}^{*\alpha\beta}\ A$$

$$\epsilon^{\alpha\beta} = \bar{\epsilon}^{\alpha\beta}\ \frac{1}{a}\ ,\quad \epsilon^{*\alpha\beta} = \bar{\epsilon}^{*\alpha\beta}\ \frac{1}{A}$$

$$\underset{\sim}{a}_{\alpha} \cdot \underset{\sim}{a}_{\beta} = \epsilon_{\alpha\beta}\ \underset{\sim}{n}\ ,\quad \underset{\sim}{a}^{\alpha} \cdot \underset{\sim}{a}^{\beta} = \epsilon^{\alpha\beta}\ \underset{\sim}{n}$$

$$\underset{\sim}{n} \cdot \underset{\sim}{a}_{\alpha} = \epsilon_{\alpha\beta}\ \underset{\sim}{a}^{\beta},\quad \underset{\sim}{n} \cdot \underset{\sim}{a}_{\beta} = -\epsilon_{\alpha\beta}\underset{\sim}{a}^{\alpha}$$

$$\underset{\sim}{n} \cdot \underset{\sim}{a}^{\alpha} = \epsilon_{\alpha\beta}\ \underset{\sim}{a}_{\beta}\ ,\quad \underset{\sim}{n} \cdot \underset{\sim}{a}_{\mu} = -\epsilon_{\alpha\mu}\underset{\sim}{a}^{\alpha}$$

$$\underset{\sim}{a}_{\beta} \cdot \underset{\sim}{n} = \epsilon_{\alpha\beta}\ \underset{\sim}{a}^{\alpha}\ ,\quad \underset{\sim}{a}_{\alpha} \cdot \underset{\sim}{n} = -\epsilon_{\alpha\beta}\ \underset{\sim}{a}^{\beta}$$

$$\underset{\sim}{a}^{\beta} \cdot \underset{\sim}{n} = \epsilon_{\alpha\beta}\ \underset{\sim}{a}_{\alpha}\ ,\quad \underset{\sim}{a}_{\mu} \cdot \underset{\sim}{n} = -\epsilon_{\mu\beta}\ \underset{\sim}{a}^{\beta}$$

$$\epsilon^{\alpha\beta}\ \epsilon_{\alpha\beta} = 1$$

Love-Kirchhoff Assumptions

(1) points which lie on one and the same normal to the undeformed middle surface also lie on one and the same normal to the deformed middle surface.

(2) the effect of the normal stress on surfaces parallel to the middle surface may be neglected in the stress-strain relations.

(3) the displacements in the direction of the normal to the middle surface are approximately equal for all points on the same normal.

Assumptions for Love's strain-energy expressions

(1) the shell is thin, i. e. $h/r \ll 1$

(2) deflections may be large but strains are small $\epsilon_{\alpha\beta} = \epsilon^{*}_{\alpha\beta}$

(3) strain energy is a quadratic function of the strain components

$$\Phi = \frac{1}{2}\ E^{ijk\ell}\gamma_{ij}\gamma_{k\ell}$$

(4) the state of stress is approximately plane, i. e., the effect of transverse shear stresses and of the transverse normal stress, acting on surfaces parallel to the middle surface, may be neglected in the strain energy density. For thin shell, terms with $z^\beta = 0$ and $\gamma^{23} = 0$. For shallow shell, $u^3_{,\alpha} \gg b_{\alpha\beta}u^\beta = 0$.

3. CALCULATION OF FUNDAMENTAL TENSORS

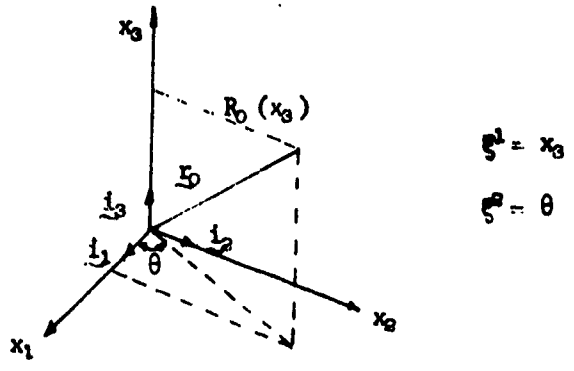

Figure A.1.3: Surfaces of Revolution

$$\underset{\sim}{r}_o(x_3, \theta) = R_o(x_3)\cos\theta\ \underset{\sim}{i}_1 + R_o(x_3)\sin\theta\ \underset{\sim}{i}_2 + x_3\underset{\sim}{i}_3$$

$$\underset{\sim}{r}_{o,1} = \underset{\sim}{a}_1 = \frac{\partial \underset{\sim}{r}_o}{\partial \xi^1} = \frac{\partial \underset{\sim}{r}_o}{\partial x^3} = R_o^1\cos\theta\ \underset{\sim}{i}_1 + R_o^1\sin\theta\ \underset{\sim}{i}_2 + \underset{\sim}{i}_3$$

$$\underset{\sim}{r}_{o,2} = \underset{\sim}{a}_2 = \frac{\partial r_o}{\partial \xi^2} = \frac{\partial \underset{\sim}{r}_o}{\partial\theta} = -R_o\sin\theta\ \underset{\sim}{i}_1 + R_o\cos\theta\ \underset{\sim}{i}_2$$

$$a_{11} = \underset{\sim}{a}_1 \cdot \underset{\sim}{a}_1 = 1 + (R_o^1)^2$$

$$a_{12} = \underset{\sim}{a}_1 \cdot \underset{\sim}{a}_2 = 0$$

$$a_{22} = \underset{\sim}{a}_2 \cdot \underset{\sim}{a}_2 = R_o^2$$

$$|a_1 \times a_2| = (a_{11}a_{22} - a_{12}^2)^{\frac{1}{2}} = R_o\{1 + (R_o')^2\}^{\frac{1}{2}}$$

$$\underset{\sim}{n} = \frac{\underset{\sim}{a}_1 \times \underset{\sim}{a}_2}{|a_1 \times a_2|} = \frac{-R_o}{\sqrt{a_{11}a_{22}}}(\cos\theta\ \underset{\sim}{i}_1 + \sin\theta\ \underset{\sim}{i}_2 - R_o'\underset{\sim}{i}_3)$$

$$= \frac{-R_o}{R_o\sqrt{1 + R_o'^2}}(\cos\theta\ \underset{\sim}{i}_1 + \sin\theta\ \underset{\sim}{i}_2 - R_o'\ \underset{\sim}{i}_3)$$

$$= -\frac{1}{\sqrt{1 + R_o'^2}}(\cos\theta\ \underset{\sim}{i}_1 + \sin\theta\ \underset{\sim}{i}_2 - R_o'\ \underset{\sim}{i}_3)$$

$$\underset{\sim}{n}_{,1} = \frac{\partial \underset{\sim}{n}}{\partial x_3} = \frac{R_o'R_o''}{\sqrt{1 + R_o'^2}}(\cos\theta\ \underset{\sim}{i}_1 + \sin\theta \quad - R_o'\ \underset{\sim}{i}_3) + \frac{R_o''}{\sqrt{1 + R_o'^2}}\ \underset{\sim}{i}_3$$

$$= \frac{R_o'R_o''}{\sqrt{1 + R_o'^2}}(\cos\theta\ \underset{\sim}{i}_1 + \sin\theta\ \underset{\sim}{i}_2) + \frac{R_o''(1 - R_o'^2)}{\sqrt{1 + R_o'^2}}\ \underset{\sim}{i}_3$$

$$\underset{\sim}{n}_{,2} = \frac{\partial \underset{\sim}{n}}{\partial\theta} = \frac{-1}{\sqrt{1 + R_o'^2}}(-\sin\theta\ \underset{\sim}{i}_1 + \cos\theta\ \underset{\sim}{i}_2)$$

$$b_{11} = -\underset{\sim}{a}_1 \cdot \underset{\sim}{n}_{,1} = -\frac{R_o'^2R_o''}{\sqrt{1 + R_o'^2}} + \frac{R_o''(1 - R_o'^2)}{\sqrt{1 + R_o'^2}} = -\frac{R_o''}{\sqrt{1 + R_o'^2}}$$

$$b_{12} = -\underset{\sim}{a}_1 \cdot \underset{\sim}{n}_{,2} = 0$$

$$b_{22} = -\underset{\sim}{a}_2 \cdot \underset{\sim}{n}_{,2} = \frac{R_o}{\sqrt{1 + R_o'^2}}$$

$$R_1 = -\frac{1}{b_1'} = -\frac{a_{11}}{b_{11}} = +\frac{(1 + R_1'^2)(\sqrt{1 + R_o'^2})}{R_o''} = \frac{(1 + R_o'^2)^{3/2}}{R_o''}$$

$$R_2 = -\frac{1}{b_2^2} = -\frac{a_{22}}{b_{22}} = -\frac{R_o^2(\sqrt{1 + R_o'^2})}{R_o} = -R_o\sqrt{1 + R_o'^2}$$

Since $a_{12} = b_{12} = 0$ we say that the meridians and parallels are lines of principal curvature.

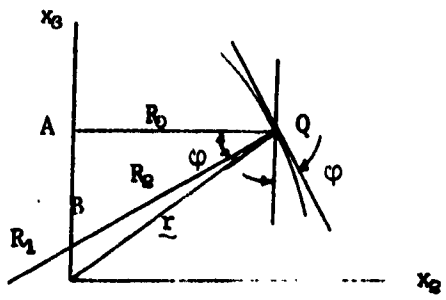

R_1 = Radius of curvature of meridian curve $R_o(x^3)$

Figure A.1.4: Principal Curvatures

$$R_o' = \frac{\partial R_o}{\partial x_3} = \tan\varphi$$

$$AB = R_o \tan\varphi = R_o R_o'$$

$$BO = \sqrt{R_o^2 + R_o^2 R_o'^2} = R_o\sqrt{1 + R_o'^2} = -R_2$$

- sign signifies R_2 is opposite to direction $\underline{n}$. To check if $a_{\alpha\beta}$ and R_1 and R_2 define is valid surface we use Coadazi equations

$$b_{\alpha\beta|\gamma} = b_{\alpha\gamma|\beta} \qquad \frac{1}{R_1}(\sqrt{a}_{22}),_1 = (\frac{\sqrt{a}_{22}}{R_2}),_1 \quad , \quad \frac{1}{R_2}(\sqrt{a}_{11}),_2 = (\frac{\sqrt{a}_{11}}{R_1}),_2$$

$$\underset{\sim}{t}_1 = \frac{\underset{\sim}{a}_1}{\sqrt{a_{11}}} \quad , \quad \underset{\sim}{t}_2 = \frac{\underset{\sim}{a}_2}{\sqrt{a_{22}}} \quad , \quad \underset{\sim}{n} = \frac{\underset{\sim}{a}_1 \times \underset{\sim}{a}_2}{\sqrt{a_{11}a_{22}}}$$

$$\underset{\sim}{n}_{,1} = c_1\underset{\sim}{t}_1 + c_2\underset{\sim}{t}_2$$

$$\underset{\sim}{t}_1 \cdot \underset{\sim}{n}_{,1} = \frac{-\underset{\sim}{a}_1 \cdot \underset{\sim}{n}_{,1}}{\sqrt{a_{11}}} = \frac{b_{11}}{\sqrt{a_{11}}} = C_1(t_1 \cdot t_1) + C_2(t_1 \cdot t_2)$$

$$\underset{\sim}{t}_2 \cdot \underset{\sim}{n}_{,1} = \frac{-\underset{\sim}{a}_2 \cdot \underset{\sim}{n}_1}{\sqrt{a_{22}}} = \frac{b_{21}}{\sqrt{a_{22}}} = C_1(t_2 \cdot t_1) + C_2(t_2 \cdot t_2)$$

$$C_1 = \frac{b_{11}}{\sqrt{a_{11}}} \quad , \quad C_2 = 0$$

$$\underset{\sim}{n}_{,1} = \frac{b_{11}}{\sqrt{a_{11}}}\underset{\sim}{t}_1$$

$$k_1 = -\frac{1}{R_1} = \frac{b_{11}}{a_{11}} \qquad b_{11} = -\frac{a_{11}}{R_1}$$

$$\underset{\sim}{n}_{,1} = \frac{\sqrt{a_{11}}}{R_1}\underset{\sim}{t}_1$$

Similarly

$$\underset{\sim}{n}_{,2} = \frac{\sqrt{a_{22}}}{R_2}\underset{\sim}{t}_2$$

$$b_{11} = -\underset{\sim}{a}_1 \cdot \underset{\sim}{n}_{,1} = -\sqrt{a_{11}}\,\underset{\sim}{t}_1 \cdot \frac{\sqrt{a_{11}}}{R_1}\underset{\sim}{t}_1 = -\frac{a_{11}}{R_1}$$

4. LINEAR STRAIN-DISPLACEMENT EQUATIONS (NOVOZHILOV)

$$e_{\alpha\beta} = \frac{1}{2}\{(u^{\mu}_{,\beta} + \Gamma^{\mu}_{\lambda\varsigma}u^{\lambda})a_{\alpha\mu} + (u^{\mu}_{,\alpha} + \Gamma^{\mu}_{\lambda\alpha}u^{\lambda})a_{\beta\mu} - 2b_{\alpha\beta}u^{3}\}$$

Let $A_1 = \sqrt{a_{11}}$, $A_2 = \sqrt{a_{22}}$, $R_1 = -\frac{a_{11}}{b_{11}}$, $R_2 = -\frac{a_{22}}{b_{22}}$

$$\bar{u}^{\mu} = u^{\mu}\sqrt{a_{\mu\mu}} \qquad \bar{e}_{\alpha\beta} = \frac{e_{\alpha\beta}}{\sqrt{a_{\alpha\alpha}a_{\beta\beta}}} \quad , \quad \Gamma^{\mu}_{\lambda 9}u^{\lambda}a_{\alpha\mu} = (\Gamma'_{11}u' + \Gamma'_{21}u^{2})a_{11}$$

$$u^{\mu}_{,\beta}a_{\alpha\mu} = \frac{1}{\sqrt{a_{\alpha\alpha}a_{\beta\beta}}}\frac{\partial}{\partial\xi_{\beta}}\left(\frac{\bar{u}^{\mu}}{\sqrt{a_{\mu\mu}}}\right)a_{\alpha\mu}$$

$$= \frac{1}{\sqrt{a_{\alpha\alpha}a_{\beta\beta}}}\left(\frac{\partial\bar{u}^{\mu}}{\partial\xi_{\beta}}\frac{1}{\sqrt{a_{\mu\mu}}} - \frac{\bar{u}^{\mu}}{a_{\mu\mu}}\frac{\partial\sqrt{a_{\mu\mu}}}{\partial\xi_{9}}\right)a_{\alpha\mu}$$

$$\bar{e}_{11} = \frac{1}{\sqrt{a_{11}a_{11}}}\left[\frac{1}{\sqrt{a_{11}}}\frac{\partial\bar{u}^{1}}{\partial\xi_{1}} - \frac{\bar{u}^{1}}{a_{11}}\frac{\partial\sqrt{a_{11}}}{\partial\xi_{1}} + \sqrt{a_{11}}\,\underset{\sim}{t}_{1}\cdot\frac{\partial\sqrt{a_{11}}}{\partial\xi_{1}}\underset{\sim}{t}_{1}\frac{\bar{u}^{1}}{\sqrt{a_{11}}}\frac{1}{\sqrt{a_{11}a_{11}}}\right.$$

$$\left. + \sqrt{a_{11}}\,\underset{\sim}{t}_{1}\cdot\frac{\partial\sqrt{a_{11}}}{\partial\xi_{2}}\underset{\sim}{t}_{1}\frac{\bar{u}^{2}}{\sqrt{a_{22}}}\frac{1}{\sqrt{a_{11}a_{11}}}\right]a_{11} - \left(\frac{-a_{11}}{R_1}\right)\bar{u}^{3}$$

$$= \frac{1}{\sqrt{a_{11}}}\frac{\partial\bar{u}^{1}}{\partial\xi_{1}} - \frac{1}{a_{11}}\frac{\partial\sqrt{a_{11}}}{\partial\xi_{1}}\bar{u}' + \sqrt{a_{11}}\frac{\partial\sqrt{a_{11}}}{\partial\xi_{1}}\frac{\bar{u}^{1}}{\sqrt{a_{11}}}\frac{a_{11}}{\sqrt{a_{11}a_{11}}}\frac{1}{\sqrt{a_{11}a_{11}}}$$

$$+ \sqrt{a_{11}}\frac{\partial\sqrt{a_{11}}}{\partial\xi_{2}}\frac{\bar{u}^{2}}{\sqrt{a_{22}}}\frac{a_{11}}{\sqrt{a_{11}a_{11}}}\frac{1}{\sqrt{a_{11}a_{11}}} + \frac{\bar{u}^{3}}{R_1}$$

Let

$$u^1 = u\ ,\quad u^2 = v,\quad u^3 = w\quad \sqrt{a_{11}} = A_1\quad \sqrt{a_{22}} = A_2$$

$$\bar{e}_{11} = \frac{1}{A_1}\frac{\partial u}{\partial \xi^1} + \frac{1}{A_1 A_2}\frac{\partial A_1}{\partial \xi^2} + \frac{w}{R_1}$$

Similarly

$$\bar{e}_2 = \frac{1}{A_2}\frac{\partial v}{\partial \xi^2} + \frac{1}{A_1 A_2}\frac{\partial A_2}{\partial \xi^1} u + \frac{w}{R_2}$$

$$\bar{e}_{12} = \frac{A_2}{A_1}\frac{\partial}{\partial \xi^1}\left(\frac{v}{A_2}\right) + \frac{A_1}{A_2}\frac{\partial}{\partial \xi^2}\left(\frac{u}{A_1}\right)$$

$$\bar{e}_{22} = \frac{1}{A_2}\frac{\partial v}{\partial \xi_2} + \frac{1}{A_1 A_2}\frac{\partial A_2}{\partial \xi_1} u + \frac{w}{R_2}$$

$$\chi_{\alpha\beta} = -u^3_{|\alpha\beta} - (u^\lambda{}_{|\alpha}\lambda^{\cdot}_{|\beta} - b^\mu_\beta(u_{\mu|\alpha} - u^3 b_{\mu\alpha})$$

$$= -u^3_{|\alpha\beta} - u^\lambda_{|\beta} b_{\alpha\lambda} - u^\lambda b_{\alpha\lambda|\beta} - b^\lambda_\beta(u_{\mu|\alpha} - u^3 b_{\mu\alpha})$$

$$= -u^3_{|\alpha\beta} - u_{\lambda|\beta} b^\lambda_\alpha - u_\lambda b^\lambda_{\alpha|\beta} - b^\mu_\beta u_{\mu|\alpha} + b^\mu_\beta b_{\mu\alpha} u^3$$

$$\bar{\chi}_{11} = -\frac{1}{A_1}\frac{\partial}{\partial \xi_1}\left(\frac{1}{A_1}\frac{\partial w}{\partial \xi_1} - \frac{u}{R_1}\right) - \frac{1}{A_1 A_2}\frac{\partial A_1}{\partial \xi_2}\left(\frac{1}{A_2}\frac{\partial w}{\partial \xi_2} - \frac{v}{R_2}\right)$$

$$\bar{\chi}_{22} = -\frac{1}{A_2}\frac{\partial}{\partial \xi_2}\left(\frac{1}{A_2}\frac{\partial w}{\partial \xi_2} - \frac{v}{R_2}\right) - \frac{1}{A_1 A_2}\frac{\partial A_2}{\partial \xi_1}\frac{1}{A_1}\frac{\partial w}{\partial \xi_1} - \frac{u}{R_1}$$

$$\bar{\chi}_{12} = -\frac{1}{A_1 A_2}\left(\frac{\partial^2 w}{\partial \xi_1 \partial \xi_2} - \frac{1}{A_1}\frac{\partial A_1}{\partial \xi_2}\frac{\partial w}{\partial \xi_1} - \frac{1}{A_2}\frac{\partial A_2}{\partial \xi_1}\frac{\partial w}{\partial \xi_2}\right)$$

$$+ \frac{1}{R_1}\left(\frac{1}{A_2}\frac{\partial u}{\partial \xi_2} - \frac{1}{A_1 A_2}\frac{\partial A_1}{\partial \xi_2} u\right) + \frac{1}{R_2}\left(\frac{1}{A_1}\frac{\partial v}{\partial \xi_1} - \frac{1}{A_1 A_2}\frac{\partial A_2}{\partial \xi_1} v\right)$$

For a shell of revolution

Let $A_1 = 1$ $\qquad A_2 = r$

$$R_1 = -\frac{\partial S}{\partial \varphi}$$

$$R_2 = \frac{r}{\cos \varphi}$$

Novozhilov strain equation

$$\bar{e}_{11} = \frac{\partial u}{\partial s} - w \frac{\partial \varphi}{\partial s}$$

$$\bar{e}_{22} = \frac{1}{r}\left(\frac{\partial v}{\partial \theta} + u \sin \varphi + w \cos \varphi\right)$$

$$\bar{e}_{12} = \frac{\partial v}{\partial s} - \frac{v}{r} \sin \varphi + \frac{1}{r} \frac{\partial u}{\partial \theta}$$

$$\bar{\chi}_{11} = -\left(\frac{\partial^2 w}{\partial s^2} + u \frac{\partial^2 \varphi}{\partial s^2} + \frac{\partial u}{\partial s} \frac{\partial \varphi}{\partial s}\right) \qquad (16)$$

$$\chi_{22} = -\frac{1}{r}\left\{\frac{1}{r} \frac{\partial^2 w}{\partial \theta^2} - \frac{\cos \varphi}{r} \frac{\partial v}{\partial \theta} + \sin \varphi\left(\frac{\partial w}{\partial s} + u \frac{\partial \varphi}{\partial s}\right)\right\}$$

$$\chi_{12} = -\frac{1}{r}\left\{\frac{\partial^2 w}{\partial s \partial \theta} - \frac{1}{r} \sin \varphi \frac{\partial w}{\partial \theta} - \frac{\partial \varphi}{\partial s} \frac{\partial u}{\partial \theta} + \cos \varphi \frac{\partial v}{\partial s} - \frac{\cos \varphi}{r} \sin \varphi v\right\}$$

APPENDIX A.2

YIELD CRITERIA

1. ISTROPIC YIELD FUNCTION

The von Mises yield criterion, one of the most widely used, is discussed herein. Von Mises suggested that yielding occurred when the second deviatoric stress invariant J reached a constant value $\bar{\sigma}$ called equivalent stress such that

$$f = \bar{\sigma}^2 = 3J = \frac{9}{2}\tau_{oct}^2 \qquad (1)$$

where f is the plastic potential function, and τ_{oct} is the octahedral stress defined as

$$\tau_{oct} = \frac{1}{3}\sqrt{(\sigma_{11}-\sigma_{22})^2 + (\sigma_{22}-\sigma_{33})^2 + (\sigma_{33}-\sigma_{11})^2 + 6(\sigma_{12}^2+\sigma_{23}^2+\sigma_{31}^2)} \qquad (2)$$

Together with Drucker's postulate that the yield surface is convex and the plastic strain rate vector is normal to the yield surface the Prandtle-Reuss flow rule for isotropic hardening material as defined in (2.8), Section 2, will be employed in the present study.

Following the procedure outlined in the expressions (2.8) through (2.19), we obtain the explicit physical components of the tensor of plastic moduli,

$$\overset{*}{\underset{\sim}{D}} = \frac{-\underset{\sim}{D}\,\underset{\sim}{Z}\,\underset{\sim}{Z}^T\,\underset{\sim}{D}}{E_{(p)} + \underset{\sim}{Z}^T\,\underset{\sim}{D}\,\underset{\sim}{Z}} \qquad (3)$$

where $\underset{\sim}{E}$ is the standard elastic matrix and

$$\underset{\sim}{Z}^T = \left[\frac{3\sigma'_{11}}{2\bar{\sigma}} \quad \frac{3\sigma'_{22}}{2\bar{\sigma}} \quad \frac{3\sigma'_{33}}{2\bar{\sigma}} \quad \frac{3\sigma_{12}}{\bar{\sigma}} \quad \frac{3\sigma_{23}}{\bar{\sigma}} \quad \frac{3\sigma_{31}}{\bar{\sigma}}\right] \tag{4}$$

in which σ'_{11}, σ'_{22}, and σ'_{33} are deviatoric stresses.

2. ANISOTROPIC YIELD FUNCTION

2.1 THREE DIMENSIONAL SOLID

Developments of anisotropic yield criteria have evolved for the last two decades. The directional anisotropy was studied by Hill [8] using the von Mises yield condition and its flow rules. He chose yield functions such that the von Mises criterion for isotropic solid is restored when anisotropy vanishes. Such yield functions were used also by Tsai [22], Fulton [7] and others. The formulation, however, is not convenient for numerical step-by-step computation. Hu [10] extended the Hill theory and introduced equivalent stress-strain relationships in appropriate form, using simple uniaxial and shear stress-strain tests on coupons cut in the directions of the orthotropy. The anisotropic parameters were held constant. However, experimental evidences show that anisotropic parameters for strain-hardening material depend on the state of stress and should be updated as the stress level changes. Such procedure was used by Jensen [11] and Whang [23]. In the present study the yield criterion of Hill as extended by Hu and further by Jensen and Whang will be specialized for fiber-reinforced shell structures. Additional discussions concerning coordinate transformations are given in Appendix A.5.

For the case of anisotropy the yield function (2.6) is given explicitly,

$$f = \bar{\sigma}^2 = \frac{1}{2}\{A_{12}(\sigma_{11}-\sigma_{22})^2 + A_{23}(\sigma_{22}-\sigma_{33})^2 + A_{31}(\sigma_{33}-\sigma_{11})^2 + 6(A_{44}\sigma_{12}^2 + A_{55}\sigma_{23}^2 + A_{66}\sigma_{31}^2)\} \quad (5)$$

where A_{12}, etc. are anisotropic parameters.

Setting

$$A_{11} = A_{12} + A_{31}$$

$$A_{22} = A_{12} + A_{23}$$

$$A_{33} = A_{23} + A_{31}$$

$$f = \bar{\sigma}^3 = \frac{1}{2}\{ A_{11}\sigma_{11}^2 + A_{22}\sigma_{22}^2 + A_{33}\sigma_{33}^2 - 2(A_{12}\sigma_{11}\sigma_{22} + A_{23}\sigma_{22}\sigma_{33} + A_{31}\sigma_{33}\sigma_{11}) + 6(A_{44}\sigma_{12}^2 + A_{55}\sigma_{23}^2 + A_{66}\sigma_{31}^2)\} \quad (6)$$

Differentiating (6),

$$d\bar{\sigma} = \frac{d\sigma_{11}}{2\bar{\sigma}}(A_{11}\sigma_{11} - A_{12}\sigma_{22} - A_{31}\sigma_{33}) + \frac{d\sigma_{22}}{2\bar{\sigma}}(-A_{12}\sigma_{11} + A_{22}\sigma_{22} - A_{23}\sigma_{33}) + \frac{d\sigma_{33}}{2\bar{\sigma}}(-A_{31}\sigma_{11} - A_{23}\sigma_{22} + A_{33}\sigma_{33}) + \frac{d\sigma_{12}}{\bar{\sigma}}(3A_{44}\sigma_{12}) + \frac{d\sigma_{23}}{\bar{\sigma}}(3A_{55}\sigma_{23}) + \frac{d\sigma_{31}}{\bar{\sigma}}(3A_{66}\sigma_{31}) \quad (7)$$

It is seen that (6) reduces to the isotropic yield function (1) if $A_{11} = A_{22} = A_{33} = 2$ and all other anisotropic parameters are equal to 1.

The anisotropic parameters initially depend on the initial yield stresses in various directions. Let $\bar{\sigma}_{(0)}$ be the equivalent initial yield stress in the 1-1 direction and all other stress components be equal to zero, and set

$$\bar{\sigma}_{(0)} = \sigma_{(0)11} \tag{8}$$

which gives from (5)

$$\bar{\sigma}^2_{(0)} = \frac{1}{2}(A_{(0)12} + A_{(0)31})\sigma^2_{(0)11}$$

or

$$A_{(0)12} + A_{(0)31} = 2 \tag{9}$$

Similarly for the 2-2 direction,

$$\sigma_{22} = \sigma_{(0)22}$$

$$\bar{\sigma}^2_{(0)} = \frac{1}{2}(A_{(0)12} + A_{(0)23})\sigma^2_{(0)22}$$

$$A_{(0)12} + A_{(0)23} = 2\left(\frac{\bar{\sigma}_{(0)}}{\sigma_{(0)22}}\right)^2 \tag{10}$$

and

$$\sigma_{33} = \sigma_{(0)33}$$

$$\bar{\sigma}^2_{(0)} = \frac{1}{2}(A_{(0)23} + A_{(0)31})\sigma^2_{(0)33}$$

$$A_{(0)23} + A_{(0)31} = 2\left(\frac{\bar{\sigma}_{(0)}}{\sigma_{(0)33}}\right)^2 \tag{11}$$

Solving for $A_{(0)12}$, $A_{(0)23}$, and $A_{(0)31}$ from (9), (10), and (11), we get.

$$A_{(0)12} = 1 + \bar{\sigma}^2_{(0)}\left(\frac{\sigma^2_{(0)33} - \sigma^2_{(0)22}}{\sigma^2_{(0)33}\sigma^2_{(0)22}}\right) \tag{12a}$$

$$A_{(0)23} = -1 + \bar{\sigma}^2_{(0)}\left(\frac{\sigma^2_{(0)33} + \sigma^2_{(0)22}}{\sigma^2_{(0)33}\sigma^2_{(0)22}}\right) \tag{12b}$$

$$A_{(0)31} = 1 + \bar{\sigma}^2_{0}\left(\frac{\sigma^2_{(0)22} - \sigma^2_{(0)33}}{\sigma^2_{(0)33}\sigma^2_{(0)22}}\right) \tag{12c}$$

Similarly, we determine $A_{(0)44}$, $A_{(0)55}$, and $A_{(0)66}$ as

$$A_{(0)44} = \frac{1}{3}\left(\frac{\bar{\sigma}_{(0)}}{\sigma_{(0)12}}\right)^2 \tag{12d}$$

$$A_{(0)55} = \frac{1}{3}\left(\frac{\bar{\sigma}_{(0)}}{\sigma_{(0)13}}\right)^2 \tag{12e}$$

$$A_{(0)66} = \frac{1}{3}\left(\frac{\bar{\sigma}_{(0)}}{\sigma_{(0)23}}\right)^2 \tag{12f}$$

Let

$$A_{(0)11} = A_{(0)12} + A_{(0)31} = 2 \tag{13a}$$

$$A_{(0)22} = A_{(0)12} + A_{(0)23} = 2\left(\frac{\bar{\sigma}_{(0)}}{\sigma_{(0)22}}\right) \tag{13b}$$

$$A_{(0)33} = A_{(0)23} + A_{(0)31} = 2\left(\frac{\bar{\sigma}_{(0)}}{\sigma_{(0)33}}\right) \tag{13c}$$

These initial parameters do not remain constant as the material undergoes strain-hardening. The subsequent anisotropic parameters should depend on the current state of stress, equivalent stress, and bilinear plastic moduli for various directions. We make use of the fact that plastic work performed in the current stress space and equivalent stress space for a given direction must be equal. For the 1-1 direction,

$$W^{(p)} = \int \sigma_{11} d\gamma_{11}^{(p)} = \int \bar{\sigma} d\bar{\gamma}^{(p)},$$

$$W^{(p)} = \int \sigma_{22} d\gamma_{22}^{(p)} = \int \bar{\sigma} d\bar{\gamma}^{(p)},$$

etc.

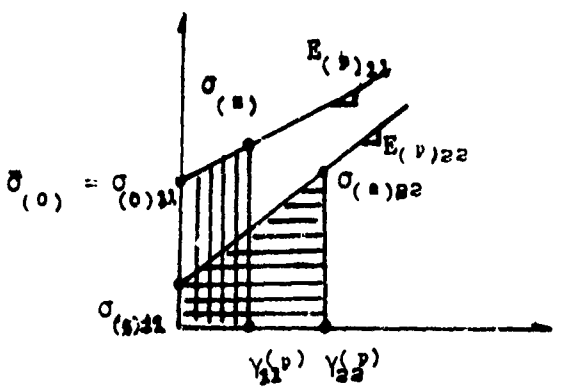

Figure A.2.1: Plastic Work

From the figure above it is easily seen that

$$\frac{\sigma_{(0)11}}{E_{(p)11}}(\sigma_{(a)11} - \sigma_{(0)11}) + \frac{1}{2E_{(p)11}}(\sigma_{(a)11} - \sigma_{(0)11})^2$$

$$= \frac{\sigma_{(0)22}}{E_{(p)22}}(\sigma_{(a)22} - \sigma_{(0)22}) + \frac{1}{2E_{(p)22}}(\sigma_{(a)22} - \sigma_{(0)22})^2$$

or

$$\sigma^2_{(a)22} = \frac{E_{(p)22}}{E_{(p)11}}[\sigma^2_{(a)11} - \sigma^2_{(0)11}] + \sigma^2_{(0)22}$$

Therefore, the subsequent anisotropic parameters are, using $\sigma_{(a)11} = \bar{\sigma}$,

$$A_{11} = 2\left(\frac{\bar{\sigma}}{\sigma_{(a)11}}\right)^2 = 2 \tag{14a}$$

$$A_{22} = 2\left(\frac{\bar{\sigma}}{\sigma_{(a)22}}\right)^2 = \frac{2\bar{\sigma}^2}{\frac{E_{(p)22}}{E_{(p)11}}(\bar{\sigma}^2 - \sigma^2_{(0)11}) + \sigma^2_{(0)22}} \tag{14b}$$

Similarly,

$$A_{33} = \frac{2\bar{\sigma}^2}{\frac{E_{(p)33}}{E_{(p)11}}(\bar{\sigma}^2 - \sigma^2_{(0)11}) + \sigma^2_{(0)33}} \tag{14c}$$

$$A_{44} = \frac{\bar{\sigma}^2}{3\left[\frac{G_{(p)12}}{E_{(p)11}}(\bar{\sigma}^2 - \sigma^2_{(0)11}) + \sigma^2_{(0)12}\right]} \tag{14d}$$

$$A_{55} = \frac{\bar{\sigma}^2}{3\left[\frac{G_{(p)13}}{E_{(p)11}}(\bar{\sigma}^2 - \sigma^2_{(0)11}) + \sigma^2_{(0)13}\right]} \tag{14e}$$

$$A_{66} = \frac{\bar{\sigma}^2}{3\left[\frac{G_{(p)23}}{E_{(p)11}}\left(\bar{\sigma}^2 - \sigma^2_{(0)11}\right) + \sigma^2_{(0)33}\right]} \tag{14f}$$

where $E_{(p)}$ and $G_{(p)}$ are the plastic modulus and plastic shear modulus in bilinear stress-strain curves.

2.2 PLANE STRESS

For the case of a shell subjected to the state of plane stress, the yield function is written in the form,

$$f = \bar{\sigma}^2 = \frac{A_{11}}{2}\sigma_{11}^2 - A_{12}\sigma_{11}\sigma_{22} + \frac{A_{22}}{2}\sigma_{22}^2 + 3A_{44}\sigma_{12}^2 \tag{15}$$

Here we can only provide two tensile tests and one shear test which are not sufficient to determine 4 parameters of anisotropy. To settle this problem the yield stress in the direction of thickness of plate or shell may be assumed to be the same as that of 1-1 or 2-2 direction [11]. This assumption was rejected by Whang [23] who suggested additional tensile test at some angle from the axis of orthotropy. In the present study, the later procedure is followed. If this tensile test is performed at an angle θ from one of the axes of orthotropy, then (15) becomes

$$\bar{\sigma}^2 = \frac{A_{11}}{2}\sigma_0^2\cos^4\theta - A_{12}\sigma_0^2\cos^2\theta\sin^2\theta$$

$$+ \frac{A_{22}}{2}\sin^4\theta + 3A_{44}\sigma_0^2\cos^2\theta\sin^2\theta \tag{16}$$

For convenience the tensile test may be performed at $\theta = 45^\circ$ which

will simplify (16) such that for initial yielding,

$$\bar{\sigma}^{2}_{(o)} = \sigma_{(o)45}{}^{2} \left\{ \frac{A_{(o)11}}{8} - \frac{A_{(o)12}}{4} + \frac{A_{(o)22}}{8} + \frac{3}{4} A_{(o)44} \right\}$$

or

$$A_{(o)12} = \frac{A_{(o)11}}{2} + \frac{A_{(o)22}}{2} + 3A_{(o)44} - 4\left(\frac{\bar{\sigma}_{(o)}}{\sigma_{(o)45}{}^{0}}\right)^{2} \tag{17}$$

where $A_{(o)11}$, $A_{(o)22}$, $A_{(o)44}$ are the same as in the three dimensional case. The subsequent parameter A_{12} for strain-hardening is

$$A_{12} = \frac{A_{11}}{2} + \frac{A_{22}}{2} + 3A_{44} - \frac{4\bar{\sigma}^{2}_{(o)}}{\frac{E_{(o)45}{}^{0}}{E_{(p)11}}\left(\bar{\sigma}^{2} - \sigma^{2}_{(o)11}\right) - \sigma^{2}_{(o)45}{}^{0}} \tag{18}$$

where A_{11}, A_{22}, and A_{44} are the same as in the 3 dimensional case.

2.3 ANISOTROPIC PLASTICITY MATRIX

With all anisotropic parameters defined it is a simple matter to apply the associated flow rule to obtain the anisotropic plasticity matrix in the form

$$\underset{\sim}{\overset{*}{D}} = \frac{-\underset{\sim}{D}\,\underset{\sim}{Z}\,\underset{\sim}{Z}^{T}\,\underset{\sim}{D}}{D_{(p)11} + \underset{\sim}{Z}^{T}\,\underset{\sim}{D}\,\underset{\sim}{Z}} \tag{19}$$

where the components of $\underset{\sim}{Z}$ are given by

$$Z_{\alpha\beta} = \frac{1}{2\bar{\sigma}} \frac{\partial f}{\partial \sigma^{\alpha\beta}}$$

3. ANALYSIS

The linear elastic analysis is first performed to calculate displacements and stresses. If the stress in any element exceeded the limiting yield stresses then the plastic matrix as derived above will be calculated.

For the case of a thin shell integration of plastic stiffness matrix must be performed with each layer integrated one at a time and summed through the thickness. Necessary equations for this process are derived in Appendix A.9.

Details of elastoplastic analysis are also given in Appendix A.9.

APPENDIX A.3

DERIVATION OF INTERNAL (HIDDEN) VARIABLES

Consider the internal variable $q^{(r)}_{ij}$

$$q^{(r)}_{ij}(t) = \int_0^t \exp\left(\frac{-(t-\tau)}{T_{(r)}}\right) \dot{\gamma}_{ij}(\tau)d\tau \qquad (1)$$

where $\dot{\gamma}_{ij}(\tau)$ may be considered to vary linearly within the small time interval Δt,

$$\dot{\gamma}_{ij}(\tau) = \dot{\gamma}_{ij}(t-\Delta t) + \frac{\tau-(t-\Delta t)}{\Delta t}[\dot{\gamma}_{ij}(t) - \dot{\gamma}_{ij}(t-\Delta t)] \qquad (2)$$

Substituting (2) in (1),

$$q^{(r)}_{ij}(t) = \int_0^{t-\Delta t} \exp\left(\frac{-(t-\tau)}{T_{(r)}}\right) \dot{\gamma}_{ij}(\tau)d\tau + \int_{t+\Delta t}^{t} \exp\left(\frac{-(t-\tau)}{T_{(r)}}\right) \dot{\gamma}_{ij}(\tau)d\tau$$

$$= \exp\left(\frac{-\Delta t}{T_{(r)}}\right) q^{(r)}_{ij}(t-\Delta t) + \int_{t-\Delta t}^{t} \exp\left(\frac{-(t-\tau)}{T_{(r)}}\right) \dot{\gamma}_{ij}(\tau)d\tau$$

$$= \exp\left(\frac{-\Delta t}{T_{(r)}}\right) q^{(r)}_{ij}(t-\Delta t) + \int_{t-\Delta t}^{t} \exp\left(\frac{-(t-\tau)}{T_{(r)}}\right)\left[\dot{\gamma}_{ij}(t-\Delta t)\right.$$

$$\left. + \frac{\Delta t-t+\tau}{\Delta t}\left[\dot{\gamma}_{ij}(t) - \dot{\gamma}_{ij}(t-\Delta t)\right]\right]d\tau$$

$$= \exp\left(\frac{-\Delta t}{T_{(r)}}\right)^{(r)}q_{ij}(t-\Delta t) + \int_{t-\Delta t}^{t} \exp\left(\frac{-(t-\tau)}{T_{(r)}}\right)\left\{\left(1-\frac{t}{\Delta t}+\frac{\tau}{\Delta t}\right)\dot{v}_{ij}(t)\right.$$

$$\left. + \left(\frac{t}{\Delta t} - \frac{\tau}{\Delta t}\right)\dot{v}_{ij}(t-\Delta t)\right\} d\tau = \exp\left(\frac{-\Delta t}{T_{(r)}}\right)^{(r)}q_{ij}(t-\Delta t) + T_{(r)}\left\{\left[\exp\left(\frac{-(t-\tau)}{T_{(r)}}\right)\right.\right.$$

$$\left. - \frac{t}{\Delta t}\exp\left(\frac{-(t-\tau)}{T_{(r)}}\right) + \frac{\tau}{\Delta t}\exp\left(\frac{-(t-\tau)}{T_{(r)}}\right) - \frac{T_{(r)}}{\Delta t}\exp\left(\frac{-(t-\tau)}{T_{(r)}}\right)\right]_{t-\Delta t}^{t}\dot{v}_{ij}(t)$$

$$\left. + \left[\frac{t}{\Delta t}\exp\left(\frac{-(t-\tau)}{T_{(r)}}\right) - \frac{\tau}{\Delta t}\exp\left(\frac{-(t-\tau)}{T_{(r)}}\right) + \frac{T_{(r)}}{\Delta t}\exp\left(\frac{-(t-\tau)}{T_{(r)}}\right)\right]_{t-\Delta t}^{t}\dot{v}_{ij}(t-\Delta t)\right\}$$

$$= \exp\left(\frac{-\Delta t}{T_{(r)}}\right)^{(r)}q_{ij}(t-\Delta t) + T_{(r)}\left[\left\{1-\exp\left(\frac{-\Delta t}{T_{(r)}}\right) - \frac{t}{\Delta t}\left[1-\exp\left(\frac{-\Delta t}{T_{(r)}}\right)\right]\right.\right.$$

$$\left. + \frac{t}{\Delta t} - \frac{t-\Delta t}{\Delta t}\exp\left(\frac{-\Delta t}{T_{(r)}}\right) - \frac{T_{(r)}}{\Delta t} + \frac{T_{(r)}}{\Delta t}\exp\left(\frac{-\Delta t}{T_{(r)}}\right)\right\}\dot{v}_{ij}(t)$$

$$+ \left\{\frac{t}{\Delta t}\left[1-\exp\left(\frac{-\Delta t}{T_{(r)}}\right)\right] - \frac{t}{\Delta t} + \frac{t-\Delta t}{\Delta t}\exp\left(\frac{-\Delta t}{T_{(r)}}\right) + \frac{T_{(r)}}{\Delta t}\right.$$

$$\left.\left. - \frac{T_{(r)}}{\Delta t}\exp\left(\frac{-\Delta t}{T_{(r)}}\right)\right\}\dot{v}_{ij}(t-\Delta t)\right] = \exp\left(\frac{-\Delta t}{T_{(r)}}\right)^{(r)}q_{ij}(t-\Delta t)$$

$$+ T_{(r)}\left[\left\{1-\exp\left(\frac{-\Delta t}{T_{(r)}}\right) + \frac{T_{(r)}}{\Delta t}\left\{1-\exp\left(\frac{-\Delta t}{T_{(r)}}\right)\right\}\dot{v}_{ij}(t-\Delta t)\right.\right.$$

$$\left.\left. + \left\{1 - \frac{T_{(r)}}{\Delta t}\left\{1-\exp\left(\frac{\Delta t}{T_{(r)}}\right)\right\}\dot{v}_{ij}(t)\right]\right. = {}^{(r)}A^{(r)}q_{ij}(t-\Delta t)$$

$$+ {}^{(r)}B\,\dot{v}_{ij}(t-\Delta t) + {}^{(r)}C\,\dot{v}_{ij}(t)$$

or

$$q_{ij}^{(r)}(s) = A^{(r)} q_{ij}^{(r)}(s-1) + B^{(r)} \dot{Y}_{ij}(s-1) + C^{(r)} \dot{Y}_{ij}(s)$$

where

$$A^{(r)} = \exp \frac{-\Delta t}{T_{(r)}}$$

$$B^{(r)} = T_{(r)} \left[\phi^{(r)} - A^{(r)} \right]$$

$$C^{(r)} = T_{(r)} \left[1 - \phi^{(r)} \right]$$

$$\phi^{(r)} = \frac{T_{(r)}}{\Delta t} \left(1 - A^{(r)} \right)$$

APPENDIX A. 4

INTERPOLATION FUNCTIONS FOR AXISYMMETRIC THIN SHELL ELEMENT

Let us consider an arbitrary axisymmetric shell as depicted in Figure A.4.1. The nodal circles passing through the nodes normal to the surface are boundaries of each element. The deformation state of each discrete element (Figure A.4.2) is described by four midsurface displacements (Ref. [24]).

(1) meridional translation Θ_1

(2) circumferential translation Θ_2

(3) transverse translation Θ_3

(4) meridional rotation Θ_4

The generalized displacements at nodes p and p + 1 for the element with meridional length ℓ are:

at s = 0	at s = ℓ
$\Theta_{1,p} = u(0)$	$\Theta_{1,p+1} = u(\ell)$
$\Theta_{2,p} = v(0)$	$\Theta_{2,p+1} = v(\ell)$
$\Theta_{3,p} = w(0)$	$\Theta_{3,p+1} = w(\ell)$
$\Theta_{4,p} = (\frac{\partial w}{\partial s} + u\frac{\partial \varphi}{\partial s})_0$	$\Theta_{4,p+1} = (\frac{\partial w}{\partial s} + u\frac{\partial \varphi}{\partial s})_\ell$

where φ is the angle between the z axis and the line tangent to the meridional surface, s is an arbitrary distance from the node p along the meridian.

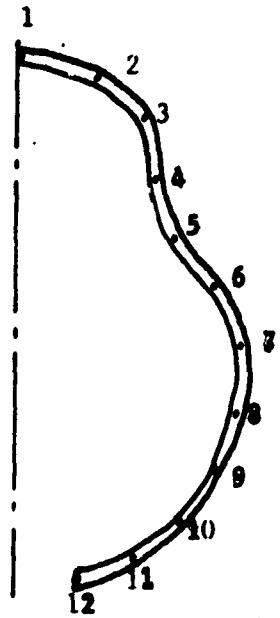

Figure A.4.1: Discretized Arbitrary Axisymmetric Shell

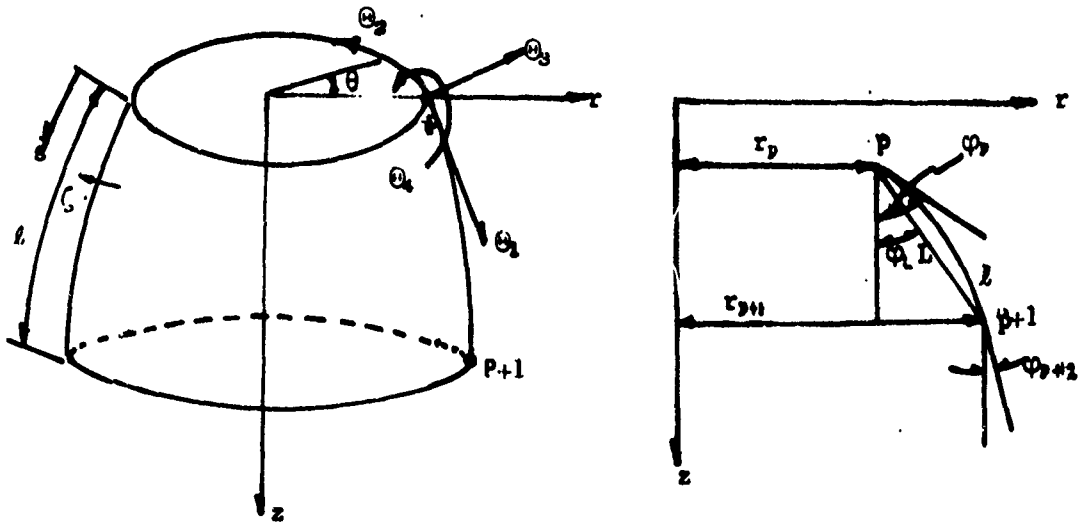

Figure A.4.2: Generalized Coordinates and Geometry of a Curved Shell Element

The midsurface meridional slope φ is assumed to vary as

$$\varphi(s) = a_0 + a_1 s + a_2 s^2$$

Assuming that the curved shell element may be approximated as a segment of a circle, the coefficients a_0, a_1, and a_2 are determined as

$$a_0 = \varphi_p$$

$$a_1 = \frac{1}{\ell}(6\varphi_L - 4\varphi_p - 2\varphi_{p+1})$$

$$a_2 = \frac{1}{\ell^2}(3\varphi_L + 3\varphi_p - 6\varphi_L)$$

The midsurface radius r(s) is given by

$$r(s) = r_p + \int_0^s \sin \varphi ds$$

The shell thickness h(s) is assumed to vary linearly so that

$$h(s) = h_p - \frac{s}{\ell}(h_p - h_{p+1})$$

The meridional variation of midsurface displacements, u, v, and w may be assumed to be of the form

$$\Theta_1(s) = u(s) = C_1 + C_2 s \tag{1a}$$

$$\Theta_2(s) = v(s) = C_3 + C_4 s \tag{1b}$$

$$\Theta_3(s) = w(s) = C_5 + C_6 s + C_7 s^2 + C_8 s^3 \tag{1c}$$

The meridional rotation is, then,

$$\Theta_4(s) = \frac{\partial w(s)}{\partial s} + u \frac{\partial \varphi(s)}{\partial s} = C_6 + 2C_7 s + 3C_8 s^2 + (C_1 + C_2 s)\varphi' \tag{1d}$$

Writing these four equations at p(s=0) and p+1(s=ℓ) we obtain 8 equations from which we can solve for the 8 constants, C_1 through C_8. Substituting these constants into (1a) through (1d) we have

$$\Theta_i = S_{iR} Q_{RN} \Theta^N \tag{2}$$

or

$$\Theta_i = \Psi_{iN} \Theta^N \tag{3}$$

In matrix form,

$$\underset{\sim}{\Theta} = \underset{\sim}{S}\,\underset{\sim}{Q}\,\underset{\sim}{\Theta} = \underset{\sim}{\Psi}\,\underset{\sim}{\Theta} \tag{4}$$

where

$$\underset{(4 \times 8)}{\underset{\sim}{\Psi}} = \underset{(4 \times 8)}{\underset{\sim}{S}} \; \underset{(8 \times 8)}{\underset{\sim}{Q}} \qquad (5)$$

$$\underset{\sim}{S} = \begin{bmatrix} 1 & s & & & & & & \\ & & 1 & s & & & & \\ & & & & 1 & s & s^2 & s^3 \\ & & & & & 1 & 2s & 3s^2 \end{bmatrix}$$

$$\underset{\sim}{Q} = \begin{bmatrix} 1 & 0 & 0 & 0 & 0 & 0 & 0 & 0 \\ -\frac{1}{\ell} & 0 & 0 & 0 & \frac{1}{\ell} & 0 & 0 & 0 \\ 0 & 1 & 0 & 0 & 0 & 0 & 0 & 0 \\ 0 & -\frac{1}{\ell} & 0 & 0 & 0 & \frac{1}{\ell} & 0 & 0 \\ 0 & 0 & 1 & 0 & 0 & 0 & 0 & 0 \\ -\varphi_0' & 0 & 0 & 1 & 0 & 0 & 0 & 0 \\ \frac{2\varphi_0'}{\ell} & 0 & \frac{-3}{\ell^2} & \frac{-2}{\ell} & \frac{\varphi\ell}{\ell} & 0 & \frac{3}{\ell} & \frac{-1}{\ell} \\ \frac{-\varphi_0'}{\ell^2} & 0 & \frac{2}{\ell^3} & \frac{1}{\ell^2} & \frac{\varphi\ell}{\ell^3} & 0 & \frac{-2}{\ell^3} & \frac{1}{\ell^3} \end{bmatrix}$$

$$\psi_{11} = \psi_{22} = 1 - \frac{s}{\ell}\,, \quad \psi_{15} = \psi_{26} = \frac{s}{\ell}$$

$$\psi_{31} = -s\varphi_0' + \frac{2\varphi_0' s^2}{\ell} - \frac{s^3\varphi_0'}{\ell}\,, \quad \psi_{33} = 1 - \frac{3s^2}{\ell^2} + \frac{2s^3}{\ell^3}\,, \quad \psi_{34} = s - \frac{2s^2}{\ell} + \frac{s^3}{\ell^2}$$

$$\psi_{35} = \frac{\varphi_0' s^2}{\ell} + \frac{\varphi_0' s^3}{\ell^2}\,, \quad \psi_{37} = \frac{3s^2}{\ell} - \frac{2s^3}{\ell^2}\,, \quad \psi_{38} = \frac{-s^2}{\ell} + \frac{s^3}{\ell^2}\,,$$

$$\psi_{41} = -\varphi_0' + \frac{4s\varphi_0'}{\ell} - \frac{3s^2\varphi_0'}{\ell^2}\,, \quad \psi_{43} = -\frac{6s}{\ell^2} + \frac{6s^2}{\ell^3}\,, \quad \psi_{44} = 1 - \frac{4s}{\ell} + \frac{3s^2}{\ell^2}$$

$$\psi_{45} = \frac{2\varphi_0' s}{\ell} + \frac{3\varphi_0' s^2}{\ell^2}\,, \quad \psi_{47} = \frac{6s}{\ell} - \frac{6s^2}{\ell^2}\,, \quad \psi_{48} = \frac{-2s}{\ell} + \frac{3s^2}{\ell^2}$$

all other $\psi_{iN} = 0$, $\varphi_0' = \left(\frac{\partial \varphi}{\partial s}\right)_0$, etc.

Thus, the strain-displacement relation may be written in the form,

$$\gamma_{\alpha\beta} = e_{\alpha\beta} + \zeta\, \chi_{\alpha\beta}$$

The engineering strain vector in matrix form considering only linear terms can be obtained by substituting the interpolation functions into the strain-displacement relations,

$$\gamma_i = e_i + \zeta x_i$$

$$\gamma_1 = \frac{\partial}{\partial s}(C_1 + C_2 s) - (C_5 + C_6 s + C_7 s^2 + C_8 s^3)\frac{\partial \varphi(s)}{\partial s}$$

$$+ \zeta\{ \frac{\partial^2}{\partial s^2}(C_5 + C_6 s + C_7 s^2 + C_8 s^3)$$

$$+ (C_1 + C_2 s)\frac{\partial^2 \varphi(s)}{\partial s^2} + \frac{\partial}{\partial s}(C_1 + C_2 s)\frac{\partial \varphi(s)}{\partial s} \}$$

Writing similarly for γ_2 and γ_{12}, performing differentiation, and substituting values of constants, we obtain

$$\underset{\sim}{\gamma} = \underset{\sim}{e} + \zeta \underset{\sim}{x} = \underset{\sim}{G}\,\underset{\sim}{W}\,\underset{\sim}{Q}\,\underset{\sim}{\Theta} + \underset{\sim}{Z}\,\underset{\sim}{W}\,\underset{\sim}{Q}\,\underset{\sim}{\Theta} \tag{6}$$

$$\underset{\sim}{e} = \underset{\sim}{G}\,\underset{\sim}{W}\,\underset{\sim}{Q}\,\underset{\sim}{\Theta}$$

$$\zeta \underset{\sim}{x} = \underset{\sim}{Z}\,\underset{\sim}{W}\,\underset{\sim}{Q}\,\underset{\sim}{\Theta}$$

where

$$\underset{\sim}{G} = \begin{bmatrix} 1 & 0 & 0 & 0 & 0 & 0 \\ 0 & 1 & 0 & 0 & 0 & 0 \\ 0 & 0 & 1 & 0 & 0 & 0 \end{bmatrix}$$

$$\underset{\sim}{Z} = \begin{bmatrix} 0 & 0 & 0 & \zeta & 0 & 0 \\ 0 & 0 & 0 & 0 & \zeta & 0 \\ 0 & 0 & 0 & 0 & 0 & \zeta \end{bmatrix}$$

The explicit form of $\underset{\sim}{W}$ will be shown in Appendix A.6.

APPENDIX A.5

TRANSFORMED ELASTICITY AND PLASTICITY MATRICES OF FIBER-REINFORCED AXISYMMETRIC SHELL

1. GENERAL

Two types of element, plane stress element of axisymmetric thin shell and isoparametric element of axisymmetric thick shell will be discussed. Shear stresses in the plane of meridional and tangential directions are included in the axisymmetric plane stress shell element whereas shear stresses in the plane of axial and radial directions are incorporated in the isoparametric solid element. Coordinate transformations between the local and global systems differ depending on the choice of either plane stress element to be used for a thin shell or isoparametric element for a thick shell. Since the global coordinates for the thick shell consist of axial and radial directions additional transformation for an inclined element is required.

2. PLANE STRESS ELEMENT

It can be shown that the transformation between the local and global components of strain for a thin shell is related by

$$\begin{bmatrix} \gamma_T \\ \gamma_{TL} \\ \gamma_L \end{bmatrix} = \begin{bmatrix} \cos^2\alpha & \cos\alpha \sin\alpha & \sin^2\alpha \\ -2\sin\alpha\cos\alpha & \cos^2\alpha-\sin^2\alpha & 2\sin\alpha\cos\alpha \\ -\sin^2\alpha & -\cos\alpha \sin\alpha & \cos^2\alpha \end{bmatrix} \begin{bmatrix} \gamma_s \\ \gamma_{s\theta} \\ \gamma_\theta \end{bmatrix} \quad (1)$$

The above notations are shown in Figure A.5.1. In matrix form (1) may be written,

$$\underset{\sim}{\gamma}^{(L)} = \underset{\sim}{T}\,\underset{\sim}{\gamma}^{(G)} \qquad (2)$$

where (L) and (G) refer to "local" and "global", respectively. It is a simple matter to show that the global elasticity matrix is in the form,

$$\underset{\sim}{D}^{(G)} = \underset{\sim}{T}^{T}\,\underset{\sim}{D}^{(L)}\,\underset{\sim}{T} \qquad (3)$$

in which $D^{(L)} = D_{(e)}^{(L)} + D_{(p)}^{(L)}$ with (e) and (p) denoting "elastic" and "plastic". The components of $\underset{\sim}{D}^{(G)}$ are

$$D_{11}^{(G)} = c^2(c^2D_{11} + s^2D_{12}) + 4s^2c^2G + s^2(c^2D_{12} + s^2D_{22})$$

$$D_{12}^{(G)} = sc(c^2D_{11} + s^2D_{12}) + (c^2-s^2)(-2scG) - cs(c^2D_{12} + s^2D_{22})$$

$$D_{13}^{(G)} = s^2(c^2D_{11} + s^2D_{12}) - 4s^2c^2G + c^2(c^2D_{12} + s^2D_{22})$$

$$D_{21}^{(G)} = c^3s(D_{11}-D_{12}) + (c^2-s^2)G(-2sc) + cs^3(D_{12}-D_{22})$$

$$D_{22}^{(G)} = c^2s^2(D_{11}-D_{12}) + (c^2-s^2)G - c^2s^2(D_{12}-D_{22})$$

$$D_{23}^{(G)} = cs^3(D_{11}-D_{12}) + 2sc(c^2-s^2)G + c^3s(D_{12}-D_{22})$$

$$D_{31}^{(G)} = c^2(s^2D_{11} + c^2D_{12}) - 4s^2c^2G + s^2(s^2D_{12} + c^2D_{22})$$

$$D_{32}^{(G)} = sc(s^2D_{11} + c^2D_{12}) + 2scG(c^2-s^2) - sc(s^2D_{12} + c^2D_{22})$$

$$D_{33}^{(G)} = s^2(s^2D_{11} + c^2D_{12}) + 4s^2c^2G + c^2(s^2D_{12} + c^2D_{22})$$

where $c = \cos\alpha$ and $s = \sin\alpha$. For axisymmetric deformations we

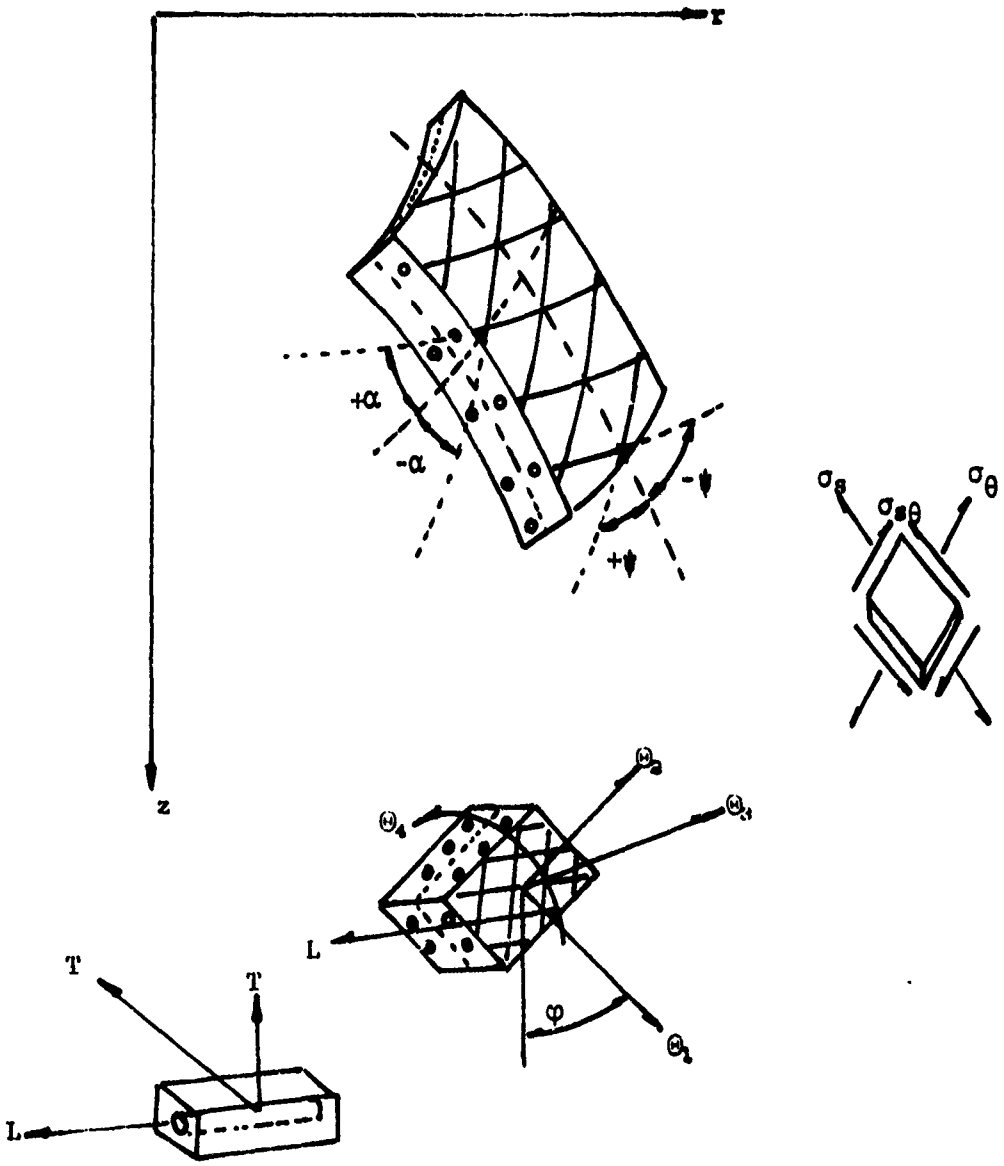

Θ_1 = Meridional displacement

Θ_2 : Tangential displacement

Θ_3 · Transverse displacement

Θ_4 Meridional rotation

Figure A.5.1: Fiber-Reinforced Axisymmetric Thin Shell

require that stresses carried by α fibers $\sigma^{\alpha\beta}_{(\alpha)}$ be the same as stresses carried $-\alpha$ fibers $\sigma^{\alpha\beta}_{(-\alpha)}$. This is satisfied by imposing the average stress to assume the form

$$\sigma^{\alpha\beta} = \frac{1}{2}(\sigma^{\alpha\beta}_{(\alpha)} + \sigma^{\alpha\beta}_{(-\alpha)})$$

However, the strain in each ply is equal to the imposed strain. This causes $D^{(a)}_{13} = D^{(a)}_{31} = D^{(a)}_{23} = D^{(a)}_{32} = 0$ and we obtain the following form of $\underset{\sim}{D}^{(a)}$.

$$\underset{\sim}{D}^{(a)} = \begin{bmatrix} D^{(a)}_{11} & 0 & D^{(a)}_{13} \\ 0 & D^{(a)}_{22} & 0 \\ D^{(a)}_{13} & 0 & D^{(a)}_{33} \end{bmatrix} \tag{4}$$

which is the globally transformed fiber reinforced elastoplasticity matrix. If the plasticity matrix is used as pseudo load the above operations are performed separately without adding together.

3. PLANE STRAIN ELEMENT

Referring to Fig.A.5.2 the coordinate transformation of the elasticity and plasticity matrix for a plane strain axisymmetric solid element for a thick shell without bending may be accomplished in the same manner as in the plane stress case if such transformation is limited to a plane(vertical cylinder). The global elastoplasticity matrix can also be given equivalently by

$$\underset{4\times4}{D}^{(a)} = \underset{4\times6}{T}^{T}\ \underset{6\times6}{D}^{(L)}\ \underset{6\times4}{T} \tag{5}$$

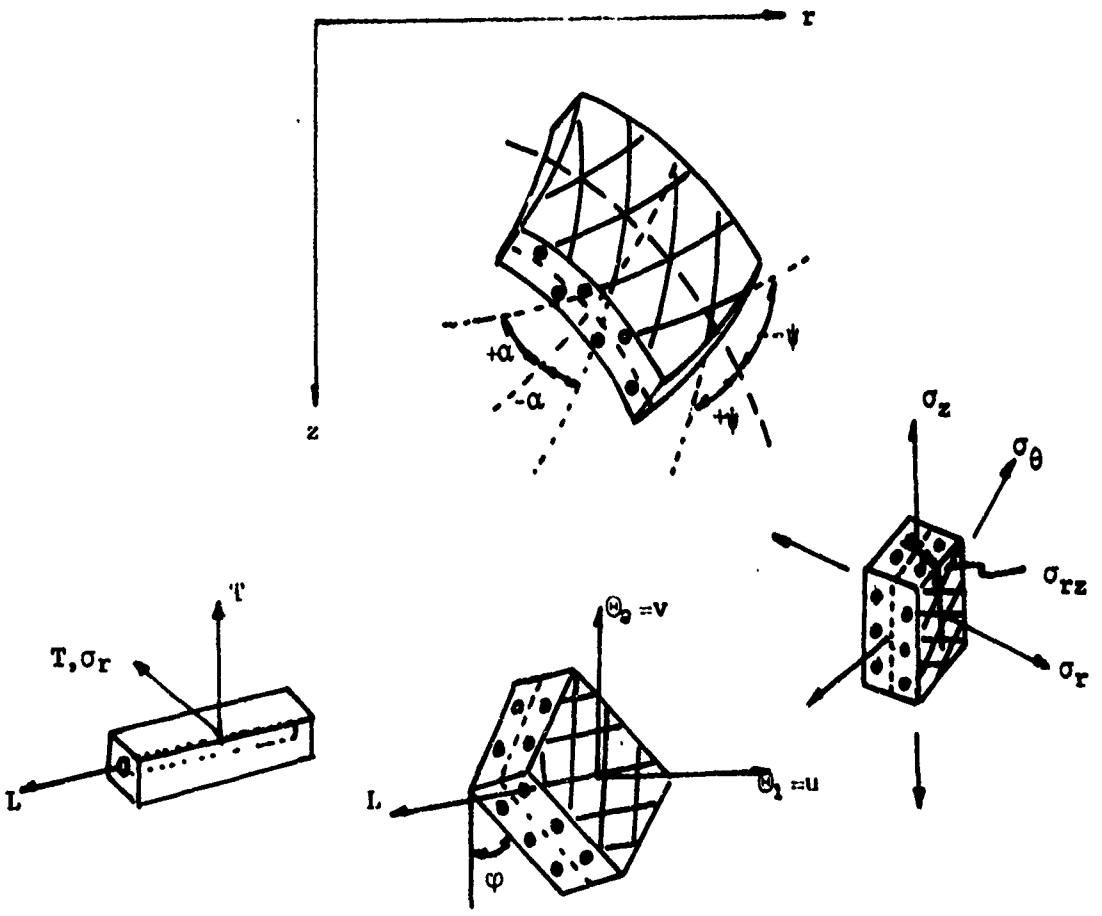

Θ_1 = u = radial displacement

Θ_2 = v = axial displacement

Figure A.5.2: Fiber-Reinforced Axisymmetric Thick Shell

in which $\underset{\sim}{D}^{(L)}$ is the sum of regular 3-dimensional elasticity and plasticity matrices and $\underset{\sim}{T}$ is related by

$$\begin{bmatrix} \gamma_r \\ \gamma_T \\ \gamma_L \\ \gamma_{rT} \\ \gamma_{rL} \\ \gamma_{TL} \end{bmatrix} = \begin{bmatrix} 1 & 0 & 0 & 0 \\ 0 & c^2 & s^2 & 0 \\ 0 & s^2 & c^2 & 0 \\ 0 & 0 & 0 & c \\ 0 & 0 & 0 & -s \\ 0 & -2cs & 2cs & 0 \end{bmatrix} \begin{bmatrix} \gamma_r \\ \gamma_z \\ \gamma_\theta \\ \gamma_{rz} \end{bmatrix}$$

where $c = \cos\alpha \quad s = \sin\alpha$

or
$$\underset{\sim}{\gamma}^{(G)} = \underset{\sim}{T}\,\underset{\sim}{\gamma}^{(L)} \tag{6}$$

If the element is inclined an angle of φ from the z axis (Fig.A.5.3), then $\underset{\sim}{T}$ must be modified as follows:

$$\begin{bmatrix} \xi^1 \\ \xi^2 \\ \xi^3 \end{bmatrix} = \begin{bmatrix} 1 & 0 & 0 \\ 0 & s & c \\ 0 & c & -s \end{bmatrix} \begin{bmatrix} \bar{c} & 0 & -\bar{s} \\ 0 & 1 & 0 \\ \bar{s} & 0 & \bar{c} \end{bmatrix} \begin{bmatrix} \eta^1 \\ \eta^2 \\ \eta^3 \end{bmatrix}$$

or

$$\underset{\sim}{\xi} = \underset{\sim}{R}\,\underset{\sim}{\eta}$$

where

$$\underset{\sim}{R} = \begin{bmatrix} \bar{c} & 0 & -\bar{s} \\ c\bar{s} & s & \bar{c}c \\ -s\bar{s} & c & -s\bar{c} \end{bmatrix}$$

and

$$\bar{c} = \cos\varphi \ , \qquad \bar{s} = \sin\varphi$$

$$\eta^1 = r \ , \quad \eta^2 = \theta \ , \quad \eta^3 = z$$

as defined in Figure A.5.2.

The modified $\bar{\underline{T}}$ then assumes the form,

$$\bar{\underline{T}} = \begin{bmatrix} \bar{c}^2 & \bar{s}^2 & 0 & -\bar{c}\bar{s} \\ c^2\bar{s}^2 & \bar{c}^2c^2 & s^2 & c^2\bar{s}\bar{c} \\ s^2\bar{s}^2 & s^2\bar{c}^2 & c^2 & s^2\bar{s}\bar{c} \\ 2\bar{c}\bar{s}c & -2\bar{s}c\bar{c} & 0 & \bar{c}^2c-\bar{s}^2c \\ -2\bar{c}cs\bar{s} & 2s\bar{s}\bar{c} & 0 & -\bar{c}^2s+\bar{s}^2s \\ -2c\bar{s}^2s & -2\bar{c}^2cs & 2sc & -2c\bar{c}cs\bar{s} \end{bmatrix}$$

Here $\bar{\underline{T}}$ replaces $\underline{T}$ in (5) for inclined element.

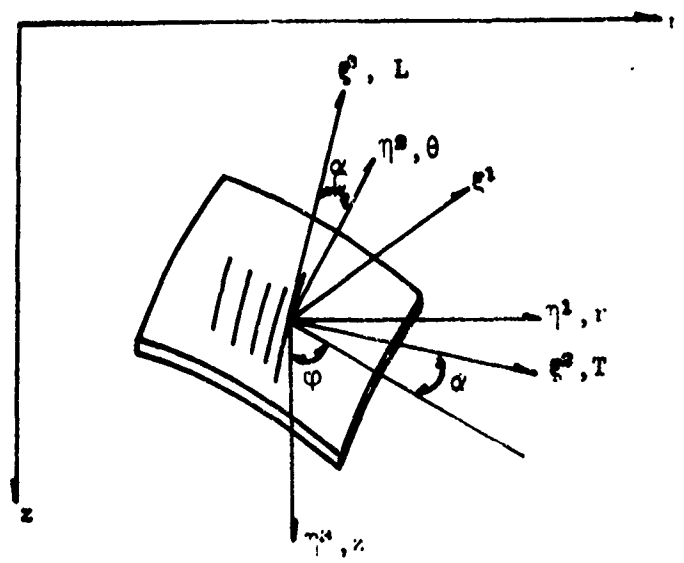

Figure A.5.3: Coordinate Transformation for Inclined Element

APPENDIX A.6

STIFFNESS MATRIX (SYMMETRIC AND ASYMMETRIC LOADING)

Since the stiffness matrix for symmetrical loading is obtained as a special case of that for asymmetric loading we discuss here the Fourier harmonically-coupled stiffness matrix. The circumferential variation of the displacements at any meridional station, s, may be expressed as

$$u(s,\theta) = u^{(o)}(s) + \sum_{j=1}^{\infty} u^{(j)}(s) \cos j\theta + \sum_{j=1}^{\infty} \bar{u}^{(j)}(s) \sin j\theta$$

$$v(s,\theta) = v^{(o)}(s) + \sum_{j=1}^{\infty} v^{(j)}(s) \sin j\theta + \sum_{j=1}^{\infty} \bar{v}^{(j)}(s) \cos j\theta \qquad (1)$$

$$w(s,\theta) = w^{(o)}(s) + \sum_{j=1}^{\infty} w^{(j)}(s) \cos j\theta + \sum_{j=1}^{\infty} \bar{w}^{(j)}(s) \sin j\theta$$

where the unbarred and barred coefficients are defined as the "A" series and "B" series, respectively. Note also that the circumferential displacement, v, varies as an odd function, and, therefore, this coefficient is associated with sin jθ (odd function) in "A" series. The "A" series harmonic number j takes on the positive sign whereas the "B" series harmonic number j takes on the negative sign.

Similarly, we may write all the midsurface strain components in the form of Fourier series as follows:

$$(e_s)_o = (e_s)_o^{(o)} + \sum_{j=1}^{\infty} (e_s)_o^{(j)} \cos j\theta + \sum_{j=1}^{\infty} (\bar{e}_s)_o^{(j)} \sin j\theta$$

$$(e_{s\theta})_o = (e_{s\theta})_o^{(o)} + \sum_{j=1}^{\infty} (e_{s\theta})_o^{(j)} \sin j\theta + \sum_{j=1}^{\infty} (\bar{e}_{s\theta})_o^{(j)} \cos j\theta \quad (2a)$$

$$(e_\theta)_o = (e_\theta)_o^{(o)} + \sum_{j=1}^{\infty} (e_\theta)_o^{(j)} \cos j\theta + \sum_{j=1}^{\infty} (\bar{e}_\theta)_o^{(j)} \sin j\theta$$

Bending Strains are

$$\chi_s = \chi_s^{(o)} + \sum_{j=1}^{\infty} \chi_s^{(j)} \cos j\theta + \sum_{j=1}^{\infty} \bar{\chi}_s^{(j)} \sin j\theta$$

$$\chi_{s\theta} = \chi_{s\theta}^{(o)} + \sum_{j=1}^{\infty} \chi_{s\theta}^{(j)} \sin j\theta + \sum_{j=1}^{\infty} \bar{\chi}_{s\theta}^{(j)} \cos j\theta \quad (2b)$$

$$\chi_\theta = \chi_\theta^{(o)} + \sum_{j=1}^{\infty} \chi_\theta^{(j)} \cos j\theta + \sum_{j=1}^{\infty} \bar{\chi}_\theta^{(j)} \sin j\theta$$

Substituting "A" series of (1) in (16) of Appendix A.1 and setting these results equal to the "A" series of (2), we obtain, considering only linear terms, the following relationships:

For the meridional strain,

$$(e_s)_o = \frac{\partial}{\partial s} \sum_{j=1}^{\infty} u_{(s)}^{(j)} \cos j\theta - \sum_{j=1}^{\infty} w_{(s)}^{(j)} \cos j\theta \quad \frac{\partial w}{\partial s} =$$

$$= \frac{\partial u^{(j)}}{\partial s} - w^{(j)} \frac{\partial w}{\partial s} \sum_{j=1}^{\infty} \cos j\theta \quad (3a)$$

From (2a), $$(e_s)_o = \sum_{j}^{\infty} (e_s)_o^{(j)} \cos j\theta \qquad (3b)$$

From Eqs. (3a) and (3b),

$$(e_s)_o^{(j)} = \frac{\partial u}{\partial s}^{(j)} - w^{(j)} \frac{\partial \varphi}{\partial s} \qquad (3c)$$

Similarly for the shear strain,

$$(e_{s\theta})_o = \frac{1}{r}\left[r \frac{\partial}{\partial s}\left(\sum_{j=1}^{\infty} v^{(j)} \sin j\theta\right) - \sum_{j=1}^{\infty} v^{(j)} \sin j\theta \sin\varphi\right.$$

$$\left. + \frac{\partial}{\partial \theta}\left(\sum_{j=1}^{\infty} u^{(j)} \cos j\theta\right)\right]$$

$$= \left(\frac{\partial v}{\partial s}^{(j)} - \frac{v}{r}^{(j)} \sin\varphi - j\frac{u}{r}^{(j)}\right) \sum_{j=1}^{\infty} \sin j\theta \qquad (4a)$$

$$(e_{s\theta})_o = \sum_{j=1}^{\infty} (e_{s\theta})_o^{(j)} \sin j\theta \qquad (4b)$$

$$(e_{s\theta})_o^{(j)} = \frac{\partial v}{\partial s}^{(j)} - \frac{v}{r}^{(j)} \sin\varphi - j\frac{u}{r}^{(j)} \qquad (4c)$$

Omitting the first two steps for the rest of the strain expressions,

$$(e_\theta)_o^{(j)} = j\frac{v}{r}^{(j)} + \frac{u}{r}^{(j)} \sin\varphi + \frac{w}{r}^{(j)} \cos\varphi \qquad (5)$$

$$\chi_s^{(j)} = \frac{\partial^2 w}{\partial s^2}^{(j)} + u^{(j)} \frac{\partial^2 \varphi}{\partial s^2} + \frac{\partial u}{\partial s}^{(j)} \frac{\partial \varphi}{\partial s} \qquad (6)$$

$$\chi_{s\theta}^{(j)} = \frac{2}{r}\left[j\frac{\partial w}{\partial s}^{(j)} - \frac{j}{r}\sin\varphi\, w^{(j)} + \cos\varphi\frac{\partial v}{\partial s}^{(j)}\right.$$

$$\left. - \frac{1}{r}\sin\varphi\cos\varphi\, v^{(j)} + j\frac{\partial\varphi}{\partial s}u^{(j)}\right] \qquad (7)$$

$$\chi_{\theta}^{(j)} = \frac{1}{r}\left[\frac{j^2}{r}w^{(j)} + \frac{j}{r}\cos\varphi\, v^{(j)} - \frac{\partial w}{\partial s}^{(j)} + u^{(j)}\frac{\partial\varphi}{\partial s}\sin\varphi\right] \qquad (8)$$

For dome-ended shells of revolution (r = 0), the strain components are obtained by taking the limit of the above equations as r approaches zero.

$$(e_s)_{\substack{o\\r=0}}^{(j)} = \lim_{r\to 0}(e_s)_o^{(j)} = (e_s)_o^{(j)} = \frac{\partial u}{\partial s}^{(j)} - w^{(j)}\frac{\partial\varphi}{\partial s} \qquad (9)$$

$$(e_{s\theta})_o^{(j)} = \lim_{r\to 0}(e_{s\theta})_o = \lim_{r\to 0}\frac{\frac{\partial}{\partial s}\left(r\frac{\partial v}{\partial s}^{(j)} - v^{(j)}\sin\varphi - ju^{(j)}\right)}{\frac{\partial r}{\partial s}}$$

$$= \lim_{r\to 0}\frac{\frac{\partial r}{\partial s}\frac{\partial v}{\partial s}^{(j)} + r\frac{\partial^2 v}{\partial s^2}^{(j)} - \frac{\partial v}{\partial s}^{(j)}\sin\varphi - j\frac{\partial u}{\partial s}^{(j)}}{\frac{\partial r}{\partial s}} = -j\frac{\partial u}{\partial s}^{(j)} \qquad (10)$$

Note that, at r = 0, we have

$$\sin\varphi = \frac{\partial r}{\partial s} = 1$$

$$(e_\theta)_{\substack{o\\r=0}}^{(j)} = \lim_{r\to 0}(e_\theta)_o^{(j)} = \lim_{r\to 0}\frac{\frac{\partial}{\partial s}\left[j\, v^{(j)} + u^{(j)}\sin\varphi + w^{(j)}\cos\varphi\right]}{\frac{\partial r}{\partial s}}$$

$$= \lim_{r\to 0}\left[j\frac{\partial v}{\partial s}^{(j)} + \frac{\partial u}{\partial s}^{(j)}\sin\varphi + \frac{\partial w}{\partial s}\cos\varphi + w\frac{\partial}{\partial s}\left(-r\frac{\partial\varphi}{\partial s}\right)\right]$$

$$= j\frac{\partial v}{\partial s}^{(j)} + \frac{\partial u}{\partial s}^{(j)} - w^{(j)}\frac{\partial \varphi}{\partial s^2} \tag{11}$$

$$\chi_s^{(j)} = \lim_{r\to 0} \chi_s^{(j)} = -\left(\frac{\partial^2 w}{\partial s^2}^{(j)} + u^{(j)}\frac{\partial^2 \varphi}{\partial s^2}\right) \tag{12}$$

$$\chi_{s\theta}^{(j)} = \lim_{r\to 0} \chi_{s\theta}^{(j)} = \lim_{r\to 0} \frac{2\frac{\partial^2}{\partial s^2}\left[jr\frac{\partial w}{\partial s}^{(j)} - \sin\varphi\, w^{(j)} + r\cos\varphi\frac{\partial v}{\partial s}^{(j)} - \sin\varphi\cos\varphi\, v^{(j)} + jr\frac{\partial \varphi}{\partial s}u^{(j)}\right]}{\frac{\partial^2 r^2}{\partial s^2}}$$

$$= j\left(\frac{\partial^2 w}{\partial s^2}^{(j)} + u^{(j)}\frac{\partial^2 \varphi}{\partial s^2}\right) \tag{13}$$

Note that the first derivative leaves the expression still singular for $r = 0$ and, therefore, the second derivative is required:

$$\chi_{s\theta}^{(j)} = \lim_{r\to 0} \chi_{\theta}^{(j)} = \lim_{r\to 0} \frac{\frac{\partial^2}{\partial s^2}\left[j^2 w^{(j)} + j\cos\varphi\, v^{(j)} - \left(r\frac{\partial w}{\partial s}^{(j)} + ru^{(j)}\frac{\partial \varphi}{\partial s}\right)\sin\varphi\right.}{}$$

$$= \frac{j^2}{2}\frac{\partial^2 w}{\partial s^2}^{(j)} - j\frac{\partial \varphi}{\partial s}\frac{\partial v}{\partial s}^{(j)} - \frac{\partial^2 w}{\partial s^2}^{(j)} - u^{(j)}\frac{\partial^2 \varphi}{\partial s^2} \tag{14}$$

Similarly, for the "B" series part, corresponding pole strain displacement relations are obtained by replacing unbarred quantities by barred quantities and j by $-j$.

Now, introducing the displacement functions of Appendix A.4 into these harmonically coupled strain expressions, it is a simple matter to obtain $\underline{W}$ in (6) of Appendix A.5 or in the expression,

$$\underline{Y}^{(j)} = \underline{G}\,\underline{W}^{(j)}\,\underline{Q}\,\underline{\Theta} + \underline{Z}\,\underline{W}^{(j)}\,\underline{Q}\,\underline{\Theta} \tag{15a}$$

$$\underset{\sim}{W} = \begin{bmatrix} 0 & 1 & 0 & 0 & -\varphi' & -\varphi s' & -\varphi s' & -\varphi' s^3 \\ -\frac{j}{r} & -\frac{js}{r} & -\frac{n}{r} & 1-\frac{ns}{r} & 0 & 0 & 0 & 0 \\ \frac{n}{r} & \frac{ns}{r} & \frac{j}{r} & \frac{js}{r} & \frac{m}{r} & \frac{ms}{r} & \frac{ms^2}{r} & \frac{ms^3}{r} \\ -\varphi'' & -(\varphi'+\varphi'' s) & 0 & 0 & 0 & 0 & -2 & 6s \\ \frac{2\varphi' j}{r} & \frac{2\varphi' js}{r} & -\frac{2mn}{r^2} & \frac{2m}{r}(1-\frac{ns}{r}) & -\frac{2jm}{r^2} & \frac{2j}{r}(1-\frac{ns}{r}) & \frac{2js}{r}(2-\frac{ns}{r}) & \frac{2js^2}{r}(3-\frac{ns}{r}) \\ -\frac{n\varphi'}{r} & -\frac{n\varphi' s}{r} & \frac{mj}{-r^2} & \frac{mjs}{r^2} & \frac{j^2}{r^2} & \frac{j^2 s}{r^2}-\frac{n}{r} & \frac{j^2 s^2}{r^2}-\frac{2ns}{r} & \frac{j^2 s^3}{r^2}-\frac{3ns^2}{r} \end{bmatrix}$$

in which $m = \cos\varphi$ and $n = \sin\varphi$.

For axisymmetric loading all terms containing j in $\underset{\sim}{W}$ are zero and

$$\underset{\sim}{Y} = \underset{\sim}{G}\,\underset{\sim}{W}\,\underset{\sim}{Q}\,\underset{\sim}{\Theta} + \underset{\sim}{Z}\,\underset{\sim}{W}\,\underset{\sim}{Q}\,\underset{\sim}{\Theta} \tag{15b}$$

Comparing this with (2.40) in Section 1 we note that

$$A_{N_{\alpha\beta}} = \underset{\sim}{G}\,\underset{\sim}{W}\,\underset{\sim}{Q} \tag{16a}$$

$$CB_{N_{\alpha\beta}} = \underset{\sim}{Z}\,\underset{\sim}{W}\,\underset{\sim}{Q} \tag{16b}$$

Note that $C_{NN_{\alpha\beta}}$ in the nonlinear membrane strain term can be determined similarly.

With (15) and (16) substituted in (2.40 a,b) of Section 1 and all stress components of $\sigma^{\alpha\beta}$ expanded in Fourier series the linear elastic

stiffness matrix of the form (2.45) of Section 1 can be derived explicitly,

$$K^{(j)} = h\int_0^{\ell}\int_0^{2\pi} \underset{\sim}{Q}^T W^{(j)T} \underset{\sim}{a}^T \underset{\sim}{D}\, \underset{\sim}{a}^T W^{(j)} \underset{\sim}{Q}\, r d\theta ds + \frac{h^3}{12}\int_0^{\ell}\int_0^{2\pi} \underset{\sim}{Q}^T \underset{\sim}{W}^{(j)T} \underset{\sim}{b}^T \underset{\sim}{D}\, \underset{\sim}{b}^T \underset{\sim}{W}^{(j)} \underset{\sim}{Q}\, r d\theta ds \qquad (17)$$

where

$$\underset{\sim}{a} = \begin{bmatrix} 1 & 0 & 0 & 0 & 0 & 0 \\ 0 & 1 & 0 & 0 & 0 & 0 \\ 0 & 0 & 1 & 0 & 0 & 0 \end{bmatrix}$$

$$\underset{\sim}{b} = \begin{bmatrix} 0 & 0 & 0 & 1 & 0 & 0 \\ 0 & 0 & 0 & 0 & 1 & 0 \\ 0 & 0 & 0 & 0 & 0 & 1 \end{bmatrix}$$

$$\underset{\sim}{D} = \frac{1}{1-\nu_{s\theta}\nu_{\theta s}} \begin{bmatrix} E_s & 0 & E_s\nu_{\theta s} \\ 0 & G & 0 \\ E_s\nu_{\theta s} & 0 & E_\theta \end{bmatrix}$$

Here integration along the meridional coordinates can be performed using Simpson's rule.

APPENDIX A.7

EQUIVALENT NODAL LOAD VECTORS

We consider arbitrary asymmetric distributed loads of $p_1(s,\theta)$, $p_2(s,\theta)$, and $p_3(s,\theta)$ acting on the midsurface of the discrete element in directions s, θ and ζ, respectively. In matrix form, these loads are expressed by Fourier series of the form,

$$\underset{\sim}{p}(s,\theta) = \underset{\sim}{p}^{(0)}(s) + \sum_{j=1}^{\infty} \underset{\sim}{C}^{(j)} \underset{\sim}{p}^{(j)}(s) + \sum_{j=1}^{\infty} \underset{\sim}{\bar{C}}^{(j)} \underset{\sim}{\bar{p}}^{(j)}(s) \qquad (1)$$

where

$$\underset{\sim}{p}(s,\theta) = [p_1(s,\theta) \ , \ p_2(s,\theta) \ , \ p_3(s,\theta) \ ]^T$$

$$\underset{\sim}{C}^{(j)} = \begin{bmatrix} \cos j\theta & 0 & 0 \\ 0 & \sin j\theta & 0 \\ 0 & 0 & \cos j\theta \end{bmatrix}$$

$$\underset{\sim}{\bar{C}}^{(j)} \begin{bmatrix} \sin j\theta & 0 & 0 \\ 0 & \cos j\theta & 0 \\ 0 & 0 & \sin j\theta \end{bmatrix}$$

Deleting the last row of matrix $\underset{\sim}{S}$ in (4), Appendix A.4, we write

$$\underset{3\times 1}{\bar{\delta}} = \underset{3\times 8}{S'} \ \underset{8\times 8}{Q} \ \underset{8\times 1}{\delta} = \underset{3\times 8}{\Psi} \ \underset{8\times 1}{\delta} \qquad (2)$$

where $\underset{\sim}{\Psi}$ is the 3 x 8 normalized interpolation function. The equivalent nodal load vector P_N in (2.38a) is derived from (2.20) for harmonically uncoupled part,

$$P_N^{(0)} = \int_0^{\ell}\int_0^{2\pi} \Psi_N \, p^{(0)}(s)\, r d\theta ds$$

or in matrix form

$$\underset{\sim}{P}^{(0)} = \int_0^{\ell}\int_0^{2\pi} \underset{\sim}{\Psi}^T p^{(0)}(s)\, r d\theta ds = [P_1^{(0)}, P_2^{(0)}, \ldots\ldots P_8^{(0)}]^T$$

where

$$P_1^{(0)} = 2\pi \int_0^{\ell} p_1^{(0)}(s)\, \lambda_1 r ds - \Phi_0' \int_0^{\ell} p_3^{(0)}(s) \lambda_4 \, r ds$$

$$P_2^{(0)} = 2\pi \int_0^{\ell} p_2^{(0)}(s)\, \lambda_2 r ds$$

$$P_3^{(0)} = 2\pi \int_0^{\ell} p_3^{(0)}(s)\, \lambda_3 r ds$$

$$P_4^{(0)} = 2\pi \int_0^{\ell} p_3^{(0)}(s)\, \lambda_4 r ds$$

$$P_5^{(0)} = 2\pi \left[\int_0^{\ell} p_1^{(0)}(s)\, \lambda_5 r ds - \Phi_{\ell}' \int_0^{\ell} p_3^{(0)}(s)\, \lambda_8 r ds \right]$$

$$P_6^{(0)} = 2\pi \int_0^{\ell} p_2^{(0)}(s)\, \lambda_6 \, r ds$$

$$P_7^{(0)} = 2\pi \int_0^{\ell} p_3^{(0)}(s)\, \lambda_7 \, r ds$$

$$P_8^{(0)} = 2\pi \int_0^{\ell} p_3^{(0)}(s)\, \lambda_8 r ds$$

where

$$\lambda_1 = \lambda_2 = 1 - \frac{s}{\ell}, \qquad \lambda_3 = 1 - 3(\frac{s}{\ell})^2 + 2(\frac{s}{\ell})^3$$

$$\lambda_4 = \ell[\frac{s}{\ell} - 2(\frac{s}{\ell})^2 + (\frac{s}{\ell})^2], \quad \lambda_5 = \lambda_6 = \frac{s}{\ell}$$

$$\lambda_7 = 3(\frac{s}{\ell})^2 - 2(\frac{s}{\ell})^3, \qquad \lambda_8 = \ell[-(\frac{s}{\ell})^2 + (\frac{s}{\ell})^3]$$

For harmonically coupled "A" series part,

$$\underset{\sim}{P}^{(j)} = \int_0^{\ell}\int_0^{2\pi} \underset{\sim}{T}^T \underset{\sim}{p}^{(j)}(s) \underset{\sim}{C}^{(j)*} \, r d\theta ds$$

Here the components of $\underset{\sim}{P}^{(j)}$ are the same as for $\underset{\sim}{P}^{(0)}$ except for 2π replaced by π and $p_i^{(0)}$, etc. by $p_i^{(j)}$, etc. The components for "B" series part are the same as in "A" series part except for j replaced by $-j$.

APPENDIX A.8

CALCULATIONS OF STRAIN AND STRESS

With nodal displacements available as a result of solving equations of motion or equilibrium we can calculate strains either by the standard finite element procedure or the finite difference representation of strain-displacement relations.

1. STRAINS

1.1 FINITE ELEMENTS

Using the notations introduced in Appendix A.4, the mid-surface normal and shear strains and bending strains are

$$\underset{6\times1}{\bar{\gamma}^{(j)}} = \underset{6\times8}{W^{(j)}}\ \underset{8\times8}{Q}\ \underset{8\times1}{\theta} \tag{1}$$

where $\bar{\gamma}^{(j)} = [e_s\ e_{s\theta}\ e_\theta\ \chi_s\ \chi_{s\theta}\ \chi_\theta]$

and j is the harmonic number. Also, the engineering strains γ may be written in the form (see (5) Appendix A.4),

$$\underset{3\times1}{\gamma^{(j)}} = \left(\underset{3\times6}{G} + \underset{3\times6}{Z}\right)\underset{6\times8}{W^{(j)}}\ \underset{8\times8}{Q}\ \underset{8\times1}{\theta} \tag{2}$$

1.2 FINITE DIFFERENCE PRESENTATION

From harmonically coupled expressions for strains as given in Appendix A.6 we write the finite difference analogue as follows:

$$e_s^{(j)} = \frac{\partial u^{(j)}}{\partial s} - w\frac{\partial \varphi}{\partial s} = u_{2i}^{(j)} - w_m^{(j)}\varphi_m' \tag{3a}$$

$$e_{s\theta} = \frac{1}{r_m}\left[r_m v_{2i}^{(j)} - v_m^{(j)}\sin\varphi_m - {}_j u_m^{(j)}\right] \tag{3b}$$

$$e_\theta^{(j)} = \frac{1}{r_m}\left[{}_j v_m^{(j)} + u_m^{(j)}\sin\varphi_m + w_m^{(j)}\cos\varphi_m\right. \tag{3c}$$

$$\chi_s^{(j)} = \beta_{2i}^{(j)} \tag{3d}$$

$$\chi_{s\theta}^{(j)} = \frac{2}{r_m}\left[{}_j w_{2i}^{(j)} - {}_j\frac{s_{in}\varphi_m w_m^{(j)}}{r_m} + \cos\varphi_m v_{2i}^{(j)} - \frac{\sin\varphi_m\cos\varphi_m}{r_m}v_m^{(j)} + {}_j\varphi_m' u_m^{(j)}\right] \tag{3e}$$

$$\chi_\theta^{(j)} = \frac{1}{r_m}\left[\frac{{}_j z}{r_m}w_m^{(j)} + {}_j\frac{\cos\varphi_m}{r_m}v_m^{(j)} - \beta_m\sin\varphi_m\right] \tag{3f}$$

where

$$u_{2i} = \frac{\theta_{1,p+1}^{(j)} - \theta_{1,p}^{(j)}}{L}, \qquad u_m = \frac{\theta_{1,p+1}^{(j)} + \theta_{1,p}^{(j)}}{2}$$

$$v_{2i} = \frac{\theta_{2,p+1}^{(j)} - \theta_{2,p}^{(j)}}{L}, \qquad v_m = \frac{\theta_{2,p+1}^{(j)} + \theta_{2,p}^{(j)}}{2}$$

$$w_{2i} = \frac{\theta_{3,p+1}^{(j)} - \theta_{3,p}^{(j)}}{L}, \qquad \beta_{2i} = \frac{\theta_{4,p+1}^{(j)} - \theta_{4,p}^{(j)}}{L}$$

$$\beta_m^{(j)} = \frac{\theta_{4,p+1}^{(j)} + \theta_{4,p}^{(j)}}{2}, \qquad \varphi_m' = \frac{\varphi_{p+1} - \varphi_p}{L}$$

with $_m$ denoting midsurface.

Writing (3) in matrix form, we get

$$\underset{6\times1}{\bar{\gamma}^{(j)}} = \underset{6\times8}{B^{(j)}}\ \underset{8\times1}{\theta^{(j)}} \tag{4}$$

and

$$\underset{3\times1}{\gamma^{(j)}} = \left(\underset{3\times6}{G} + \underset{3\times6}{Z}\right)\underset{6\times8}{B^{(j)}}\ \underset{8\times1}{\theta^{(j)}} \tag{5}$$

2. STRESSES

The Fourier series representation of stresses is

$$\sigma = \sigma^{(o)} + \sum_{j=1}^{n} C^{(j)}\sigma^{(j)} + \sum_{j=1}^{n} \bar{C}^{(j)}\bar{\sigma}^{(j)}$$

where $C^{(j)}$ and $\bar{C}^{(j)}$ are defined in Appendix A.7.

and $\sigma^{(j)} = E\,\gamma^{(j)}$, etc.

3. STRESS RESULTANTS

The inplane stress resultants are

$$N_s = \int_{-\frac{h}{2}}^{\frac{h}{2}} \sigma_s d\zeta \quad , \qquad M_s = \int_{-\frac{h}{2}}^{\frac{h}{2}} \sigma_s \zeta d\zeta$$

$$N_{s\theta} = \int_{-\frac{h}{2}}^{\frac{h}{2}} \sigma_{s\theta} d\zeta \quad , \qquad M_{s\theta} = \int_{-\frac{h}{2}}^{\frac{h}{2}} \sigma_{s\theta}\zeta d\zeta \tag{6}$$

$$N_\theta = \int_{-\frac{h}{2}}^{\frac{h}{2}} \sigma_\theta d\zeta \quad , \qquad M_\theta = \int_{-\frac{h}{2}}^{\frac{h}{2}} \sigma_\theta \zeta d\zeta$$

The stress resultants in the ζ-direction are given by

$$Q_s = \frac{\partial M_s}{\partial s} + \frac{\sin\varphi}{r} M_s + \frac{1}{r}\frac{\partial M_{s\theta}}{\partial \theta} - \frac{\sin\varphi}{r} M_\theta$$

$$Q_\theta = \frac{1}{r}\frac{\partial M_\theta}{\partial \theta} + \frac{2\sin\varphi}{r} M_{s\theta} + \frac{\partial M_{s\theta}}{\partial s} \tag{7a}$$

Once again these equations are expanded into Fourier series for summation. It is also convenient to write (7a) in harmonically coupled finite difference form,

$$Q_s^{(j)} = \frac{M_{s,p+1}^{(j)} - M_{s,p}^{(j)}}{L} + \frac{\sin\varphi_n}{r_n}\left[(M_s)_n^{(j)} - (M_\theta)_n^{(j)}\right] + \frac{j}{r_n}(M_{s\theta})_n^{(j)}$$

$$Q_\theta^{(j)} = -\frac{j}{r}(M_s)_n^{(j)} + \frac{2\sin\varphi_n}{r_n}(M_{s\theta})_n^{(j)} + \frac{M_{s\theta,p+1}^{(j)} - M_{s\theta,p}^{(j)}}{L} \tag{7b}$$

4. STRESS RESULTANTS THROUGH LAYERS OF COMPOSITES

If the shell thickness consists of n layers of composites we write (6) in matrix form,

$$\underset{\sim}{N} = \sum_{k=1}^{n} \int_{h_{k-1}}^{h_k} \underset{\sim}{\sigma}^k \, d\zeta \tag{8a}$$

$$\underset{\sim}{M} = \sum_{k=1}^{n} \int_{h_{k-1}}^{h_k} \underset{\sim}{\sigma}^k \, \zeta d\zeta \tag{8b}$$

where k denotes the $k^{\underline{th}}$ layer.

APPENDIX A.9

ELASTOPLASTIC ANALYSIS PROCEDURE

1. GENERAL

The yield criteria and coordinate transformation of plasticity matrix together with elasticity matrix are discussed in Appendix A.2 and A.5, respectively. The yield criterion to be satisfied is checked in the local coordinates of the fibers, which requires transformation of global strains and stresses to those of the local coordinates before the state of yielding can be determined. In what follows we discuss procedures involved in static loading. The viscoelastoplastic analysis for dynamic loading is discussed in Section 2.8.

2. INCREMENTAL LOADING PROCEDURE

As demonstrated in Section 2, the incremental equations of equilibrium is of the form

$$(\overset{(e)}{K}_{NM} + \overset{(p)}{K}_{NM})d\Theta^M = dF_N \tag{1a}$$

or

$$\overset{(t)}{K}_{NM}\, d\Theta^M = dF_N \tag{1b}$$

in which $\overset{(e)}{K}_{NM}$ and $\overset{(p)}{K}_{NM}$ are elastic and plastic stiffness matrices, respectively; and $d\Theta^N$ and dF_N are incremental displacements and applied forces. It should be noted that in the above equation only the static elastoplastic behavior is considered for simplicity.

The given load is applied in increments as shown in Figure A.9.1. For convenience one dimensional case is illustrated here. For a typical incremental load the incremental strain to be reached is shown in Figure A.9.1(b). Point C is reached through several steps, each step consisting of solving (1b) with updated plasticity stiffness matrix $K^{(p)}_{NM}$ which is calculated from plasticity matrix $\overset{*}{E}{}^{\alpha\beta\lambda\mu}$. The above procedure is referrred to as the tangent stiffness matrix.

An alternate approach is to rewrite (1b) in the form

$$K^{(e)}_{MN}\, d\Theta^M = dF_N - K^{(p)}_{MN}\, d\Theta^M \tag{2a}$$

If the load increment is sufficiently small it is possible to write (2a) for a load increment step (s) as

$$K^{(e)}_{ss}\, d\Theta^N(s) = dF_N(s) - K^{(p)}_{MN}(s) d\Theta^M(s-1) \tag{2b}$$

This procedure, called initial stiffness method, is illustrated in Figure A.9.1(c). In this case each iterative cycle is controlled from initially calculated elastic stiffness matrix. The product of plastic stiffness matrix and the incremental displacements of the previous step serve as a pseudo plastic load. Although this procedure is simpler than the tangent stiffness method, it requires more iterative cycles before convergence.

The transitional and unloading elements which turn to plastic from elastic and plastic to elastic, respectively, must be treated accordingly. For an element whose equivalent yield stress $\bar{\sigma}$ is less than the current yield stress $\bar{\sigma}_{max}$ at the end of elastic analysis or

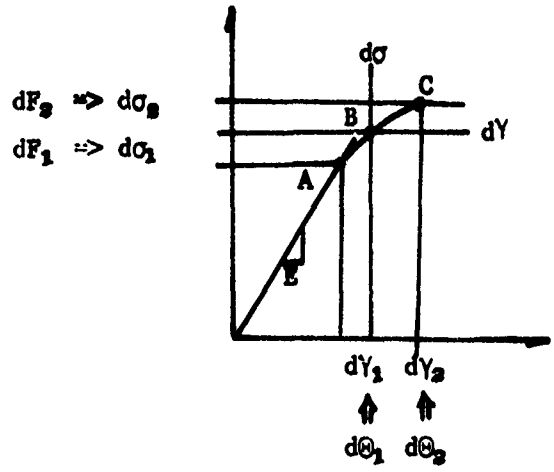

(a) One Dimensional Representation of Stress-Strain Curve

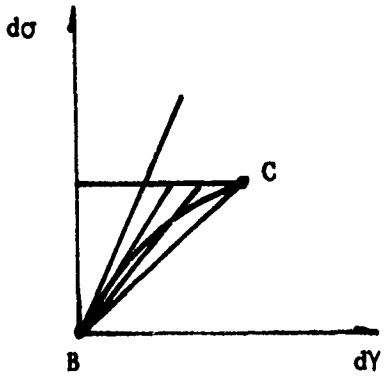

(b) Tangent Stiffness

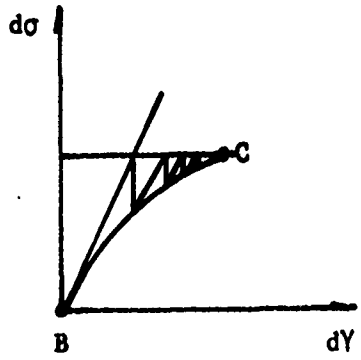

(c) Initial Stiffness

Figure A.9.1: Procedure of Incremental Loadings

previous increment, it is likely to expect faulty incremental equivalent stress $d\bar{\sigma}_1$ larger than actual. It is easy to show, however, that correct $d\bar{\sigma}_2$ for such transitional element is given by

$$d\bar{\sigma}_2 = E_{(p)} d\bar{\gamma}_1^{(p)} + \bar{\sigma}_{max} - \bar{\sigma} \tag{3}$$

where

$$d\bar{\gamma}_1^{(p)} = (\bar{\sigma} + d\bar{\sigma}_1 - \bar{\sigma}_{max})/(E + E_{(p)}) \tag{4}$$

For the next cycle this element is no longer transitional but elastoplastic. In this case $d\bar{\gamma}_1^{(p)}$ above is modified to

$$d\bar{\gamma}_2^{(p)} = [d\bar{\gamma}_1^{(p)} + (\bar{\sigma} + d\bar{\sigma}_1 - \bar{\sigma}_{max})/E] \frac{E}{E+E_{(p)}} \tag{5}$$

which is to replace $d\bar{\gamma}_1^{(p)}$ in (3).

For unloading element $d\bar{\sigma}$ becomes negative. In this case we simply set $\overset{*}{D}^{\alpha\beta\lambda\mu}$ equal to zero and only the elastic properties are used in the next cycle.

Whether tangent or initial stiffness method is used, the procedure begins by scaling displacement and stress in order to create impending yield (the elastic load limit of the structure under the given loading pattern). After the elastic limit is found status of yielding is checked for each element and the plastic stiffness matrix is developed. The incremental displacements are calculated until convergence with updated plastic stiffness matrix. The acceptable percent convergence ϵ may be defined as

$$\epsilon = [\{\Sigma(\bar{\sigma} + d\bar{\sigma}_1)^2 + \Sigma(\bar{\sigma} + d\bar{\sigma}_2)^2\}/\Sigma(\bar{\sigma} + d\bar{\sigma}_1)^2]^{\frac{1}{2}}$$

An acceptable convergence is considered to have been reached if ϵ is small, say, $\epsilon \leq 5\% - 10\%$. A new load increment is initiated and the above steps are repeated until application of total load is completed.

3. INTEGRATION THROUGH THICKNESS

Calculation of plastic stiffness matrix $K_{NM}^{(p)}$ is performed by summing the integrated plastic matrix $\underset{\sim}{\overset{*}{D}}^{(\kappa)}$ through the thickness of the shell. It is possible to write

$$\underset{\sim}{K}^{(p)} = \int_V \underset{\sim}{Q}^T \underset{\sim}{W}^T \begin{bmatrix} \overset{*}{D} & \zeta\overset{*}{D} \\ \zeta\overset{*}{D} & \zeta^2\overset{*}{D} \end{bmatrix} \underset{\sim}{W}\,\underset{\sim}{Q}\, dv$$

Since

$$\int \underset{\sim}{\overset{*}{D}}\, d\zeta = \sum_{\kappa=1}^{n} \underset{\sim}{\overset{*}{D}}^{(\kappa)} (h_{(\kappa)} - h_{(\kappa-1)})$$

$$\int \overset{*}{D}\zeta d\zeta = \sum_{\kappa=1}^{n} \underset{\sim}{\overset{*}{D}}^{(\kappa)} (h^2_{(\kappa)} - h^2_{(\kappa-1)})/2$$

and

$$\int \overset{*}{D}\zeta^2 d\zeta = \sum_{\kappa=1}^{n} \underset{\sim}{\overset{*}{D}}^{(\kappa)} (h^3_{(\kappa)} - h^3_{(\kappa-1)})/3$$

we obtain

$$\underset{\sim}{K}^{(p)} = \int_0^{\ell} \int_0^{2\pi} \underset{\sim}{Q}^T \underset{\sim}{W}^T \left\{ \sum_{\kappa=1}^{n} \underset{\sim}{\overset{*}{D}}^{(\kappa)} \begin{bmatrix} h_{(\kappa)} - h_{(\kappa-1)} & (h^2_{(\kappa)} - h^2_{(\kappa-1)})/2 \\ (h^2_{(\kappa)} - h_{(\kappa-1)})/2 & (h^3_{(\kappa)} - h^3_{(\kappa-1)})/3 \end{bmatrix} \right\} \underset{\sim}{W}\,\underset{\sim}{Q}\, r d\theta d\zeta$$

Here h is the thickness, (κ) represents the layer number, and $\underset{\sim}{Q}$ and $\underset{\sim}{W}$ are defined in Appendices A.4 and A.6, respectively.

APPENDIX A.10

DIRECT NUMERICAL TIME INTEGRATION SCHEMES

1. GENERAL

If the dynamical system is linear and has a simple geometry, the mode superposition method may be used, in which the forced response for each mode is calculated by way of the Duhamel integral or any equivalent method and the total response is obtained through superposition. This approach is especially attractive if low frequency bands of excitation dominate the applied loading. Even for a large system, condensation or component modal reduction schemes can reduce the problem to manageable size without significant loss in accuracy, provided the applied loading has this low frequency domination.

When high frequency excitation is significant, however, the coupled equations of motion of the system can best be solved by direct step-by-step integration. However, choice of inadequate integration operators result in unbounded solution or unstable solution. In the following, we discuss various integration operators and the solution stability.

2. FINITE DIFFERENCE OPERATORS AND ERRORS

The basic differential equations of motion are expressed in the form of recurrence matrix of finite differences to solve dynamic response of structures based on the following assumptions:

(1) The continuous lapse of time during the motion is divided into a series of small finite and equal time intervals. Within each time

interval, the motion of the structural system can be described by an ordinary linear differential equation of motion.

(2) The force excitation, or the displacement excitation applied to any part of the structure can be evaluated numerically at any designated time.

Numerical integration techniques fall into three rather broad categories - explicit, implicit, and predictor-corrector techniques.

1. Explicit method
   a. Forward Euler formulas
   b. Runge-Kutta formulas
   c. Open-end integration formulas (predictor formulas)
2. Implicit Method
   a. Backward Euler formulas
   b. Closed-end integration formulas (corrector formulas)
3. Predictor-correction method (mixed explicit-implicit method)

3. PARABOLIC COORDINATE

The choice of the finite-difference equivalents directly governs the accuracy and performance of the procedure. Consider the equation of motion,

$$\underset{\sim}{M}\ddot{\underset{\sim}{\Theta}} + \underset{\sim}{K}\underset{\sim}{\Theta} = \underset{\sim}{F}$$

Introduce a small time interval Δt,

$$\Delta t = t_n - t_{n-1}$$

Writing $\ddot{\underset{\sim}{\Theta}}$ for a parabolic variation of $\underset{\sim}{\Theta}$ within the time increment,

$$\ddot{\underline{\Theta}}_n = \frac{1}{(\Delta t)^2}[\underline{\Theta}_{n+1} - 2\underline{\Theta}_n + \underline{\Theta}_{n-1}) \tag{1}$$

Substituting in the equation of motion

$$\underline{M}\,\frac{1}{(\Delta t)^2}\,[\underline{\Theta}_{n+1} - 2\underline{\Theta}_n + \underline{\Theta}_{n-1}] + \underline{K}\underline{\Theta}_n = \underline{F} \tag{2}$$

$$\underline{\Theta}_{n+1} = \underline{M}^{-1}\underline{F}(\Delta t)^2 + [2 - \underline{M}^{-1}\underline{K}(\Delta t)^2]\,\underline{\Theta}_n - \underline{\Theta}_{n-1} \tag{3}$$

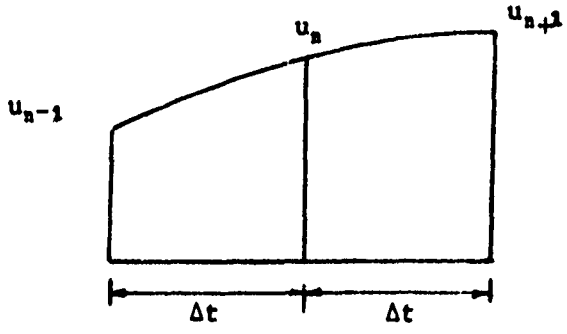

Figure A.10.1 Parabolic Variation of Displacement

For free vibration with single degree of freedom

$$\Theta_{n+1} = [2 - \frac{k}{m}(\Delta t)^2]\Theta_n - \Theta_{n-1} \tag{4}$$

Introducing

$$\Theta_n = A\beta^n \tag{5}$$

where A is the arbitrary constant to be determined from initial conditions and β is a number to be so chosen that (4) is satisfied. Substituting,

$$A\beta^{n+1} + \left[\frac{k}{m}(\Delta t)^2 - 2\right]A\beta^n + A\beta^{n-1} = 0$$

Dividing through by $A\beta^{n-1}$

$$\beta^2 + \left[\frac{k}{m}(\Delta t)^2 - 2\right]\beta + 1 = 0 \tag{6}$$

Consider various ranges of Δt

$$(1) \quad 0 < \Delta t < 2\sqrt{\frac{m}{k}}$$

First investigate $\Delta t = \sqrt{2}\sqrt{\frac{m}{k}} = .225(2\pi)\sqrt{\frac{m}{k}}$ so that $\Delta t = .225\ T$ where $T = \frac{2\pi}{\omega}$, natural period of the system. In this case Eq. (6) becomes

$$\beta^2 + 1 = 0 \tag{7}$$

$$\beta = \pm\sqrt{-1} = \pm i = e^{\pm\frac{i\pi}{2}} \tag{8}$$

Substituting in (5),

$$\theta_n = Ae^{\frac{i\pi n}{2}} + Be^{\frac{i\pi n}{2}} = A' \sin\frac{\pi n}{2} + B' \cos\frac{\pi n}{2} \tag{9}$$

Since

$$n = \frac{t}{\Delta t} = t\sqrt{\frac{\frac{k}{m}}{2}}$$

Eq. (9) can be written,

$$\theta_n = A' \sin 1.11\ t\sqrt{\frac{k}{m}} + B' \cos 1.11\ t\sqrt{\frac{k}{m}} \tag{10}$$

In this case, the effect of the numerical integration method is to increase the effective natural frequency from $\sqrt{\frac{k}{m}}$ to $1.11\sqrt{\frac{k}{m}}$ without introducing damping or build-up of the response.

As Δt changes from 0 to $2\sqrt{\frac{m}{k}}$, the factor in (10) varies from 1 to $\frac{\pi}{2}$.

(2) $\Delta t > \sqrt{\frac{m}{k}}$

Consider first $\Delta t = 3\sqrt{\frac{m}{k}}$, Eq. (6) becomes

$$\beta^2 + 7\beta + 1 = 0 \tag{11}$$

giving

$$\beta = -.1459 = -e^{-1.925}$$

$$\beta = -6.8541 = -e^{1.925}$$

Substituting these into (5),

$$\Theta_n = A(-1)^n e^{-1.925n} + B(-1)^n e^{1.925n}$$

$$= A'\cos n\pi \sinh 1.925n + B' \cos n\pi \cosh 1.925n \tag{12}$$

Substituting $n = \frac{t}{\Delta t} = t\sqrt{\frac{k}{\frac{m}{3}}}$

$$\Theta_n = [A' \sinh .642\, t\sqrt{\frac{k}{m}} + B' \cosh .642\, t\sqrt{\frac{k}{m}}\ ] \cos 1.047\, t\sqrt{\frac{k}{m}} \tag{13}$$

The primary effect of numerical integration methods is to introduce hyperbolic functions of time in the answer. Since these functions increase indefinitely with time, the result is divergent.

For all values of the time increment $\Delta t > \sqrt{\frac{m}{k}}$, divergent solutions of the time (13) result.

4. CUBIC COORDINATE

Writing the acceleration and velocity for a cubic variation of $\underset{\sim}{\Theta}$ within the time increment,

$$\ddot{\underset{\sim}{\Theta}}_n = \frac{1}{(\Delta t)^2}\left[\, 2\underset{\sim}{\Theta}_n - 5\underset{\sim}{\Theta}_{n-1} + 4\underset{\sim}{\Theta}_{n-2} - \underset{\sim}{\Theta}_{n-3}\right],$$

$$\dot{\underset{\sim}{\Theta}}_n = \frac{1}{6\Delta t}\left[\, 11\underset{\sim}{\Theta}_n - 18\underset{\sim}{\Theta}_{n-1} + 9\underset{\sim}{\Theta}_{n-2} - 2\underset{\sim}{\Theta}_{n-3}\,\right] \tag{14}$$

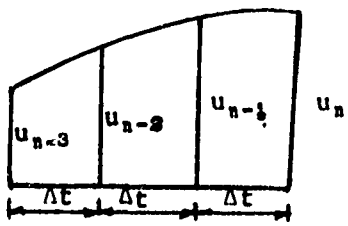

Figure A.10.2 Cubic Variation of Displacement

Substituting into equation of motion

$$\underset{\sim}{M}\frac{1}{(\Delta t)^2}\left[2\underset{\sim}{\Theta}_n - 5\underset{\sim}{\Theta}_{n-1} + 4\underset{\sim}{\Theta}_{n-2} - \underset{\sim}{\Theta}_{n-3}\right] + \underset{\sim}{K}\underset{\sim}{\Theta}_n = \underset{\sim}{F} \tag{15}$$

or

$$(2 + \underset{\sim}{M}^{-1}\underset{\sim}{K}(\Delta t)^2)\underset{\sim}{\Theta}_n = \underset{\sim}{M}^{-1}\underset{\sim}{F}\Delta t^2 + 5\underset{\sim}{\Theta}_{n-1} - 4\underset{\sim}{\Theta}_{n-2} + \underset{\sim}{\Theta}_{n-3} \tag{16}$$

For free vibration with a single degree of freedom

$$\left[2 + \frac{k}{m}(\Delta t)^2\right]\Theta_n - 5\Theta_{n-1} + 4\Theta_{n-2} - \Theta_{n-3} = 0 \tag{17}$$

Substituting (5)

$$\left[2 + \frac{k}{m}\Delta t^2\right]A\beta^n - 5A\beta^{n-1} + 4A\beta^{n-2} - A\beta^{n-3} = 0 \qquad (18)$$

Dividing through by $A\beta^{n-3}$

$$\left[2 + \frac{k}{m}(\Delta t)^2\right]\beta^3 - 5\beta^2 + 4\beta - 1 = 0 \qquad (19)$$

In this case, the errors are a small drop in natural frequency, .961 in place of 1 due to the presence of decaying exponentials. In the limit when $\Delta t \to 0$, the coefficients $2.32 \to \infty$, $.0095 \to 0$, $.961 \to 1$. The solution approaches the exact solution as Δt approaches zero.

Case (3). To judge the errors for large values of Δt consider $\Delta t = 98\sqrt{\frac{m}{k}}$

$$\theta = Ae^{-11805_t\sqrt{\frac{k}{m}}} + \left(e^{-.1424_t\sqrt{\frac{k}{m}}}\right)$$

$$x\left(B' \sin .183t\sqrt{\frac{k}{m}} + C' \cos .183t\sqrt{\frac{k}{m}}\right)$$

The errors are a large drop in natural frequency, .183 in place of 1. As $\Delta t \to \infty$ we have coefficients .805, .1424, and .183 $\to 0$. It is seen that large errors may result for large values of Δt, but they will be always convergent.

5. GENERAL FORMULAS

Consider a time interval Δt and assume variations of acceleration to be constant, linear, of a step function, or of any other form. For example let us take a linear variation,

$$\ddot{\underset{\sim}{\Theta}} = \ddot{\underset{\sim}{\Theta}}_n + (\ddot{\underset{\sim}{\Theta}}_{n+1} - \ddot{\underset{\sim}{\Theta}}_n) \frac{t}{\Delta t}$$

By integration,

$$\dot{\underset{\sim}{\Theta}} = \ddot{\underset{\sim}{\Theta}}_n t + (\ddot{\underset{\sim}{\Theta}}_{n+1} - \ddot{\underset{\sim}{\Theta}}_n)\frac{t^2}{2\Delta t} + c_1$$

where $c_1 = \dot{\underset{\sim}{\Theta}}_n$. By substituting $t = 0$

$$\dot{\underset{\sim}{\Theta}} = \ddot{\underset{\sim}{\Theta}}_n\, t + (\ddot{\underset{\sim}{\Theta}}_{n+1} - \ddot{\underset{\sim}{\Theta}}_n) \frac{t^2}{2\Delta t} + \dot{\underset{\sim}{\Theta}}_n$$

By further integration,

$$\underset{\sim}{\Theta} = \ddot{\underset{\sim}{\Theta}}_n \frac{t^2}{2} + (\ddot{\underset{\sim}{\Theta}}_{n+1} - \ddot{\underset{\sim}{\Theta}}_n) \frac{t^3}{6\Delta t} + \dot{\underset{\sim}{\Theta}}_n + c_2 \qquad (20)$$

where $c_2 = \underset{\sim}{\Theta}_n$. By substituting $t = 0$

$$\underset{\sim}{\Theta} = \ddot{\underset{\sim}{\Theta}}_n \frac{t^2}{2} + (\ddot{\underset{\sim}{\Theta}}_{n+1} - \ddot{\underset{\sim}{\Theta}}_n)\frac{t^3}{6\Delta t} + \dot{\underset{\sim}{\Theta}}_n t + \underset{\sim}{\Theta}_n$$

At $t = \Delta t$ we have $\dot{\underset{\sim}{\Theta}} = \dot{\underset{\sim}{\Theta}}_{n+1}$, $\underset{\sim}{\Theta} = \underset{\sim}{\Theta}_{n+1}$

$$\dot{\underset{\sim}{\Theta}}_{n+1} = \ddot{\underset{\sim}{\Theta}}_n \Delta t + (\ddot{\underset{\sim}{\Theta}}_{n+1} - \ddot{\underset{\sim}{\Theta}}_n) \frac{\Delta t}{2} + \dot{\underset{\sim}{\Theta}}_n = \dot{\underset{\sim}{\Theta}}_n + \ddot{\underset{\sim}{\Theta}}_n \frac{\Delta t}{2} + \ddot{\underset{\sim}{\Theta}}_{n+1}\frac{\Delta t}{2}$$

$$\underset{\sim}{\Theta}_{n+1} = \ddot{\underset{\sim}{\Theta}}_n \frac{\Delta t^2}{2} + (\ddot{\underset{\sim}{\Theta}}_{n+1} - \ddot{\underset{\sim}{\Theta}}_n) \frac{(\Delta t)^2}{6} + \dot{\underset{\sim}{\Theta}}_n \Delta t + \underset{\sim}{\Theta}_n$$

$$= \underset{\sim}{\Theta}_n \Delta t + \frac{1}{3} \ddot{\underset{\sim}{\Theta}}_n (\Delta t)^2 + \frac{1}{6} \ddot{\underset{\sim}{\Theta}}_{n+1} (\Delta t)^2$$

Newmark suggested the following general form of $\dot{\underset{\sim}{\Theta}}_{n+1}$ and $\underset{\sim}{\Theta}_{n+1}$ by introducing parameters γ and β which characterize, respectively, artificial damping and patterns of acceleration between the time interval:

$$\dot{\underset{\sim}{\Theta}}_{n+1} = \dot{\underset{\sim}{\Theta}}_n + (1 - \gamma)\, \ddot{\underset{\sim}{\Theta}}_n \Delta t + \gamma \ddot{\underset{\sim}{\Theta}}_{n+1} \Delta t \qquad (21)$$

$$\underset{\sim}{\Theta}_{n+1} = \underset{\sim}{\Theta}_n + \dot{\underset{\sim}{\Theta}}_n \Delta t + (\frac{1}{2} - \beta)\ddot{\underset{\sim}{\Theta}}_n (\Delta t)^2 + \beta \ddot{\underset{\sim}{\Theta}}_{n+1} (\Delta t)^2 \qquad (22)$$

For $\gamma = 0$ produces negative damping

$\gamma > \frac{1}{2}$ produces positive damping

$$\gamma = \frac{1}{2} \dot{\underset{\sim}{\Theta}}_{n+1} = \dot{\underset{\sim}{\Theta}}_n + \frac{1}{2} \Delta t (\ddot{\underset{\sim}{\Theta}}_{n+1})$$

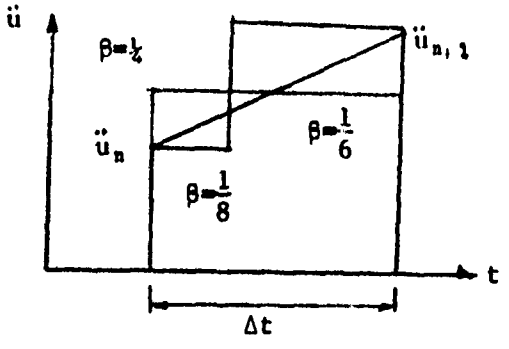

Figure A.10.2 Step, Constant, and Linear Variation of Displacement

It can easily be seen that we must choose $\gamma = \frac{1}{2}$ to avoid artificial damping and $\beta = \frac{1}{4}$, $\beta = \frac{1}{6}$, and $\beta = \frac{1}{8}$ correspond to accelerations of constant, linear, and step function, respectively.

It is interesting to note that Eq. (21) resembles the truncated Taylor series expansion with particular choice of coefficients,

$$\underset{\sim}{\Theta}_{n+1} = \underset{\sim}{\Theta}_n + \underset{\sim}{\Theta}'_n \Delta t + \Theta''_n \frac{(\Delta t)^2}{2} + \ldots$$

For constant acceleration, $\beta = \frac{1}{4}$, we have

$$\underset{\sim}{\Theta}_{n+1} = \underset{\sim}{\Theta}_n + \dot{\underset{\sim}{\Theta}}_n \Delta t + \frac{1}{4} \ddot{\underset{\sim}{\Theta}}_n \Delta t^2 + \frac{1}{4} \ddot{\underset{\sim}{\Theta}}_{n+1} \Delta t^2$$

$$\dot{\underset{\sim}{\Theta}}_{n+1} = \dot{\underset{\sim}{\Theta}}_n + \frac{\Delta t}{2} \ddot{\underset{\sim}{\Theta}}_n + \frac{\Delta t}{2} \ddot{\underset{\sim}{\Theta}}_{n+1} \qquad (23)$$

Substituting these into the equation of motion for the time step corresponding to n+1,

$$\underline{M}\ddot{\underline{\Theta}}_{n+1} + \underline{K}(\underline{\Theta}_n + \dot{\underline{\Theta}}_n\Delta t + \frac{\Delta t^2}{4}\ddot{\underline{\Theta}}_n + \frac{\Delta t^2}{4}\ddot{\underline{\Theta}}_{n+1}\Delta t^2) = \underline{F}_{n+1} \tag{24}$$

or

$$(\underline{M} + \underline{K}\frac{\Delta t^2}{4})\ddot{\underline{\Theta}}_{n+1} = \underline{F}_{n+1} - \underline{K}(\underline{\Theta}_n + \dot{\underline{\Theta}}_n\Delta t + \ddot{\underline{\Theta}}_n\frac{\Delta t^2}{4} \tag{25}$$

From this we calculate $\ddot{\underline{\Theta}}_{n+1}$ and $\underline{\Theta}_{n+1}$, subsequently.

6. RATE-DEPENDENT PROBLEM

If viscosity is present the general form of equation of motion becomes

$$\underline{M}\,\ddot{\underline{\Theta}} + \underline{C}\,\dot{\underline{\Theta}} + \underline{K}\,\underline{\Theta} = \underline{F} \tag{26}$$

where $\underline{C}$ is the viscosity matrix.

Considering a constant acceleration and substituting (22) and (23) into (26) for the n+1 step,

$$\underline{M}\,\ddot{\underline{\Theta}}_{n+1} + \underline{C}\,(\dot{\underline{\Theta}}_n + \frac{\Delta t}{2}\ddot{\underline{\Theta}}_n + \frac{\Delta t}{2}\ddot{\underline{\Theta}}_{n+1}) + \underline{K}\,(\underline{\Theta}_n + \Delta t\,\dot{\underline{\Theta}}_n + \frac{\Delta t}{4}\ddot{\underline{\Theta}}_n + \frac{\Delta t}{4}\ddot{\underline{\Theta}}_{n+1}) = \underline{F}_{n+1}$$

or

$$(\underline{M} + \frac{\Delta t}{2}\underline{C} + \frac{\Delta t^2}{4}\underline{K})\ddot{\underline{\Theta}}_{n+1} = \underline{F}_{n+1} - \underline{R}_{n+1} \tag{27}$$

where

$$\underline{R}_{n+1} = \underline{C}(\dot{\underline{\Theta}}_n + \frac{\Delta t}{2}\ddot{\underline{\Theta}}_n) + \underline{K}(\underline{\Theta}_n + \Delta t\dot{\underline{\Theta}}_n + \frac{\Delta t^2}{4}\ddot{\underline{\Theta}}_n)$$

Recursive equations are then (27), (23) and (22) to be solved repeatedly for all time increments.

7. QUASI-STATIC PROBLEM

In the absence of inertia force we have the equation of the form,

$$\underset{\sim}{C}\,\dot{\underset{\sim}{\Theta}} + \underset{\sim}{K}\,\underset{\sim}{\Theta} = \underset{\sim}{F} \tag{28}$$

Either the displacement or displacement rate may be assumed to vary linearly within a small time increment. Both cases are considered below.

7.1 LINEAR VARIATION OF DISPLACEMENT RATE

For a given time interval,

$$\dot{\underset{\sim}{\Theta}} = \dot{\underset{\sim}{\Theta}}_n + \frac{t}{\Delta t}(\dot{\underset{\sim}{\Theta}}_{n+1} - \dot{\underset{\sim}{\Theta}}_n)$$

$$\underset{\sim}{\Theta} = \dot{\underset{\sim}{\Theta}}_n + \frac{t}{2\Delta t}(\dot{\underset{\sim}{\Theta}}_{n+1} - \dot{\underset{\sim}{\Theta}}_n) + \underset{\sim}{\Theta}_n$$

For $t=\Delta t$

$$\underset{\sim}{\Theta}_{n+1} = \dot{\underset{\sim}{\Theta}}_n \Delta t + \frac{\Delta t}{2}(\dot{\underset{\sim}{\Theta}}_{n+1} - \dot{\underset{\sim}{\Theta}}_n) + \underset{\sim}{\Theta}_n$$

or

$$\underset{\sim}{\Theta}_{n+1} = \underset{\sim}{\Theta}_n + \frac{\Delta t}{2}\dot{\underset{\sim}{\Theta}}_n + \frac{\Delta t}{2}\dot{\underset{\sim}{\Theta}}_{n+1} \tag{29}$$

Substituting (29) into (28) for the $n+1$ step

$$\underset{\sim}{C}\,\dot{\underset{\sim}{\Theta}}_{n+1} + \underset{\sim}{K}(\underset{\sim}{\Theta}_n + \frac{\Delta t}{2}\dot{\underset{\sim}{\Theta}}_n + \frac{\Delta t}{2}\dot{\underset{\sim}{\Theta}}_{n+1}) = \underset{\sim}{F}_{n+1}$$

or

$$(\underset{\sim}{C} + \frac{\Delta t}{2}\,\underset{\sim}{K})\dot{\underset{\sim}{\theta}}_{n+1} = \underset{\sim}{F}_{n+1} - \underset{\sim}{R}_{n+1} \tag{30}$$

where

$$\underset{\sim}{R}_{n+1} = \underset{\sim}{K}(\underset{\sim}{\theta}_n + \frac{\Delta t}{2}\,\dot{\underset{\sim}{\theta}}_n) \tag{31}$$

Here (30) and (29) constitute recursive equations.

7.2 LINEAR VARIATION OF DISPLACEMENT

We consider a linear variation of displacement so that the average displacement at the mid-interval is

$$\underset{\sim}{\theta}_{n+\frac{1}{2}} = (\underset{\sim}{\theta}_{n+1} + \underset{\sim}{\theta}_n)/2 \tag{32}$$

The displacement rate at the mid-intervals is approximated as

$$\dot{\underset{\sim}{\theta}}_{n+\frac{1}{2}} = (\underset{\sim}{\theta}_{n+1} - \underset{\sim}{\theta}_n)/\Delta t \tag{33}$$

In view of (32) and (33) and rewriting (28) for the mid-interval $n+\frac{1}{2}$, we obtain

$$\underset{\sim}{C}\left(\frac{2\underset{\sim}{\theta}_{n+1} - 2\underset{\sim}{\theta}_n}{\Delta t}\right) + \underset{\sim}{K}\,\underset{\sim}{\theta}_{n+\frac{1}{2}} = \underset{\sim}{F}_{n+\frac{1}{2}}$$

or

$$(\frac{2}{\Delta t}\,\underset{\sim}{C} + \underset{\sim}{K})\underset{\sim}{\theta}_{n+\frac{1}{2}} = \underset{\sim}{F}_{n+\frac{1}{2}} + \frac{2}{\Delta t}\,\underset{\sim}{C}\,\underset{\sim}{\theta}_n$$

using (32) once again,

$$\underset{\sim}{\theta}_{n+1} = 2(\frac{2}{\Delta t}\,\underset{\sim}{C} + \underset{\sim}{K})(\underset{\sim}{F}_{n+\frac{1}{2}} + \frac{2}{\Delta t}\,\underset{\sim}{C}\,\underset{\sim}{\theta}_n) - \underset{\sim}{\theta}_n \tag{34}$$

which may be solved repeatedly to any extent of time desired.

APPENDIX A.11

MASS MATRICES

1. GENERAL

There are two types of mass matrices in use: lumped mass matrix and consistent mass matrix. The lumped mass matrix is a diagonal matrix contributed by the tributary area around the node with equivalent mass (weight divided by gravitational acceleration). The consistent mass matrix is derived in Section 2 and given by (2.39) in terms of the normalized interpolation function. Although the lumped mass matrix is simpler we use the consistent mass matrix in the present study because computer coding does not present any special difficulty.

2. THIN SHELL

The general form of consistent mass matrix (2.39) is

$$M_{NM} = \int_0^{\ell}\int_0^{2\pi} \rho \psi_N^i \psi_{iM} r(s) d\theta ds$$

or in matrix form

$$\underset{\sim}{M} = 2\pi\rho \int_0^{\ell} \underset{\sim}{\psi}^T(s)\, \underset{\sim}{\psi}(s)\, r(s) ds$$

or

$$\underset{8\times8}{\underset{\sim}{M}} = 2\pi\rho\, \underset{8\times8}{\underset{\sim}{Q}^T}\ \underset{8\times8}{\underset{\sim}{L}}\ \underset{8\times8}{\underset{\sim}{Q}} \qquad (1)$$

in which

$$\underset{8\times8}{\underset{\sim}{L}} = \int_0^{\ell} \underset{8\times4}{\underset{\sim}{S}^T}\ \underset{4\times8}{\underset{\sim}{S}}\ r(s) ds \qquad (2)$$

Here $\underset{\sim}{Q}$ and $\underset{\sim}{S}$ are given in (5), Appendix A.4 and the integral $\underset{\sim}{L}$ is easily obtained by computer program using Simpson's rule.

3. THICK SHELL

The consistent mass matrix corresponding to a thick shell without bending represented by the plane strain element described in Appendix A.12 can be obtained similarly as in the previous section. We have

$$\underset{\sim}{M} = 2\pi\rho \int_{-1}^{1}\int_{-1}^{1} \underset{\sim}{\tilde{\psi}}^T \underset{\sim}{\tilde{\psi}} \, |J| r \, d\xi d\eta \tag{3}$$

in which $\underset{\sim}{\tilde{\psi}}$ and $|J|$ are given in Appendix A.12.

Explicit forms are not presented here because the computer coding by means of Gaussian quadrature is quite simple.

APPENDIX A.12

THICK SHELL ISOPARAMETRIC ELEMENT

1. INTERPOLATION FUNCTION

Consider the four-sided element with nodes 1, 2, 3, and 4 characterized by two coordinate systems r-z (cartesian coordinate) and ξ-η (isoparametric coordinate) as shown in Figure A.12.1. The isoparametric nodal values are either 1 or -1 measured from the origin of ξ-η coordinate. It is possible to write

$$r = \underset{\sim}{R}\,\underset{\sim}{a} \tag{1}$$

where

$$\underset{\sim}{R} = [\ 1 \quad \xi \quad \eta \quad \xi\eta\ ]$$

$$\underset{\sim}{a} = [\ a_1 \quad a_2 \quad a_3 \quad a_4\ ]$$

Here a_1, etc., are constants to be determined writing the nodal values of $\underset{\sim}{X}$ by substituting the nodal values of ξ and η we obtain

$$\underset{\sim}{r} = \underset{\sim}{A}\,\underset{\sim}{a} \tag{2}$$

where $\underset{\sim}{r} = [\ r_1 \quad r_2 \quad r_3 \quad r_4\ ]^T$

$$\underset{\sim}{A} = \begin{bmatrix} 1 & -1 & -1 & 1 \\ 1 & 1 & -1 & -1 \\ 1 & 1 & 1 & 1 \\ 1 & -1 & 1 & -1 \end{bmatrix}$$

from which

$$\underset{\sim}{a} = \underset{\sim}{A}^{-1}\,\underset{\sim}{r}$$

Substituting the above into the expression for r gives

$$r = \begin{bmatrix} 1 & \xi & \eta & \xi\eta \end{bmatrix} \frac{1}{4} \begin{bmatrix} 1 & 1 & 1 & 1 \\ -1 & 1 & 1 & -1 \\ -1 & -1 & 1 & 1 \\ 1 & -1 & 1 & -1 \end{bmatrix} \begin{bmatrix} r_1 \\ r_2 \\ r_3 \\ r_4 \end{bmatrix}$$

or

$$r = \underset{\sim}{\psi}\, \underset{\sim}{r} \tag{3}$$

where

$$\psi_1 = \frac{1}{4}(1-\xi)(1-\eta)$$
$$\psi_2 = \frac{1}{4}(1+\xi)(1-\eta)$$
$$\psi_3 = \frac{1}{4}(1+\xi)(1+\eta)$$
$$\psi_4 = \frac{1}{4}(1-\xi)(1+\eta)$$

Similarly z can be written

$$z = \underset{\sim}{\psi}\, \underset{\sim}{z} \tag{4}$$

Here $\underset{\sim}{\psi}$ is called the isoparametric interpolation function.

Combining (3) and (4) we can also write

$$X_i = \psi_N X^N \quad , \qquad \text{or} \qquad X_i = \psi_{ir} X^r$$

In matrix form,

$$\underset{\sim}{X} = \begin{bmatrix} r \\ z \end{bmatrix} = \underset{\sim}{\psi}\, \underset{\sim}{X} \quad , \text{ or} \qquad \underset{\sim}{X} = \begin{bmatrix} r \\ z \end{bmatrix} = \overline{\underset{\sim}{\psi}}\, \underset{\sim}{X}$$

where

$$\underset{\sim}{\psi} = \begin{bmatrix} \psi_1 & \psi_2 & \psi_3 & \psi_4 \\ \psi_1 & \psi_2 & \psi_3 & \psi_4 \end{bmatrix}$$

$$\overline{\underset{\sim}{\psi}} = \begin{bmatrix} \psi_1 & 0 & \psi_2 & 0 & \psi_3 & 0 & \psi_4 & 0 \\ 0 & \psi_1 & 0 & \psi_2 & 0 & \psi_3 & 0 & \psi_4 \end{bmatrix}$$

$$\underset{\sim}{X} = [\, r_1 \; r_2 \; r_3 \; r_4 \; z_1 \; z_2 \; z_3 \; z_4 \,]$$

$$\underset{\sim}{\bar{X}} = [\, r_1 \; z_1 \; r_2 \; z_2 \; r_3 \; z_3 \; r_4 \; z_4 \,]$$

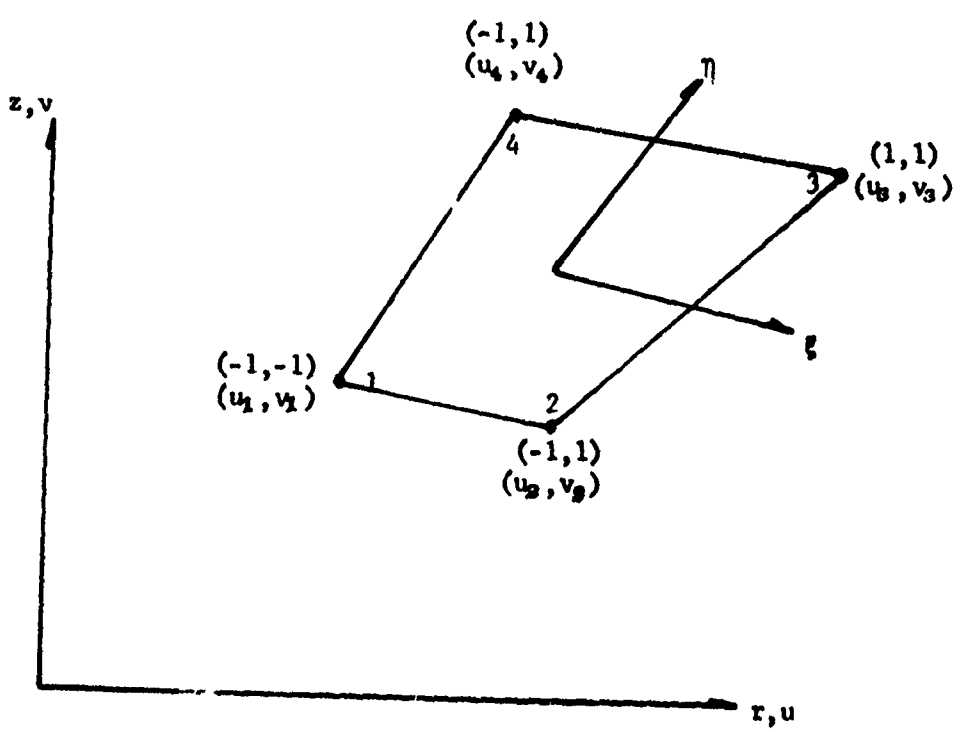

Figure A.12.1: Isoparametric Element

Here 1, 2, 3, and 4 indicate the node numbers.

It is now assumed that the displacements u and v are also related by the same interpolation functions such that

$$u = \underset{\sim}{\psi}\,\underset{\sim}{u}, \quad v = \underset{\sim}{\psi}\,\underset{\sim}{v}$$

where

$$\underset{\sim}{u} = [u_1\ u_2\ u_3\ u_4]^T, \quad \underset{\sim}{v} = [v_1\ v_2\ v_3\ v_4]^T$$

or
$$\underset{\sim}{u} = \tfrac{1}{4}[(1-\xi-\eta+\xi\eta)u_1 + (1+\xi-\eta-\xi\eta)u_2$$
$$+ (1+\xi+\eta+\xi\eta)u_3 + (1-\xi+\eta-\xi\eta)u_4]$$
$$= \tfrac{1}{4}\sum_{n=1}^{4}(1 + B_n\,\xi + C_n\,\eta + D_n\,\xi\eta)u_n \qquad (5a)$$

$B_1 = -1$	$C_1 = -1$	$D_1 = 1$
$B_2 = 1$	$C_2 = -1$	$D_2 = -1$
$B_3 = 1$	$C_3 = 1$	$D_3 = 1$
$B_4 = -1$	$C_4 = 1$	$D_4 = -1$

Similarly

$$v = \tfrac{1}{4}\sum_{n=1}^{8}(1 + B_n\,\xi + C_n\,\eta + D_n\,\xi\eta)v_n \qquad (5b)$$

Since r is given by

$$r = \tfrac{1}{4}[(1-\xi)(1-\eta)r_1 + (1+\xi)(1-\eta)r_2 + (1+\xi)(1+\eta)r_3 + (1-\xi)(1+\eta)r_4]$$

or
$$r = \tfrac{1}{4}[R_T + (R_A)\xi + (R_B)\eta + (R_C)\xi\eta] \qquad (6)$$

where

$$R_T = (r_1 + r_2 + r_3 + r_4)$$
$$R_A = (-r_1 + r_2 + r_3 - r_4)$$
$$R_B = (-r_1 - r_2 + r_3 + r_4)$$
$$R_C = (r_1 - r_2 + r_3 - r_4)$$

Similarly,

$$z = \tfrac{1}{4}(Q_1 + Q_A\xi + Q_B\eta + Q_C\xi\eta) \tag{7}$$

where

$$Q_1 = (z_1 + z_2 + z_3 + z_4)$$

$$Q_A = (-z_1 + z_2 + z_3 - z_4)$$

$$Q_B = (-z_1 - z_2 + z_3 + z_4)$$

$$Q_C = (r_1 - r_2 + r_3 - r_4)$$

Substitution of interpolation functions into the strain-displacement relations will lead to partial differentiation of these functions. Thus,

$$\frac{\partial\psi}{\partial r} = \frac{\partial\psi}{\partial r}\cdot\frac{\partial r}{\partial\xi} + \frac{\partial\psi}{\partial z}\cdot\frac{\partial z}{\partial\xi}$$

$$\frac{\partial\psi}{\partial\eta} = \frac{\partial\psi}{\partial r}\cdot\frac{\partial r}{\partial\eta} + \frac{\partial\psi}{\partial z}\cdot\frac{\partial z}{\partial\eta}$$

or

$$\begin{bmatrix}\frac{\partial\psi}{\partial\xi}\\ \frac{\partial\psi}{\partial\eta}\end{bmatrix} = \begin{bmatrix}\frac{\partial r}{\partial\xi} & \frac{\partial z}{\partial\xi}\\ \frac{\partial r}{\partial\eta} & \frac{\partial z}{\partial\eta}\end{bmatrix}\begin{bmatrix}\frac{\partial\psi}{\partial r}\\ \frac{\partial\psi}{\partial z}\end{bmatrix} = \underset{\sim}{J}\begin{bmatrix}\frac{\partial\psi}{\partial r}\\ \frac{\partial\psi}{\partial z}\end{bmatrix} \tag{8}$$

This gives

$$\begin{bmatrix}\frac{\partial\psi}{\partial r}\\ \frac{\partial\psi}{\partial z}\end{bmatrix} = \frac{1}{\Delta}\begin{bmatrix}\frac{\partial z}{\partial\eta} & -\frac{\partial z}{\partial\xi}\\ -\frac{\partial r}{\partial\eta} & \frac{\partial r}{\partial\xi}\end{bmatrix}\begin{bmatrix}\frac{\partial\psi}{\partial\xi}\\ \frac{\partial\psi}{\partial\eta}\end{bmatrix} \tag{9}$$

in which

$$\Delta = \begin{bmatrix}\frac{\partial r}{\partial\xi}\cdot\frac{\partial z}{\partial\eta} - \frac{\partial z}{\partial\xi}\cdot\frac{\partial r}{\partial\eta}\end{bmatrix} \tag{10}$$

Here $\underset{\sim}{J}$ is called Jacobian matrix. Performing the partial differentiation required in (8),

$$\frac{\partial r}{\partial \xi} = \tfrac{1}{4}[\,(-r_1 + r_2 + r_3 - r_4) + (r_1 - r_2 + r_3 - r_4)\eta] \qquad (11a)$$

Similarly,

$$\frac{\partial z}{\partial \xi} = \tfrac{1}{4}[(-z_1 + z_2 + z_3 - z_4) + (z_1 - z_2 + z_3 - z_4)\eta] \qquad (11b)$$

$$\frac{\partial r}{\partial \eta} = \frac{1}{4}\,[(-r_1 - r_2 + r_3 + r_4) + (r_1 - r_2 + r_3 - r_4)\xi] \qquad (11c)$$

$$\frac{\partial z}{\partial \eta} = \frac{1}{4}\,[(-z_1 - z_2 + z_3 + z_4) + (z_1 - z_2 + z_3 - z_4)\xi] \qquad (11d)$$

$$\frac{\partial r}{\partial \xi}\frac{\partial z}{\partial \eta} = \frac{1}{16}\,[(-r_1 + r_1 + r_3 - r_4)(-z_1 - z_2 + z_3 + z_4) + (r_1 - r_2 + r_3 - r_4)(-z_1 - z_2 + z_3 + z_4)\eta + (-r_1 + r_2 + r_3 - r_4)(z_1 - z_2 + z_3 - z_4)\xi + (r_1 - r_2 + r_3 - r_4)(z_1 - z_2 + z_3 - z_4)\xi\eta]$$

And

$$\frac{\partial z}{\partial \xi}\frac{\partial r}{\partial \eta} = \frac{1}{16}\,[\,(-r_1 - r_2 + r_3 + r_4)(-z_1 + z_2 + z_3 - z_4) + (-r_1 - r_2 + r_3 + r_4)(z_1 - z_2 + z_3 - z_4)\eta + (r_1 - r_2 + r_3 - r_4)(-z_1 + z_2 + z_3 - z_4)\xi + (r_1 - r_2 + r_3 - r_4)(z_1 - z_2 + z_3 - z_4)\xi\eta]$$

Substituting these into Equation (8) and denoting that $r_{12} = r_1 - r_2$, etc.,

$$\Delta = \frac{1}{8}\,[(r_{42}z_{13} - r_{13}z_{42}) + (r_{34}z_{12} - r_{12}z_{34})\xi + (r_{41}z_{23} - r_{23}z_{41})\eta\,] \qquad (12)$$

Similarly,

$$\frac{\partial v}{\partial \xi} = \tfrac{1}{4}[(-v_1 + v_2 + v_3 - v_4) + (v_1 - v_2 + v_3 - v_4)\eta] \qquad (13a)$$

$$\frac{\partial v}{\partial \eta} = \tfrac{1}{4}[(-v_1 - v_2 + v_3 + v_4) + (v_1 - v_2 + v_3 - v_4)\xi\,] \qquad (13b)$$

$$\frac{\partial v}{\partial \xi}\frac{\partial r}{\partial \eta} = \frac{1}{16}\{(-v_1+v_2+v_3-v_4)(-r_1-r_2+r_3+r_4) +$$
$$(-v_1+v_2+v_3-v_4)(r_1-r_2+r_3-r_4)\xi +$$
$$(v_1-v_2+v_3-v_4)(-r_1-r_2+r_3+r_4)\eta +$$
$$(v_1-v_2+v_3-v_4)(r_1-r_2+r_3-r_4)\xi\eta\}$$

$$\frac{\partial v}{\partial \eta}\frac{\partial r}{\partial \xi} - \frac{\partial v}{\partial \xi}\frac{\partial r}{\partial \eta} = \frac{1}{8}[(v_1 r_{42}+v_2 r_{13}+v_3 r_{24}+v_4 r_{31}) + \quad (14a)$$
$$(v_1 r_{34}+v_2 r_{43}+v_3 r_{21}+v_4 r_{12})\xi +$$
$$(v_1 r_{23}+v_2 r_{41}+v_3 r_{14}+v_4 r_{32})\eta]$$

$$\frac{\partial v}{\partial \xi}\frac{\partial z}{\partial \eta} = \frac{1}{16}\{(-v_1+v_2+v_3-v_4)(z_1-z_2+z_3+z_4) +$$
$$(-v_1+v_2+v_3-v_4)(z_1-z_2+z_3-z_4)\xi +$$
$$(v_1-v_2+v_3-v_4)(-z_1-z_2+z_3+z_4)\eta + (v_1-v_2+v_3-v_4)(z_1-z_2-z_3-z_4)\xi\eta\}$$

$$\frac{\partial v}{\partial \eta}\frac{\partial z}{\partial \xi} = \frac{1}{16}\{(-v_1-v_2+v_3+v_4)(-z_1+z_2+z_3-z_4) +$$
$$(v_1-v_2+v_3-v_4)(-z_1+z_2+z_3-z_4)\xi +$$
$$(-v_1-v_2+v_3+v_4)(z_1-z_2+z_3-z_4)\eta+(v_1-v_2+v_3-v_4)(z_1-z_2+z_3-z_4)\xi\eta\}$$

therefore

$$\frac{\partial v}{\partial \xi}\frac{\partial z}{\partial \eta} - \frac{\partial v}{\partial \eta}\frac{\partial z}{\partial \xi} = \frac{1}{8}\{(v_1 z_{24}+v_2 z_{31}+v_3 z_{42}+v_4 z_{13}) +$$
$$(v_1 z_{43}+v_2 z_{34}+v_3 z_{12}+v_4 z_{21})\xi +$$
$$(v_1 z_{32}+v_2 z_{14}+v_3 z_{41}+v_4 z_{23})\eta\} \quad (14b)$$

We will make use of equations (14a) and (14b) in evaluating $\frac{\partial v}{\partial z}$ in terms of v_1, v_2, v_3, v_4 and nodal coordinates (r_1, z_1), (r_2, z_2), (r_3, z_3) and (r_4, z_4).

From equation (.9.) we can write,

$$\frac{\partial v}{\partial z} = \frac{1}{\Delta}\left[\frac{\partial r}{\partial \eta}\cdot\frac{\partial v}{\partial \xi} + \frac{\partial r}{\partial \xi}\cdot\frac{\partial v}{\partial \eta}\right] \quad (15a)$$

and

$$\frac{\partial v}{\partial r} = \frac{1}{\Delta}\left[\frac{\partial z}{\partial \eta}\cdot\frac{\partial v}{\partial \xi} - \frac{\partial z}{\partial \xi}\frac{\partial v}{\partial \eta}\right] \tag{15b}$$

Using equation (14a) and (14b),

$$\frac{\partial v}{\partial z} = \frac{1}{8\Delta}\{(v_1 r_{42}+v_2 r_{13}+v_3 r_{24}+v_4 r_{31}) + (v_1 r_{34}+v_2 r_{43}+v_3 r_{21}+v_4 r_{12})\xi + (v_1 r_{23}+v_2 r_{41}+v_3 r_{14}+v_4 r_{32})\eta\} \tag{16a}$$

and

$$\frac{\partial v}{\partial r} = \frac{1}{8\Delta}\{(v_1 z_{24}+v_2 z_{31}+v_3 z_{42}+v_4 z_{13}) + (v_1 z_{43}+v_2 z_{34}+v_3 z_{12}+v_4 z_{21})\xi + (v_1 z_{32}+v_2 z_{14}+v_3 z_{41}+v_4 z_{23})\eta\} \tag{16b}$$

Denote $\Omega = \frac{1}{8\Delta}$

$$M_1 = \Omega(r_{42}+r_{34}\xi+r_{23}\eta)$$
$$M_2 = \Omega(r_{13}+r_{43}\xi+r_{41}\eta)$$
$$M_3 = \Omega(r_{24}+r_{21}\xi+r_{14}\eta)$$
$$M_4 = \Omega(r_{31}+r_{12}\xi+r_{32}\eta)$$

$$L_1 = \Omega(z_{24}+z_{43}\xi+z_{32}\eta)$$
$$L_2 = \Omega(z_{31}+z_{34}\xi+z_{14}\eta)$$
$$L_3 = \Omega(z_{42}+z_{12}\xi+z_{41}\eta)$$
$$L_4 = \Omega(z_{13}+z_{21}\xi+z_{23}\eta)$$

Substituting these into equations (16a) and (16b) yields

$$\frac{\partial v}{\partial z} = \underset{\sim}{M}\ \underset{\sim}{v} \tag{17a}$$

$$\frac{\partial v}{\partial r} = \underset{\sim}{L}\ \underset{\sim}{v} \tag{17b}$$

where

$$\underset{\sim}{M} = [M_1 \; M_2 \; M_3 \; M_4]$$

$$\underset{\sim}{L} = [L_1 \; L_2 \; L_3 \; L_4]$$

and

$$\underset{\sim}{v} = [v_1 \; v_2 \; v_3 \; v_4]$$

Equations (1-17a) and (1-17b) can also be written as

$$\frac{\partial v}{\partial z} = \sum_{n=1}^{4} \Omega \, (A_{rn} + B_{rn}\xi + C_{rn}\eta) v_n \qquad (18a)$$

$$\frac{\partial v}{\partial r} = \sum_{n=1}^{4} \Omega \, (A_{zn} + B_{zn}\xi + C_{zn}\eta) v_n \qquad (18b)$$

where

$Ar_1 = r_4 - r_3$ $\quad$ $Br_1 = r_3 - r_4$ $\quad$ $Cr_1 = r_2 - r_3$

$Ar_2 = r_1 - r_3$ $\quad$ $Br_2 = r_4 - r_3$ $\quad$ $Cr_2 = r_4 - r_1$

$Ar_3 = r_2 - r_4$ $\quad$ $Br_3 = r_2 - r_1$ $\quad$ $Cr_3 = r_1 - r_4$

$Ar_4 = r_3 - r_1$ $\quad$ $Br_4 = r_1 - r_2$ $\quad$ $Cr_4 = r_3 - r_2$

and

$Az_1 = z_2 - z_4$ $\quad$ $Bz_1 = z_4 - z_3$ $\quad$ $Cz_1 = z_3 - z_2$

$Az_2 = z_3 - z_1$ $\quad$ $Bz_2 = z_3 - z_4$ $\quad$ $Cz_2 = z_1 - z_4$

$Az_3 = z_4 - z_2$ $\quad$ $Bz_3 = z_1 - z_2$ $\quad$ $Cz_3 = z_4 - z_1$

$Az_4 = z_1 - z_3$ $\quad$ $Bz_4 = z_2 - z_1$ $\quad$ $Cz_4 = z_2 - z_3$

Similarly,

$$\frac{\partial u}{\partial r} = \sum_{n=1}^{4} \Omega \, (A_{zn} + B_{zn}\xi + C_{zn}\eta) u_n \qquad (19a)$$

$$\frac{\partial u}{\partial z} = \sum_{n=1}^{4} \Omega \, (A_{rn} + B_{rn}\xi + C_{rn}\eta) u_n \qquad (19b)$$

Using equations (18a,b), (19a,b), (5a,b) and (5b) the following relations can be obtained:

$$\frac{\partial v}{\partial z}\,\frac{\partial v}{\partial z} = \sum_{m=1}^{4}\sum_{n=1}^{4} \Omega^2\{ A_{rm}A_{rn}+(A_{rm}B_{rn}+B_{rm}A_{rn})\xi+(A_{rm}C_{rn}+C_{rm}A_{rn})\eta+$$

$$(B_{rm}C_{rn}+C_{rm}B_{rn})\xi\eta + B_{rm}B_{rn}\xi^2 + C_{rm}C_{rn}\eta^2\}v_m v_n$$

$$\frac{\partial v}{\partial z}\,\frac{\partial u}{\partial r} = \sum_{m=1}^{4}\sum_{n=1}^{4} \Omega^2\{A_{rm}A_{zn}+(A_{rm}B_{zn}+B_{rm}A_{zn})\xi+(A_{rm}C_{zn}+C_{rm}A_{zn})\eta+$$

$$(B_{rm}C_{zn}+C_{rm}B_{zn})\xi\eta + B_{rm}B_{zn}\xi^2 + C_{rm}C_{zn}\eta^2\}v_m u_n$$

$$\frac{\partial v}{\partial r}\,\frac{\partial v}{\partial r} = \sum_{m=1}^{4}\sum_{n=1}^{4} \Omega^2\{A_{zm}A_{zn}+(A_{zm}B_{zn}+A_{zn}B_{zm})\xi+(A_{zm}C_{zn}+C_{zm}A_{zn})\eta+$$

$$(C_{zn}B_{zm}+B_{zn}C_{zm})\xi\eta + B_{zm}B_{zn}\xi^2 + C_{zm}C_{zn}\eta^2\}v_m v_n$$

$$\frac{\partial v}{\partial r}\,\frac{\partial u}{\partial z} = \sum_{m=1}^{4}\sum_{n=1}^{4} \Omega^2\{A_{zm}A_{rn}+(A_{zm}B_{rn}+B_{zm}A_{rn})\xi+(A_{zm}C_{rn}+A_{rn}C_{zm})\eta+$$

$$(B_{zm}C_{rn}+C_{zm}B_{rn})\xi\eta + B_{zm}B_{rn}\xi^2 + C_{zm}C_{rn}\eta^2\}v_m u_n$$

$$\frac{\partial v}{\partial z}\,\frac{u}{r} = \sum_{m=1}^{4}\sum_{n=1}^{4} \frac{\Omega}{4\pi}\{A_{rm}+(B_{rm}+A_{rm}B_n)\xi+(C_{rm}+A_{rm}C_n)\eta+$$

$$(C_{rm}B_n+B_{rm}C_n+A_{rm}D_n)\xi\eta + B_{rm}B_n\xi^2 + C_{rm}C_n\eta^2 + B_{rm}D_n\xi^2\eta+$$

$$C_{rm}D_n\xi\eta^2\}v_m u_n$$

$$\frac{\partial v}{\partial r}\,\frac{u}{r} = \sum_{m=1}^{4}\sum_{n=1}^{4} \frac{\Omega}{4\pi}\{A_{zm}+(A_{zm}B_n+B_{zm})\xi+(A_{zm}C_n+C_{zn})\eta+$$

$$(B_{zm}C_n+C_{zm}B_n+A_{zm}D_n)\xi\eta + B_{zm}B_n\xi^2 + C_{zm}C_n\eta + B_{zm}D_n\xi^2\eta+C_{zm}D_n\xi\eta^2\}v_m u_n$$

$$\frac{u}{r}\,\frac{\partial u}{\partial z} = \sum_{m=1}^{4}\sum_{n=1}^{4} \frac{\Omega}{4\pi}\{A_{rn}+(B_{rn}+B_m A_{rn})\xi+(C_m A_{rn}+C_{rn})\eta+$$

$$(B_m C_{rn}+C_m B_{rn}+D_m A_{rn})\xi\eta + B_m B_{rn}\xi^2 + C_m C_{rn}\eta^2 + D_m B_{rn}\xi^2\eta+$$

$$D_m C_{rn}\xi\eta^2\}u_m u_n$$

$$\frac{u}{r}\,\frac{\partial u}{\partial r} = \sum_{m=1}^{4}\sum_{n=1}^{4} \frac{\Omega}{4\pi}\{A_{zn}+(B_{zn}+B_m A_{zn})\xi+(C_m A_{zn}+C_{zn})\eta+(B_m C_{zn}+$$

$$C_m B_{zn}+D_m A_{zn})\xi\eta + B_m B_{zn}\xi^2 + C_m C_{zn}\eta + D_m B_{zn}\xi^2\eta + D_m C_{zn}\xi\eta^2\}u_m u_n$$

$$\frac{u}{r}\frac{u}{r} = \sum_{m=1}^{4}\sum_{n=1}^{4}\{1 + (B_m+B_n)\xi + (C_m+C_n)\eta + (D_m+D_n + B_m C_n + C_m B_n)\xi\eta +$$

$$B_m B_n \xi^2 + C_m C_n \eta^2 + (B_m D_n + D_m B_n)\xi\eta^2 + (C_m D_n + D_m C_n)\xi^2\eta + D_m D_n \xi^2\eta^2\}$$

2. STRAIN ENERGY AND ELEMENT STIFFNESS MATRIX

Strains in the element are given by

$$\underset{\sim}{\gamma} = \begin{bmatrix} \gamma_z \\ \gamma_r \\ \gamma_\theta \\ \gamma_{zr} \end{bmatrix} = \begin{bmatrix} \frac{\partial v}{\partial z} \\ \frac{\partial u}{\partial r} \\ u/r \\ \frac{\partial u}{\partial z} + \frac{\partial v}{\partial r} \end{bmatrix}$$

Element stress strain relationship can be written as

$$\begin{bmatrix} \sigma_z \\ \sigma_r \\ \sigma_\theta \\ \sigma_{rz} \end{bmatrix} = \begin{bmatrix} D_{11} & D_{12} & D_{13} & 0 \\ D_{21} & D_{22} & D_{23} & 0 \\ D_{31} & D_{32} & D_{33} & 0 \\ 0 & 0 & 0 & D_{44} \end{bmatrix} \begin{bmatrix} \gamma_z \\ \gamma_r \\ \gamma_\theta \\ \gamma_{rz} \end{bmatrix}$$

in which

$$D_{11} = CE_T(E_L - E_T\nu_{TL}^2)$$

$$D_{12} = CE_T(E_L\nu_{TT} + E_T\nu_{TT}^2)$$

$$D_{13} = D_{23} = CE_TE_L\nu_{TL}(1+\nu_{TT})$$

$$D_{22} = CE_T(E_L - E_T\nu_{TL}^2)$$

$$D_{33} = CE_L^2(1-\nu_{TT}^2)$$

$$D_{44} = G_T$$

$$C = [E_T(1-\nu_{TT}^2) - 2E_T\nu_{TL}^2(1+\nu_{TT})]^{-1}$$

Strain energy in the element is given by

$$U = \frac{1}{2}\int_V \underset{\sim}{\gamma}^T \underset{\sim}{\sigma}\, dV$$

$$= \frac{1}{2}\iiint (\gamma_z\sigma_z + \gamma_r\sigma_r + \gamma_\theta\sigma_\theta + \gamma_{zr}\sigma_{zr})dv$$

$$= \frac{1}{2}\iiint \gamma_z(D_{11}\gamma_z + D_{12}\gamma_r + D_{13}\gamma_\theta + \gamma_r(D_{21}\gamma_z + D_{22}\gamma_r + D_{23}\gamma_\theta)$$

$$+ \gamma_\theta(D_{31}\gamma_z + D_{32}\gamma_r + D_{33}\gamma_\theta) + \gamma_{rz}(D_{44}\gamma_{rz})\}\, r\,d\theta\,dr\,dz$$

Since $\int_0^{2\pi} d\theta = 2\pi$, $\iint dr\,dz = \int_{-1}^{1}\int_{-1}^{1} |J|\, d\xi\, d\eta$

$$U = \frac{1}{2}\,(2\pi\int_{-1}^{1}\int_{-1}^{1} \{(D_{11}\frac{\partial v}{\partial z}\,\frac{\partial v}{\partial z} + D_{12}\frac{\partial v}{\partial z}\,\frac{\partial v}{\partial r} + D_{13}\frac{\partial v}{\partial z}\,\frac{u}{r} +$$

$$(D_{21}\frac{\partial u}{\partial r}\frac{\partial v}{\partial z} + D_{22}\frac{\partial u}{\partial r}\frac{\partial u}{\partial r} + D_{23}\frac{\partial u}{\partial r}\frac{u}{r}) +$$

$$(D_{31}\frac{u}{r}\frac{\partial v}{\partial z} + D_{32}\frac{u}{r}\frac{\partial u}{\partial r} + D_{33}\frac{u}{r}\frac{u}{r}) +$$

$$(D_{44}\{\frac{\partial v}{\partial r}\frac{\partial v}{\partial r} + \frac{\partial v}{\partial r}\frac{\partial u}{\partial z} + \frac{\partial u}{\partial z}\frac{\partial v}{\partial r} + \frac{\partial u}{\partial z}\frac{\partial u}{\partial z}\})\, r\, |J|\, d\eta\, d\xi \quad (20)$$

Denote

$$F_{mn} = \int_{-1}^{1}\int_{-1}^{1} \frac{\Omega}{8}\{A_{rm}A_{rn} + (A_{rm}B_{rn} + B_{rm}A_{rn})\xi + (A_{rm}C_{rn} + C_{rm}A_{rn})\eta + (B_{rm}C_{rn} + C_{rm}B_{rn})\xi\eta$$

$$+ B_{rm}B_{rn}\xi^2 + C_{rm}C_{rn}\eta^2\}\, r\, d\eta\, d\xi$$

$$G_{mn} = \int_{-1}^{1}\int_{-1}^{1} \frac{\Omega}{8}\{A_{rm}A_{zn} + (A_{rm}B_{zn} + B_{rm}A_{zn})\xi + (A_{rm}C_{zn} + C_{rm}A_{zn})\eta +$$

$$(B_{rm}C_{zn} + C_{rm}B_{zn})\xi\eta + B_{rm}B_{zn}\xi^2 + C_{rm}C_{zn}\eta^2\}\, r\, d\eta\, d\xi$$

$$I_{mn} = \int_{-1}^{1}\int_{-1}^{1} \frac{\Omega}{8}\{A_{zm}A_{zn} + (A_{zm}B_{zn} + A_{zn}B_{zm})\xi + (A_{zm}C_{zn} + C_{zm}A_{zn})\eta +$$

$$(C_{zn}B_{zm} + B_{zn}C_{zm})\xi\eta + B_{zm}B_{zn}\xi^2 + C_{zm}C_{zn}\eta^2\}\, r\, d\eta\, d\xi$$

$$L_{mn} = \int_{-1}^{1}\int_{-1}^{1} \frac{\Omega}{8}\{A_{zm}A_{rn} + (A_{zm}B_{rn} + B_{zm}A_{rn})\xi + (A_{zm}C_{rn} + A_{rm}C_{zn})\eta +$$

$$(B_{zm}C_{rn} + C_{zm}B_{rn})\xi\eta + B_{zm}B_{rn}\xi^2 + C_{zm}C_{rn}\eta^2\}\, r\, d\eta\, d\xi$$

$$P_{sn} = \int_{-1}^{1}\int_{-1}^{1} \frac{1}{32}\{A_{rs}+(B_{rs}+A_{rs}B_n)\xi+(C_{rs}+A_{rs}C_n)\eta + (C_{rs}B_n+B_{rs}C_n+A_{rs}D_n)\xi\eta$$

$$+ B_{rs}B_n\xi^2 + C_{rs}C_n\eta^2 + B_{rs}D_n\xi^2\eta + C_{rs}D_n\xi\eta^2\}\,d\eta d\xi$$

$$Q_{sn} = \int_{-1}^{1}\int_{-1}^{1} \frac{1}{32}\{A_{zs}+(A_{zs}B_n+B_{zs})\xi+(A_{zs}C_n+C_{zn})\eta+(B_{zs}C_n+C_{zs}B_n+A_{zs}D_n)\xi\eta +$$

$$B_{zs}B_n\xi^2+C_{zs}C_n\eta^2+B_{zs}D_n\xi^2\eta+C_{zs}D_n\xi\eta^2\}d\eta d\xi$$

$$R_{sn} = \int_{-1}^{1}\int_{-1}^{1} \frac{1}{32}\{A_{rn}+(B_{rn}+B_m A_{rn})\xi+(C_m A_{rn}+C_{rn})\eta+(B_m C_{rn}+C_m B_{rn}+D_m A_{rs})\xi\eta +$$

$$B_m B_{rn}\xi^2+C_m C_{rn}\eta^2+D_m B_{rn}\xi^2\eta+D_m C_{rn}\xi\eta^2\}d\eta d\xi = P_{nm}$$

$$S_{sn} = \int_{-1}^{1}\int_{-1}^{1} \frac{1}{32}\{A_{zn}+(B_{zn}+B_m A_{zn})\xi+(C_m A_{zn}+C_{zn})\eta+(B_m C_{zn}+C_m B_{zn}+D_m A_{rn})\xi\eta$$

$$+ B_m B_{zn}\xi^2 + C_m C_{zn}\eta^2 + D_m B_{zn}\xi^2\eta + D_m C_{zn}\xi\eta^2\}d\eta d\xi = Q_{nm}$$

$$T_{sn} = \int_{-1}^{1}\int_{-1}^{1} \frac{1}{128\,r}\{1+(B_m+B_n)\xi+(C_m+C_n)\eta+(D_m+D_n+B_m C_n+C_m B_n)\xi\eta +$$

$$B_m B_n\xi^2 + C_m C_n\eta^2 + (B_m D_n+D_m B_n)\xi^2\eta$$

$$(C_m D_n+D_m C_n)\xi\eta^2 + D_s D_n\xi^2\eta^2\}\,|J|\,d\eta d\xi$$

These integrals to appear in (20) are evaluated by using six point Gaussian quadrature. With the notations above we can rewrite (18) in the form,

$$U = \frac{1}{2}(2\pi)\sum_{s=1}^{4}\sum_{n=1}^{4}\{D_{11}F_{sn}v_s v_n+D_{12}G_{sn}v_s u_n+D_{13}P_{sn}v_m u_n+D_{21}G_{ns}u_s v_n$$

$$+ D_{22}I_{sn}u_s u_n+D_{23}Q_{sn}u_s u_n+D_{31}P_{nm}u_s v_n+D_{32}Q_{ns}u_s u_n$$

$$+ D_{33}T_{sn}u_s u_n+D_{44}(I_{sn}v_s v_n+L_{ns}u_s v_n+{}_{sn}{}_s u_n)\}$$

or

$$U = \frac{1}{2}(2\pi)\sum_{s=1}^{4}\sum_{n=1}^{4}\{A_{sn}v_s v_n+B_{sn}v_s u_n+C_{sn}u_s v_n+E_{sn}u_s u_n\}$$

or

$$U = \frac{1}{2}(2\pi)\sum_{m=1}^{4}\sum_{n=1}^{4}[v_m u_m]\begin{bmatrix} A_{mn} & B_{mn} \\ C_{mn} & E_{mn} \end{bmatrix}\begin{bmatrix} v_n \\ u_n \end{bmatrix}$$

The stiffness matrix $\underset{\sim}{K}$ is identified as

$$\underset{\sim}{K} = \sum_{m=1}^{4}\sum_{n=1}^{4}\begin{bmatrix} A_{mn} & B_{mn} \\ C_{mn} & E_{mn} \end{bmatrix} \tag{21}$$

where

$$A_{mn} = D_{11}F_{mn}+D_{44}I_{mn}$$

$$B_{mn} = D_{12}G_{mn}+D_{13}P_{mn}+D_{44}L_{mn}$$

$$C_{mn} = D_{21}G_{nm}+D_{31}P_{nm}+D_{44}L_{nm}$$

$$E_{mn} = D_{22}I_{mn}+D_{23}Q_{mn}+D_{32}Q_{nm}+D_{33}T_{mn}+D_{44}F_{mn}$$

The stiffness matrix obtained from Eq. (21) is of the form,

$$K = \left[\begin{array}{cccc:cccc} v_1 & v_2 & v_3 & v_4 & u_1 & u_2 & u_3 & u_4 & \\ A_{11} & A_{12} & A_{13} & A_{14} & B_{11} & B_{12} & B_{13} & B_{14} & v_1 \\ A_{21} & A_{22} & A_{23} & A_{24} & B_{21} & B_{22} & B_{23} & B_{24} & v_2 \\ A_{31} & A_{32} & A_{33} & A_{34} & B_{31} & B_{32} & B_{33} & B_{34} & v_3 \\ A_{41} & A_{42} & A_{43} & A_{44} & B_{41} & B_{42} & B_{43} & B_{44} & v_4 \\ \hdashline C_{11} & C_{12} & C_{13} & C_{14} & E_{11} & E_{12} & E_{13} & E_{14} & u_1 \\ C_{21} & C_{22} & C_{23} & C_{24} & E_{21} & E_{22} & E_{23} & E_{24} & u_2 \\ C_{31} & C_{32} & C_{33} & C_{34} & E_{31} & E_{32} & E_{33} & E_{34} & u_3 \\ C_{41} & C_{42} & C_{43} & C_{44} & E_{41} & E_{42} & E_{43} & E_{44} & u_4 \end{array}\right]$$

Elements of stiffness matrix thus obtained should be rearranged so that they conform to the applied force vector (or computed displacement vector).

3. FORCE VECTOR DUE TO BODY FORCES

Let p_z be the density of body of element. The force vector due to dead load is given by

$$F_N^K = 2\pi \int_{-1}^{1}\int_{-1}^{1} \psi_N p_{(z)}^K |J| r d\eta d\xi$$

or

$$\underset{\sim}{F} = 2\pi \int_{-1}^{1}\int_{-1}^{1} \underset{\sim}{\bar{\psi}}^T \underset{\sim}{P} |J| r d\eta d\xi$$

where

$$\underset{\sim}{\bar{\psi}} = \begin{bmatrix} \psi_1 & 0 & \psi_2 & 0 & \psi_3 & 0 & \psi_4 & 0 \\ 0 & \psi_1 & 0 & \psi_2 & 0 & \psi_3 & 0 & \psi_4 \end{bmatrix}$$

$$\underset{\sim}{P} = [0 \quad p_{(z)}]^T$$

The components of force vector become

$$\underset{\sim}{F} = [0 \quad F_{1z} \quad 0 \quad F_{2z} \quad 0 \quad F_{3z} \quad 0 \quad F_{4z}]^T$$

in which

$$F_{1z} = -2\pi p_z \int_{-1}^{1}\int_{-1}^{1} (1-\xi-\eta+\xi\eta) r |J| d\eta d\xi$$

$$F_{2z} = -2\pi p_z \int_{-1}^{1}\int_{-1}^{1} (1+\xi-\eta-\xi\eta) r |J| d\eta d\xi$$

$$F_{3z} = -2\pi p_z \int_{-1}^{1}\int_{-1}^{1} (1+\xi+\eta+\xi\eta) r |J| d\eta d\xi$$

$$F_{4z} = -2\pi p_z \int_{-1}^{1}\int_{-1}^{1} (1-\xi+\eta-\xi\eta) r |J| d\eta d\xi$$

4. STRESSES AT ELEMENT CENTROID

From earlier developments of strain-displacement relations it is possible to write

$$\underset{\sim}{\gamma} = \left[\frac{\partial v}{\partial z} \quad \frac{\partial u}{\partial r} \quad \frac{u}{r} \quad \frac{\partial v}{\partial r} + \frac{\partial u}{\partial z}\right]^T$$

or

$$\underset{\sim}{\gamma} = \sum_{n=1}^{4} \Omega \begin{bmatrix} (A_{rn} + B_{rn}\xi + C_{rn}\eta)v_n \\ (A_{zn} + B_{zn}\xi + C_{zn}\eta)u_n \\ \frac{1}{4\Omega r}(1 + B_n\,\xi + C_n\,\eta + D_n\,\xi\eta)u_n \\ A_{rn} + B_{rn}\xi + C_{rn}\eta)u_n + (A_{zn} + B_{zn} + C_{zn}\eta)v_n \end{bmatrix}$$

in which all notations are defined earlier.

If stresses are sought at the centroid of an element we have $\xi = \eta = 0$. Therefore,

$$\underset{\sim}{\gamma_0} = \sum_{n=1}^{4} \Omega \begin{bmatrix} A_{rn}\,v_n \\ A_{zn}\,u_n \\ \frac{1}{4\Omega r}\,u_n \\ A_{rn}\,u_n + A_{zn}\,v_n \end{bmatrix}$$

The stresses at the centroid are then obtained from the standard stress-strain relations.

APPENDIX B

COMPUTER PROGRAMS

There are six independent computer programs in the present report:

(1) SP1 - This program performs static elastoplastic analysis for a fiber-reinforced thin shell.

(2) SVP1 - This program performs static viscoelastoplastic analysis for a fiber-reinforced thin shell.

(3) DVP1 - This program performs dynamic viscoelastoplastic analysis for a fiber-reinforced thin shell. Dynamic elastoplastic analysis is obtained as a special case.

(4) SP2 - This program performs static elastoplastic analysis for a fiber-reinforced thick shell.

(5) SVP2 - This program performs static viscoelastoplastic analysis for a fiber-reinforced thick shell.

(6) DVP2 - This program performs dynamic viscoelastoplastic analysis for a fiber-reinforced thick shell. Dynamic elastoplastic analysis is obtained as a special case. This program is also capable of analyzing a body composed of several monolithic and composite materials.

It should be noted that all of these 6 programs can handle isotropic materials and linear elastic behavior as special cases.

A summary of the basic theories used and various features available in the programs is given below:

1. Thin Shell

   a. Novozhilov's linear thin shell theory is used.

   b. Curved finite element is used. Interpolation functions are based on linear variations of meridional and tangential displacement and cubic variation of transverse displacement.

   c. Modified Hill's anisotropic yield parameters are derived and specialized for layers of angle or cross plys.

   d. Internal or hidden variables are used for viscous effects.

   e. Solution of governing equations is based on incremental approach with increments in loading for time-independent problems and increments in time for time dependent problems.

2. Thick Shell

   a. Three dimensional theory for strain-displacement is used and specialized for axisymmetric deformations.

   b. Plane strain isoparametric finite element is used with linear variation of radial and axial displacements.

   c. Treatment of inelastic and viscous properties and solution procedures are the same as in a thin shell.

Descriptions of each program including subroutine organization chart, subroutine descriptions, flow chart, and data input format are given in the following subappendices.

APPENDIX B.1.1

SP1 - SUBROUTINE ORGANIZATION CHART

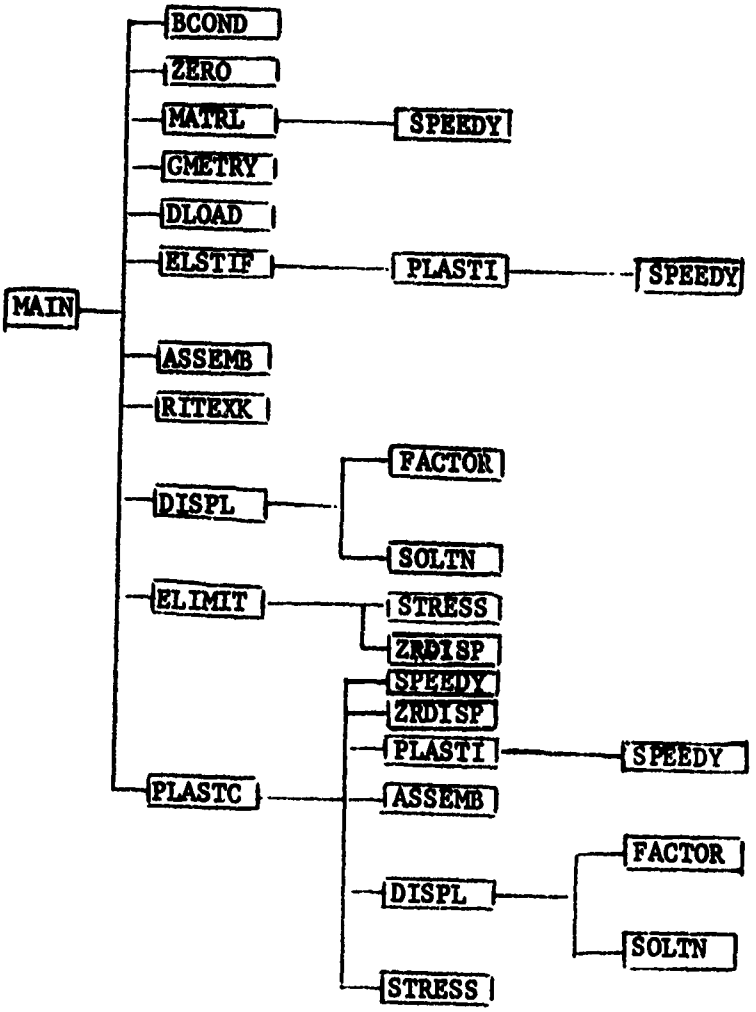

APPENDIX B.1.2

SP1 - DESCRIPTIONS OF SUBROUTINES

SUBROUTINE NAME	DESCRIPTION
ASSEMB	Assembles stiffness matrix and force vector in a single subscripted array with boundary conditions imposed.
BCOND	Reads boundary conditions and initializes the row-column indices for assembling.
DISPL	Calls FACTOR and SOLTN, and writes nodal forces and displacements.
DLOAD	Computes the equivalent nodal forces.
ELIMIT	Computes and writes the elastic limit displacements, elastic limit stresses, and elastic limit load.
ELSTIF	Forms elastic stiffness matrix.
FACTOR SOLTN	Solves given simultaneous equations in a single subscripted array.
GMETRY	Calculates, for each element, the geometrical quantities necessary for Simpson's integration along the line element.
MATRL	Reads all material properties and constructs transformation matrices and local and global elasticity matrices.
PLASTC	Performs incremental elastoplastic analysis.
PLASTI	Performs Simpson's integration with given stress-strain relations to form the element stiffness matrix.
RITEXK	Writes non-zero elements of the lower half of the global stiffness matrix with row number.
SPEEDY	Performs matrix multiplication.
STRESS	Computes strains and stresses.
ZERO	Zeroes out the given matrix.
ZRDISP	Transforms displacements into Z-R coordinate system and writes.

APPENDIX B.1.3

SP1 - FLOW CHART

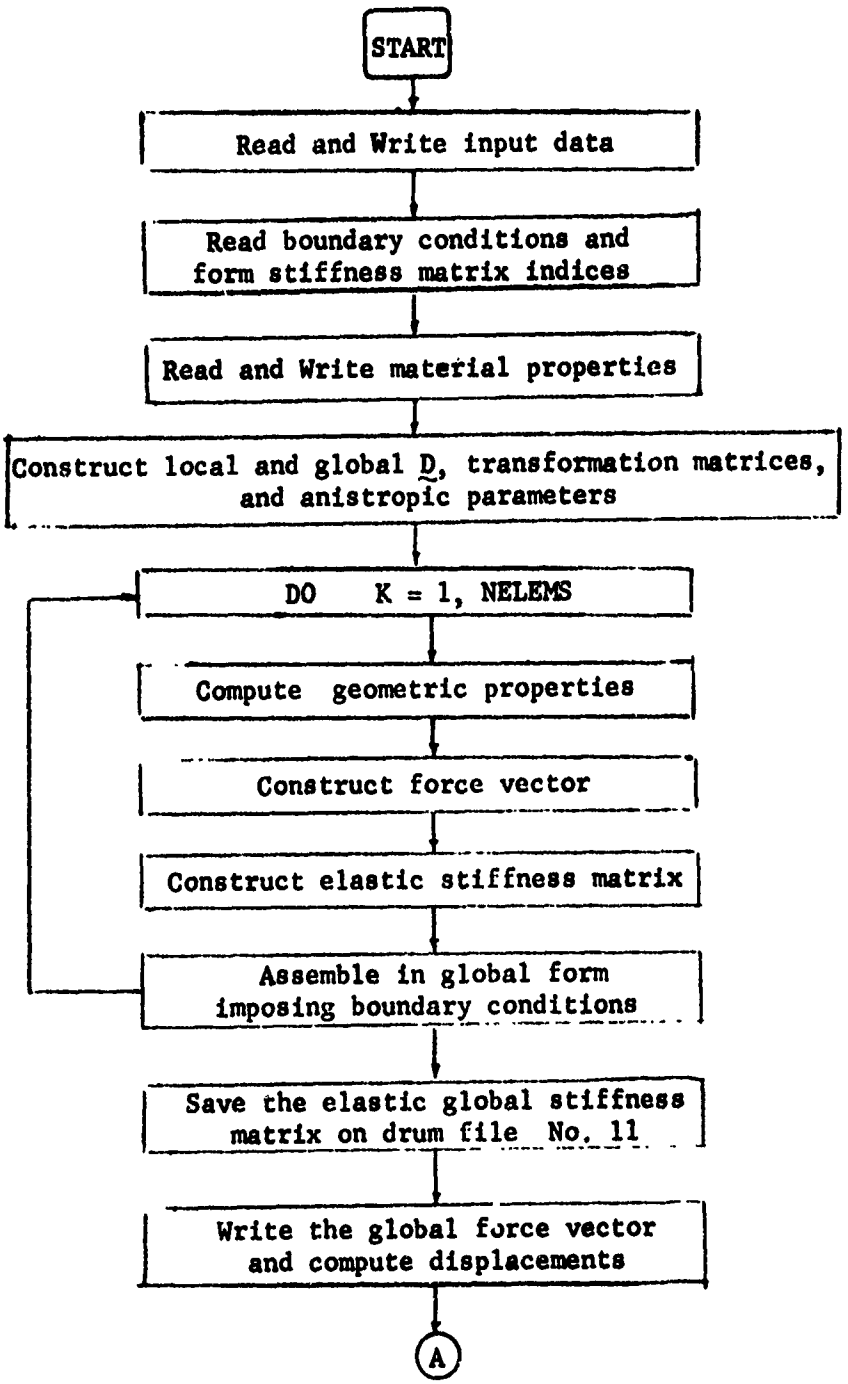

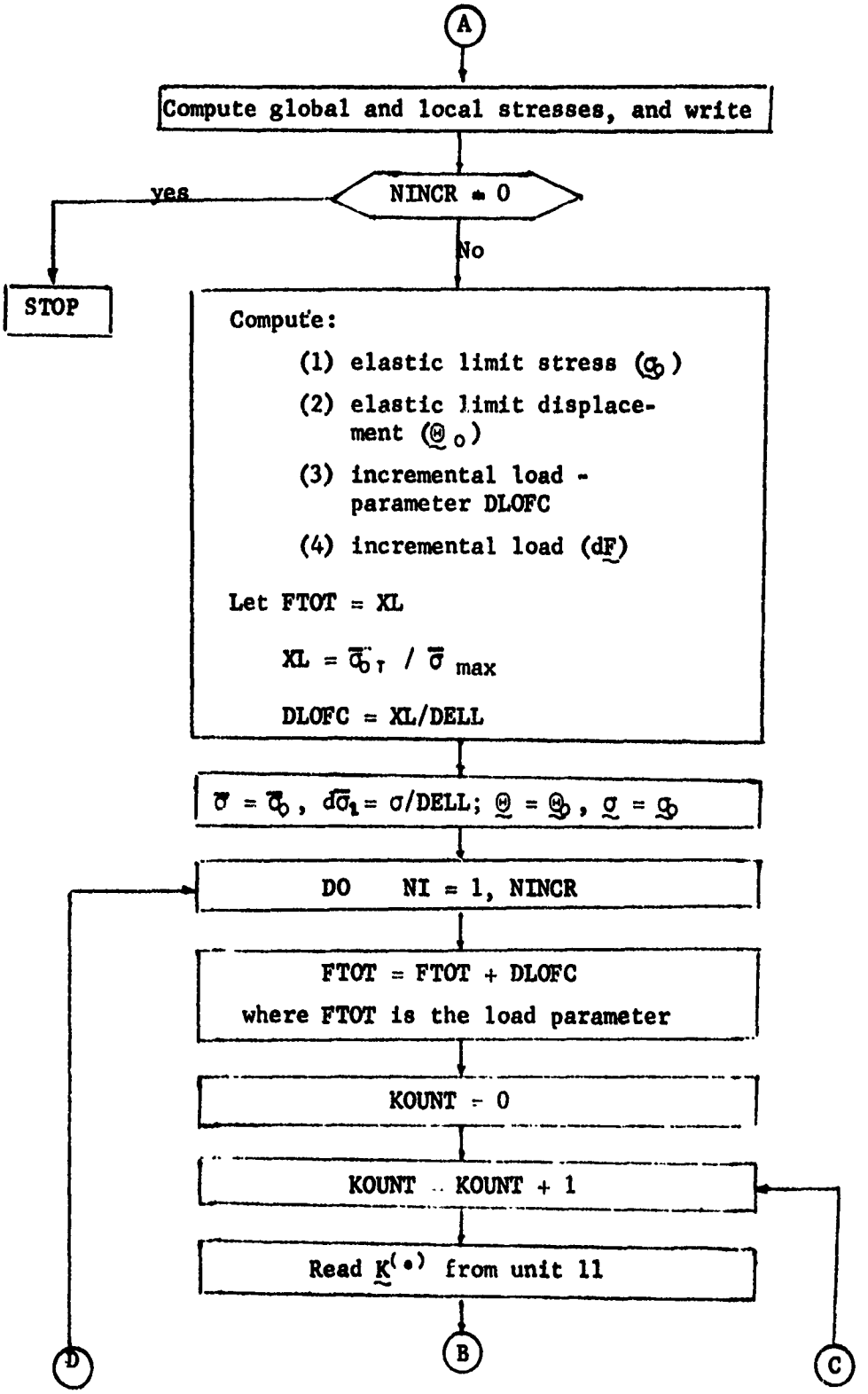
A
Compute global and local stresses, and write
NINCR = 0
yes
No
STOP
Compute:
(1) elastic limit stress (σ_0)
(2) elastic limit displacement ($\underset{\sim}{u}_0$)
(3) incremental load - parameter DLOFC
(4) incremental load ($d\underset{\sim}{F}$)
Let FTOT = XL
XL = $\bar{\sigma}_{0T}$ / $\bar{\sigma}_{max}$
DLOFC = XL/DELL
$\bar{\sigma} = \bar{\sigma}_0$, $d\bar{\sigma}_1 = \sigma$/DELL; $\underset{\sim}{u} = \underset{\sim}{u}_0$, $\underset{\sim}{\sigma} = \underset{\sim}{\sigma}_0$
DO NI = 1, NINCR
FTOT = FTOT + DLOFC
where FTOT is the load parameter
KOUNT = 0
KOUNT = KOUNT + 1
Read $\underset{\sim}{K}^{(\bullet)}$ from unit 11
B
C
D

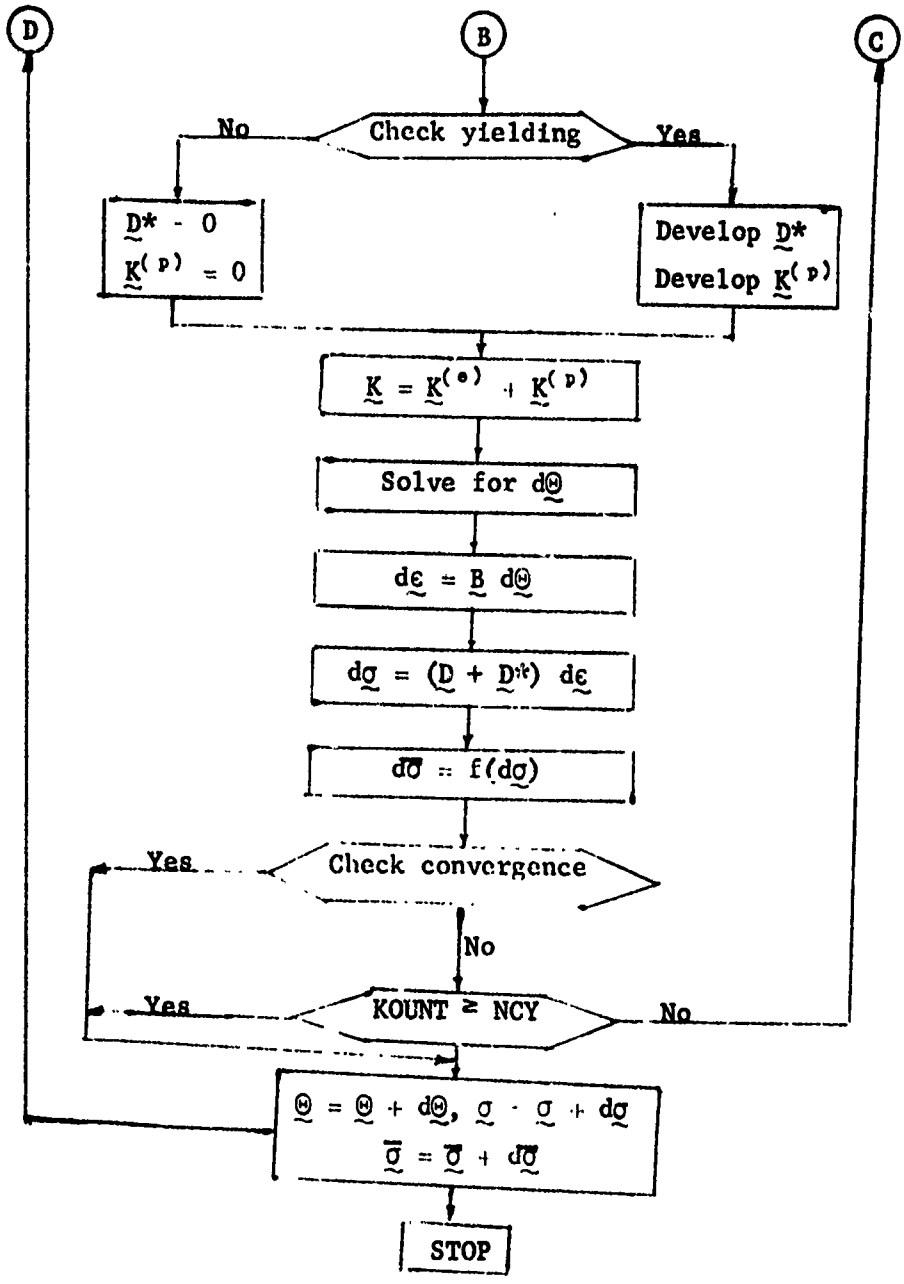
D
B
C
No
Check yielding
Yes
D* - 0
K(p) = 0
Develop D*
Develop K(p)
K = K(e) + K(p)
Solve for dΘ
dε = B dΘ
dσ = (D + D*) dε
dσ̄ = f(dσ)
Yes
Check convergence
No
Yes
KOUNT ≥ NCY
No
Θ = Θ + dΘ, σ = σ + dσ
σ̄ = σ̄ + dσ̄
STOP

APPENDIX B.1.4

SP1 - DATA INPUT FORMAT

Card 1: FORMAT (20A4)

TITLE (I) Title of the problem

Card 2: FORMAT (10I5, 3F10.4)

(1) NELEMS - No. of elements

(2) NNODES - No. of nodes

(3) NET - No. of stations for Simpson's integration

Suggested values of NET

$\phi_2 - \phi_1$	NET
$0 \sim 3^o$	15
$3^o \sim 5^o$	19
$5^o \sim 9^o$	23
$9^o \sim 14^o$	29

The program assumes NET = 15, if NET = 0

(4) MECH - Signal for distributed load

0, if a force vector for distributed loads is not wanted

1, if a force vector for distributed loads is wanted

(5) NDITO - Signal for uniform or irregular distributed load

0, uniform pressure

1, pressure varies meridionally

(6) NINCR - No. of load increment desired

Set NINCR = DELL if two times the elastic limit load is to be applied.

Suggested values of NINCR and DELL

NINCR = 40 ~ 100
DELL = 40 ~ 100 if NCY = 0

NINCR = 20 ~ 50
DELL = 20 ~ 50 if NCY ≥ 3

NINCR = 0 for elastic analysis

(7) NLA - No. of layers for angle or cross plys

(8) NBC - No. of nodes with boundary condition(s)

(9) NCY - No. of iterations within a load increment

(10) NCON - No. of node(s) with concentrated load(s)

(11) DELL - Fraction of elastic limit load to be applied for each load increment.

(12) PER - Percent error allowed for convergence in elastoplastic analysis. Suggested value: 5 ~ 10

(13) PCTARC- Fraction of arc length ignored at a pole. Suggested value: .01

Cards 3: FORMAT (3X, 2E12.6)

(1) Z(N) - Z - coordinate value

(2) R(N) - R - coordinate value

Note: Provide one card for each node in the order of node number. The node number may be recorded in 3X spaces.

Cards 4: FORMAT (2I3, 4E12.6)

(1) NODE1 - first node of the element

(2) NODE2 - second node of the element

(3) PHI1 - ϕ_1

(4) PHI2 - ϕ_2

(5) H1 - thickness at NODE1

(6) H2 - thickness at NODE2

Note: Repeat NELEMS times in the order of element number.

The sign convention for ϕ is shown below

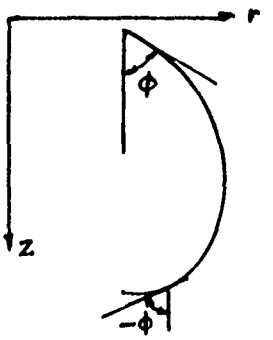

Card(s) 5: FORMAT (5I5)

(1) NOD - node number with boundary condition(s)

(2) NDIR(1) = 1, if meridional displacement is not allowed
0, if free

(3) NDIR(2) = 1, if circumferential displacement is not allowed
0, if free

(4) NDIR(3) = 1, if normal displacement is not allowed
0, if free

(5) NDIR(4) = 1, if the rotation of the normal is not allowed
0, if free

Note: Repeat NBC times.

Card 6: FORMAT (I5)

IANG = 0, if fiber angles are same for every element
1, if not

Card 7: FORMAT (8F10.0)

SIGS(I) - Yield stress in the direction of the normal to fiber for each layer.

Card 8: FORMAT (8F10.0)

SIGT(I) - Yield stress in fiber direction for each layer.

Card 9: FORMAT (8F10.0)

SIG4(I) - Yield stress in 45^{o} from fiber direction for each layer.

Card 10: FORMAT (8F10.0)

TAUT(I) - Yield stress in shear for each layer

Card 11: FORMAT (8F10.0)

EPX(I) - Elastic modulus normal to fiber for each layer

Card 12: FORMAT (8F10.0)

EPY(I) - Elastic modulus in fiber direction for each layer

Note: EPX(I) = EPY(I) for isotropic case

Card 13: FORMAT (8F10.0)

GP(I) - Elastic shear modulus for each layer

Card 14: FORMAT (8F10.0)

XNU(I) - Poisson's ratio (normal to fiber) for each layer

Card 15: FORMAT (8F10.0)

YNU(I) - Poisson's ratio (in fiber direction) for each layer

Note: XNU(I) = YNU(I) for isotropic case

Card 16: FORMAT (8F10.0)

EPX(I) - Plastic modulus normal to fiber for each layer

Card 17: FORMAT (8F10.0)

EPY(I) - Plastic modulus in fiber direction for each layer

Card 18: FORMAT (8F10.0)

EP4(I) - Plastic modulus in 45^{o} from fiber direction for each layer

Card 19: FORMAT (8F10.0)

GP(I) - Plastic shear modulus for each layer

Card(s) 20: FORMAT (8F10.0)

ALPHA(I) - fiber angles for each layer measured from horizontal line.

Note: Repeat Card(s) 20 NELEMS times in the order of element number if IANG ≠ 0.

Card(s) 21: FORMAT (6E10.0)

(1) PP1(1) - distributed pressure in direction 1 at node 1

(2) PP2(1) - distributed pressure in direction 2 at node 1

(3) PP3(1) - distributed pressure in direction 3 at node 1

(4) PP1(2) - distributed pressure in direction 1 at node 2

(5) PP2(2) - distributed pressure in direction 2 at node 2

(6) PP3(3) - distributed pressure in direction 3 at node 2

Note: Repeat NELEMS times in the order of element number if NDITO = 1

Card(s) 22: FORMAT (I5, 4E15.6)

(1) NOD - node number

(2) CL(1) - concentrated force in direction 1

(3) CL(2) - concentrated force in direction 2

(4) CL(3) - concentrated force in direction 3

(5) CL(4) - concentrated force in direction 4

Note: Repeat NCON times.

Omit if NCON = 0.

APPENDIX B.2.1

SVP1 - SUBROUTINE ORGANIZATION CHART

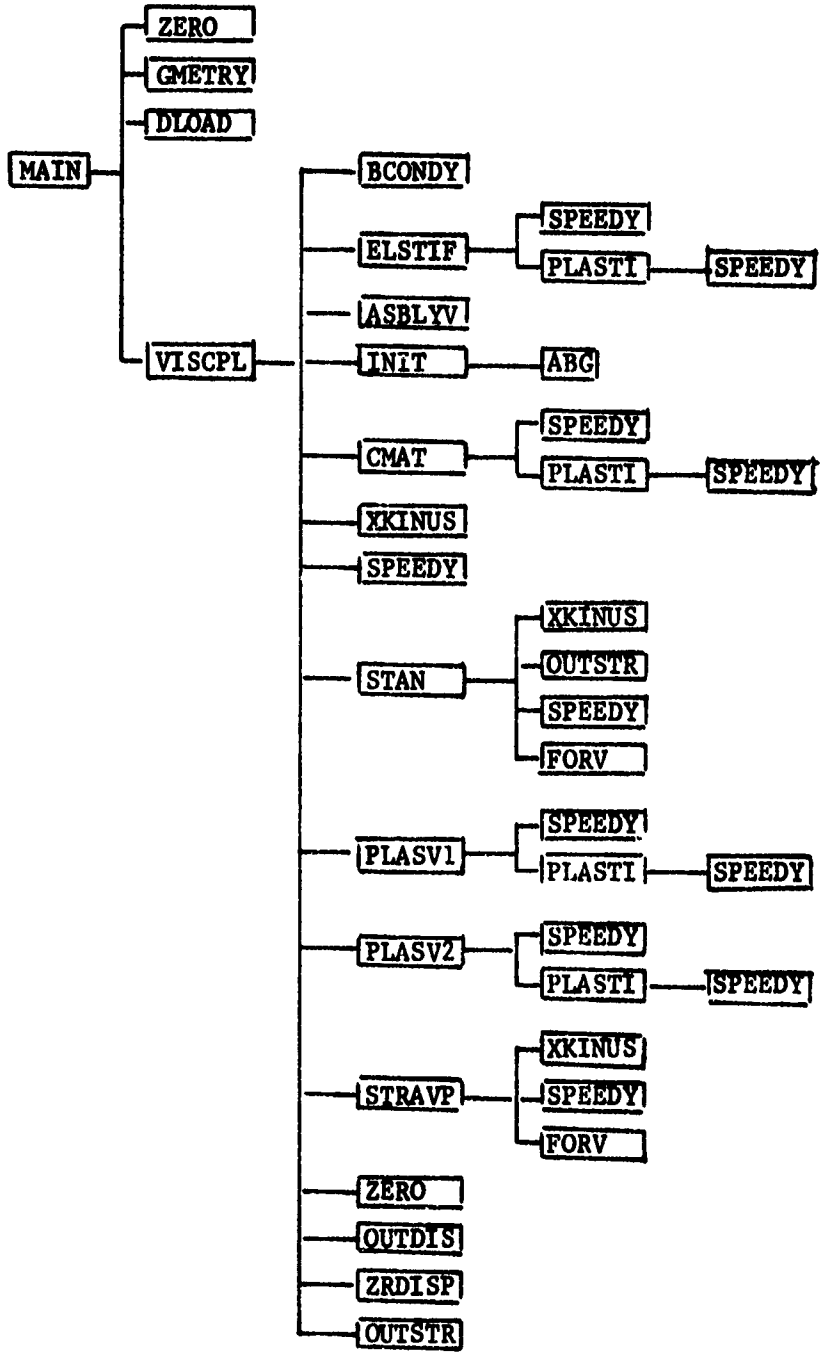

APPENDIX B.2.2

SVP1 - DESCRIPTIONS OF SUBROUTINES

SUBROUTINE NAME	DESCRIPTION
ABG	Calculates viscous constants $A^{(r)}$, $B^{(r)}$, $C^{(r)}$.
ASBLYV	Assembles in global form.
BCONDY	Imposes boundary condition(s).
CMAT	Forms the viscosity matrix.
DLOAD	Computes the equivalent nodal forces.
ELSTIF	Reads the material properties and forms the elastic stiffness matrix.
FORV	Performs integration for viscous force vector.
GMETRY	Calculates, for each element, the geometrical quantities necessary for Simpson's integration along the line element.
INIT	Reads the viscous property and forms submatrices for viscosity matrix.
OUTDIS	Writes the displacements.
OUTSTR	Writes the stresses and the equivalent stresses.
PLASTI	Performs the Simpson's integration to form stiffness or viscosity matrix.
PLASV1	Develops plastic stiffness matrix.
PLASV2	Develops plastic stiffness matrix.
SPEEDY	Performs matrix multiplication.
STAN	Calculates viscous and elastic stresses, checks yielding.
STRAVP	Calculates incremental viscous and plastic stresses, incremental equivalent stresses, and per cent error.
VISCP	Performs step by step integration.

APPENDIX B.2.2 (Cont.)

SUBROUTINE NAME	DESCRIPTION
XKINVS	Inverts a given symmetric matrix.
ZERO	Zeroes out a given matrix.
ZRDISP	Transforms the displacements into the Z-R coordinate system and writes.

APPENDIX B.2.3

SVP1 - FLOW CHART

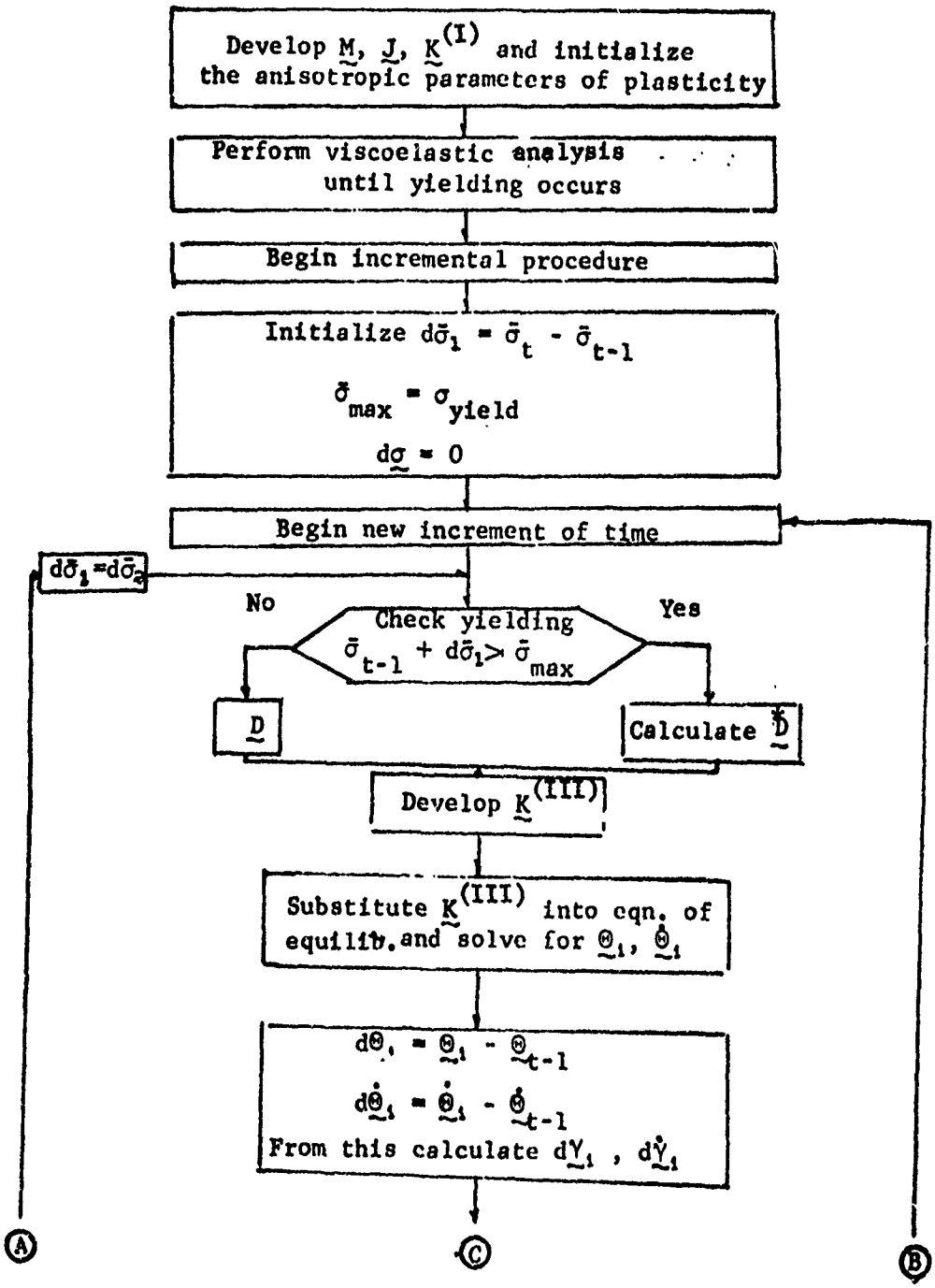

APPENDIX B.2.3 (continued)

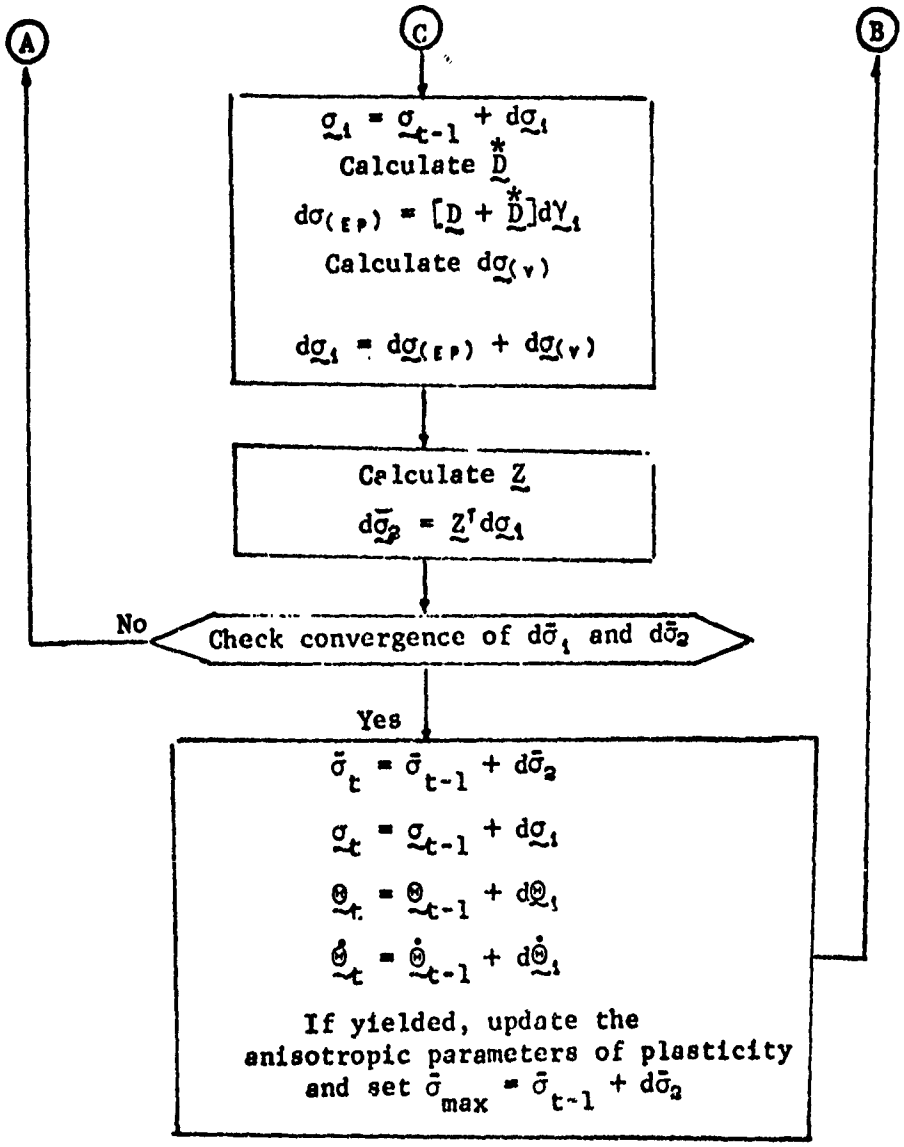

APPENDIX B.2.4

SVP1 - DATA INPUT FORMAT

Card 1: FORMAT (20AA)

TITLE(I) Title of the Problem

Card 2: FORMAT (10I5, 3F10.4)

(1) NELEMS - No. of elements

(2) NNODES - No. of nodes

(3) NET - No. of stations for Simpson's integration

Suggested value of NET:

$\varphi_2 - \varphi_1$	NET
$0 \sim 3^0$	15
$3^0 \sim 5^0$	19
$5^0 \sim 9^0$	23
$9^0 \sim 15^0$	29

The program assumes NET = 15, if NET = 0.

(4) MECH - Signal for distributed load

0, if a force vector for distributed load is not wanted.

1, if a force vector for distributed load is wanted.

(5) NDITO - Signal for uniform of irregular distributed load

0, uniform pressure

1, pressure varies meridionally

(6) NDELT - No. of time steps desired.

(7) NLA - No. of layers for angle or cross plys.

(8) NBC - No. of boundary condition(s).

(9) NCY - No. of iterations within a time step.

(10) NCON - No. of node(s) with concentrated load(s).

(11) PER - Percent error allowed for convergence in plastic analysis.

Suggested value: PER = 5 ~ 10

(12) PCTARC - Fraction of arc length ignored at a pole.

Suggested value: 0.01

The program assumes PCTARC = 0.01, if PCTARC = 0.

Card 3: FORMAT (4I5)

(1) IS(1) - 1, if elastic analysis is wanted.

0, if plastic analysis is wanted

(2) IS(2) - 1, if nonviscous analysis is wanted

- 0, if viscous analysis is wanted

(3) IS(3) - Print signal

Print displacements and stresses at every IS(3)$^{\underline{th}}$ step.

The program assumes IS(3) = 5, if IS(3) = 0.

(4) IS(4) - Transformation signal.

Transform the displacements into the Z-R coordinate system and print for every IS(4)$^{\underline{th}}$ step.

The program assumes IS(4) = NDELT, if IS(4) = 0.

Card 4: FORMAT (3X, E12.6)

DELT - Size of the time step in seconds (Δt).

Cards 5: FORMAT (3X, 2E12.6)

(1) Z(N) - Z - coordinate value.

(2) R(N) - R - coordinate value.

Note: Provide one card for each node in the order of node number. The node number may be recorded in 3X spaces.

Cards 6: FORMAT (2I3, 4E12.6)

(1) NODE1 - First node of the element

(2) NODE2 - Second node of the element

(3) PHI1 - φ_1

(4) PHI2 - φ_2

(5) H1 - Thickness at NODE1

(6) H2 - Thickness at NODE2

Note: Repeat NELEMS times in the order of element number. The sign convention for φ is shown below.

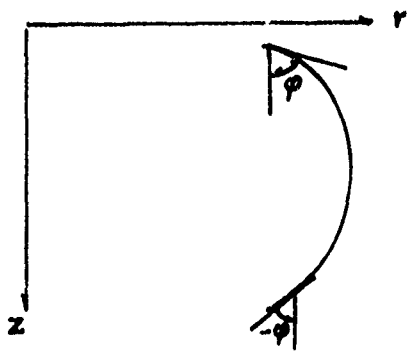

Card(s) 7: FORMAT (6E10.0)

(1) PP1(1) - Distributed pressure in direction 1 at node 1.

(2) PP2(1) - Distributed pressure in direction 2 at node 1.

(3) PP3(1) - Distributed pressure in direction 3 at node 1.

(4) PP1(2) - Distributed pressure in direction 1 at node 2.

(5) PP2(2) - Distributed pressure in direction 2 at node 2.

(6) PP3(3) - Distributed pressure in direction 3 at node 2.

Note: Repeat NELEMS times in the order of element number if NDITO = 1.

Card(s) 8: FORMAT (I5, 4E15.6)

(1) NOD - Node number

(2) CL(1) - Concentrated force in direction 1.

(3) CL(2) - Concentrated force in direction 2.

(4) CL(3) - Concentrated force in direction 3.

(5) CL(4) - Concentrated force in direction 4.

Note: Repeat NCON times.

Omit if NCON = 0.

Card(s) 9: FORMAT (2I5)

(1) NOD - Node number with boundary condition(s).

(2) NDEGF - The coordinate number of which freedom is restrained.

Note: Repeat NBC times.

Card 10: FORMAT (8F10.0)

SIGS(I) - Yield stress in the direction of the normal to fiber for each layer.

Card 11: FORMAT (8F10.0)

SIGT(I) - Yield stress in fiber direction for each layer.

Card 12: FORMAT (8F10.0)

SIG4(I) - Yield stress in 45° from fiber direction for each layer.

Card 13: FORMAT (8F10.0)

TAUT(1) - Yield stress in shear for each layer.

Card 14: FORMAT (8F10.0)

EPX(I) - Plastic modulus normal to fiber for each layer.

Card 15: FORMAT(8F10.0)

EPY(I) - Elastic modulus in fiber direction for each layer.

Note: EPX(I) = EPY(I) for isotropic case.

Card 16: FORMAT (8F10.0)

GP(I) - Elastic shear modulus for each layer.

Card 17: FORMAT (8F10.0)

XNU(I) - Poisson's ratio (normal to fiber) for each layer.

Card 18: FORMAT (8F10.0)

YNU(I) - Poisson's ratio (in fiber direction) for each layer.

Note: XNU(I) = YNU(I) for isotropic case.

Card 19: FORMAT (8F10.0)

EPX(I) - Plastic modulus normal to fiber for each layer.

Card 20: FORMAT (8F10.0)

EPY(I) - Plastic modulus in fiber direction for each layer.

Card 21: FORMAT (8F10.0)

EPr(I) - Plastic modulus in 45° from fiber direction for each layer.

Card 22: FORMAT (8F10.0)

GP(I) - Plastic shear modulus for each layer.

Card 23: FORMAT (8F10.0)

ALPHA(I) - Fiber angles for each layer measured from horizontal line.

Note: Repeat NELEMS times.

Card 24: FORMAT (8F10.0)

(1) TL - Relaxation time in fiber direction.

(2) TT - Relaxation time in the direction of normal to fiber.

(3) DSL - EPY(I) (see Card 15)

(4) DST - EPX(I) (see Card 14)

Note: Not required if IS(2) ≠ 0.

APPENDIX B.3.1

DVP1 - SUBROUTINE ORGANIZATION CHART

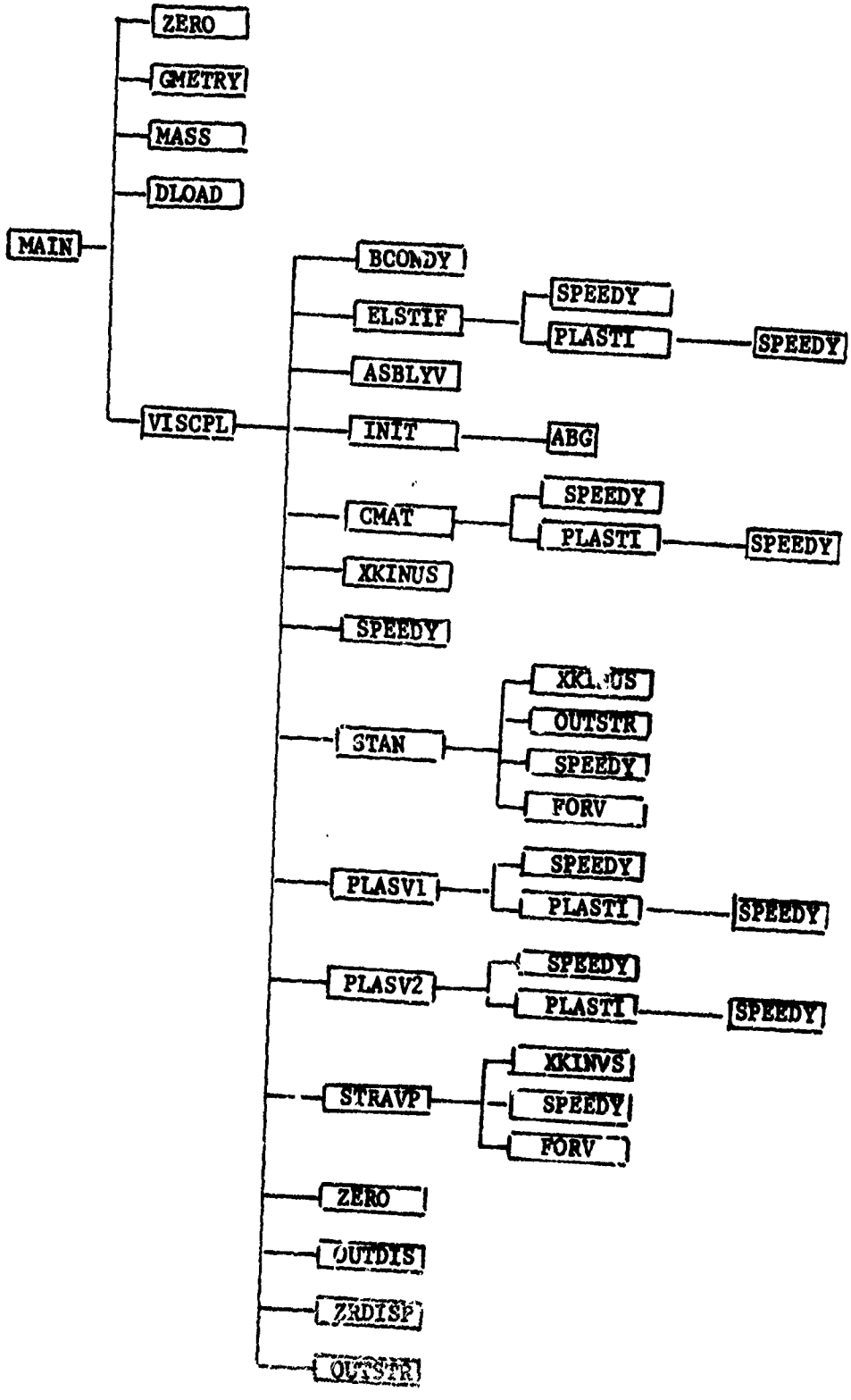

APPENDIX B.3.2

DVP1 - DESCRIPTIONS OF SUBROUTINES

SUBROUTINE NAME	DESCRIPTION
ABG	Calculates viscous constants $A^{(r)}, B^{(r)}, C^{(r)}$.
ASBKTV	Assembles in global form.
BCONDY	Imposes boundary condition(s).
CMAT	Forms the viscosity matrix.
DLOAD	Computes the equivalent nodal forces
ELSTIF	Reads the material properties and forms the elastic stiffness matrix.
FORV	Performs integration for viscous force vector.
GMETRY	Calculates, for each element, the geometrical quantities necessary for Simpson's integration along the line element.
INIT	Reads the viscous property and forms submatrices for viscosity matrix.
MASS	Forms, for each element, the consistent mass matrix.
OUTDIS	Writes the displacements.
OUTSTR	Writes the stresses and the equivalent stresses.
PLASTI	Performs Simpson's integration to form stiffness or viscousity matrix.
PLASV1	Develops plastic stiffness matrix.
PLASV2	Develops plastic stiffness matrix.
SPEEDY	Performs matrix multiplication.
STAN	Calculates viscous and elastic stresses, checks yielding.
STRAUP	Calculates incremental viscous and plastic stresses, incremental equivalent stresses, and per cent error.
VISCP	Performs step-by-step integration.

APPENDIX B.3.2 (cont.)

DVPI - DESCRIPTIONS OF SUBROUTINES

SUBROUTINE NAME	DESCRIPTION
XKINVS	Inverts a given symmetric matrix.
ZERO	Zeroes out a given matrix.
ZRDISP	Transforms the displacements into the Z-R coordinate system and writes.

APPENDIX B.3.3

DVPI - FLOW CHART

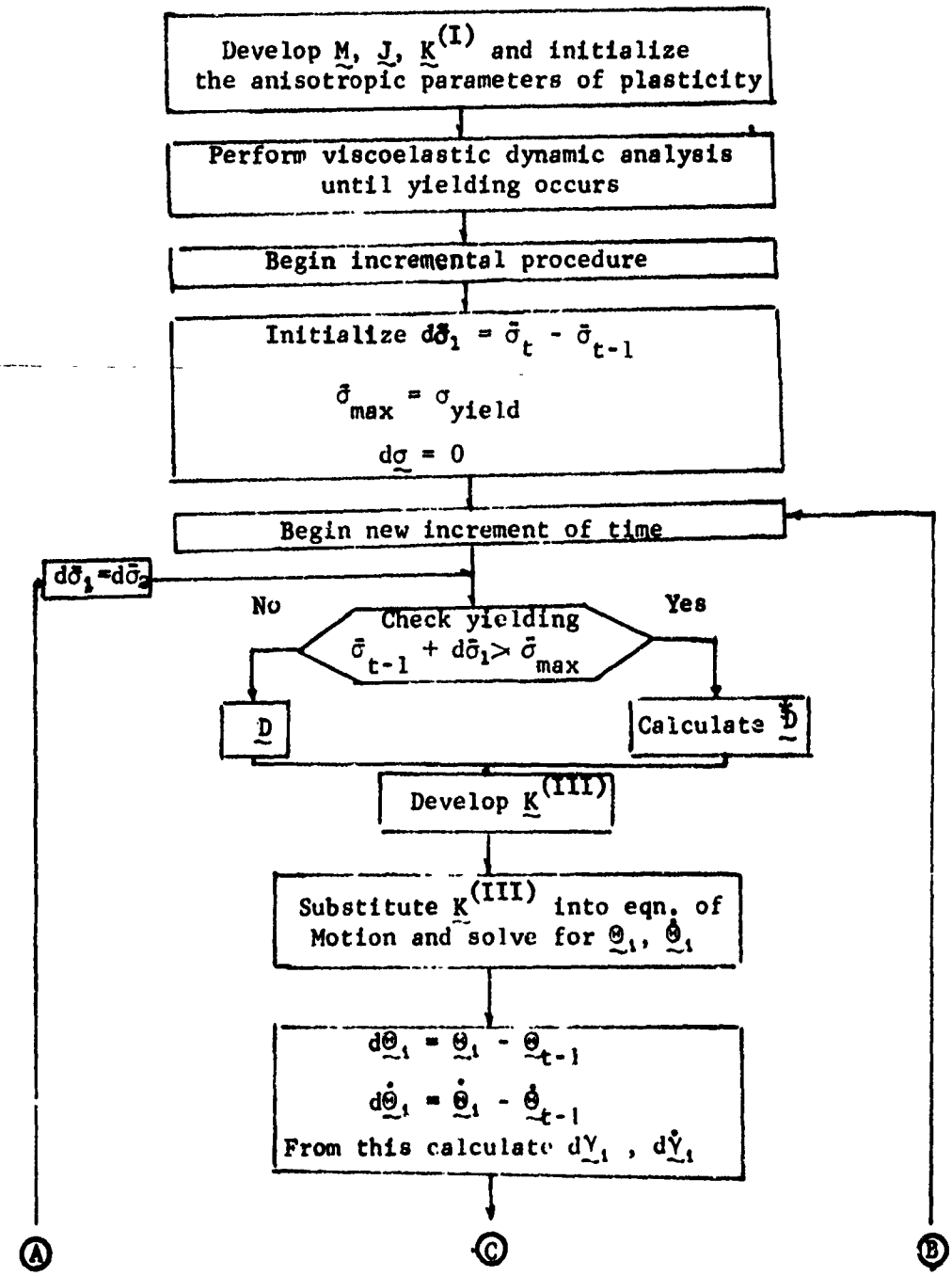

APPENDIX B.3.3 (continued)

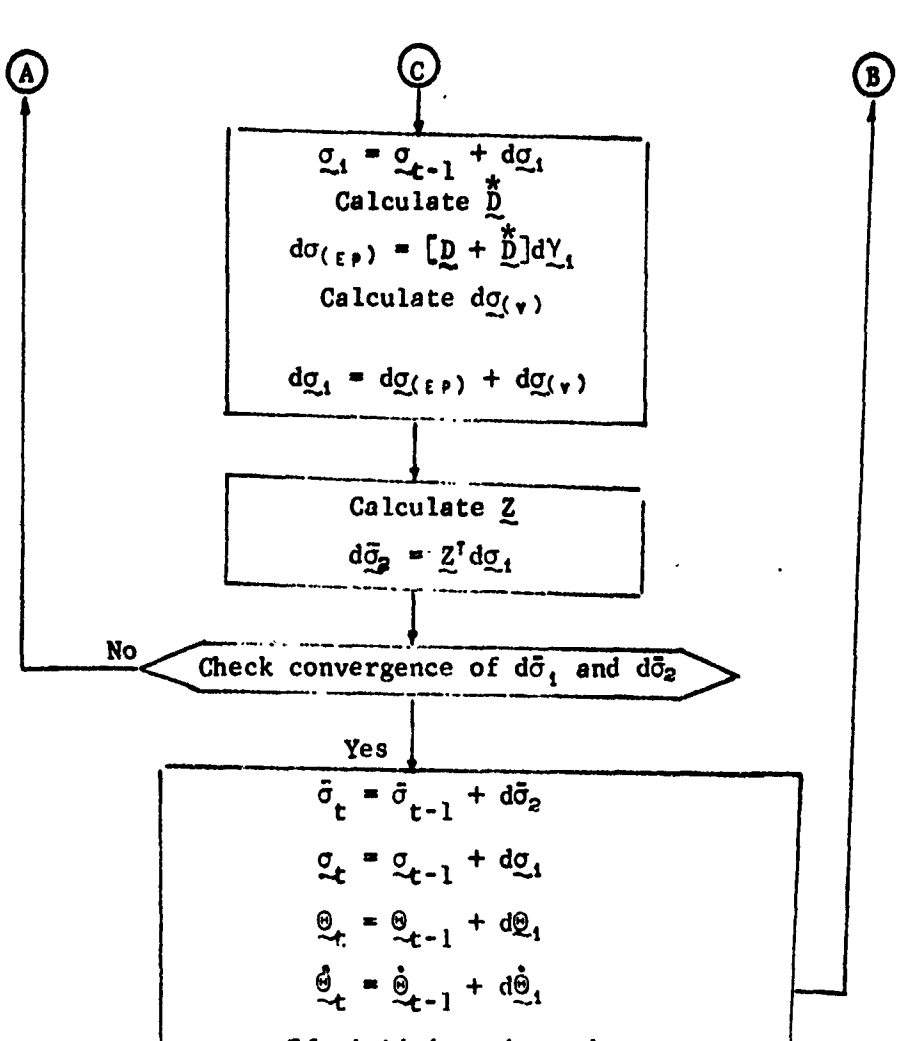

APPENDIX B.3.4

DVP1 - DATA INPUT FORMAT

Card 1: FORMAT (20A4)

TITLE(I) Title of the problem

Card 2: FORMAT (1015,3F10.4)

(1) NELEMS - No. of elements

(2) NNODES - No. of nodes

(3) NET - No. of stations for Simpson's integration

Suggested value of NET

$\varphi_2 - \varphi_1$	NET
$0 \sim 3^0$	15
$3^0 \sim 5^0$	19
$5^0 \sim 9^0$	23
$9^0 \sim 15^0$	29

The program assumes NET = 15, if NET = 0.

(4) MECH - Signal for distributed load

0, if a force vector for distributed load is not wanted.

1, if a force vector for distributed load is wanted.

(5) NDITO - Signal for uniform of irregular distributed load

0, uniform pressure

1, pressure varies meridionally

(6) NDELT - No. of time steps desired

(7) NLA - No. of layers for angle or cross plys

(8) NBC - No. of boundary condition(s)

(9) NCY - No. of iterations within a time step

(10) NCON - No. of node(s) with concentrated load(s)

(11) PER - Percent error allowed for convergence in plastic analysis

Suggested value PER = 5 ~ 10

(12) PCTARC - Fraction of arc length ignored at a pole

Suggested value: 0.01

The program assumes PCTARC = 0.01, if PCTARC = 0.

Card 3: FORMAT (415)

(1) IS(1) - 1, if elastic analysis is wanted

0, if plastic analysis is wanted

(2) IS(2) - 1, if nonviscous analysis is wanted

0, if viscous analysis is wanted

(3) IS(3) - Print signal

Print displacements and stresses at every IS(3)$^{\underline{th}}$ time step.

The program assumes IS(3) = 5, if IS(3) = 0

(4) IS(4) - Transformation signal

Transform the displacements into the z-R coordinate system and print for every IS(4)$^{\underline{th}}$ step.

The program assumes IS(4) = NDELT, if IS(4) = 0.

Card 4: FORMAT(3X,2E12.6)

(1) RHO - Average density of the material to compute the mass matrix in lbs/in^3

(2) DELT - Size of the time step in seconds (Δt)

Note: $\Delta t \leq 10^{-6}$ sec. for metals.

Cards 5: FORMAT (3X,2F12.6)

(1) Z(N) - Z - coordinate value

(2) R(N) - R - coordinate value

Note: Provide one card for each node in the order of node number. The node number may be recorded in 3X spaces.

Cards 6: FORMAT (213, 4E12.6)

(1) NODE1 - First node of the element

(2) NODE2 - Second node of the element

(3) PHI1 - φ_1

(4) PHI2 - φ_2

(5) H1 - Thickness at NODE1

(6) H2 - Thickness at NODE2

Note: Repeat NELEMS times in the order of element number. The sign convention for φ is shown below.

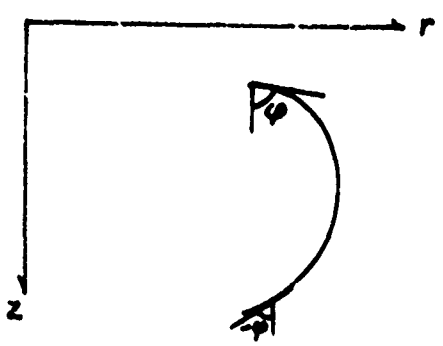

Card(s) 7: FORMAT (6E10.0)

(1) PP1(1) - Distributed pressure in direction 1 at node 1

(2) PP2(1) - Distributed pressure in direction 2 at node 1

(3) PP3(1) - Distributed pressure in direction 3 at node 1

(4) PP1(2) - Distributed pressure in direction 1 at node 2

(5) PP2(2) - Distributed pressure in direction 2 at node 2

(6) PP3(3) - Distributed pressure in direction 3 at node 2

Note: Repeat NELEMS times in the order of element number if NDITO = 1.

Card(s) 8: FORMAT (15, 4E15.6)

(1) NOD - Node number

(2) CL(1) - Concentrated force in direction 1

(3) CL(2) - Concentrated force in direction 2

(4) CL(3) - Concentrated force in direction 3

(5) CL(4) - Concentrated force in direction 4

Note: Repeat NCON times.

Omit if NCON = 0.

Card(s) 9: FORMAT (215)

(1) NOD - Node number with boundary condition(s)

(2) NDEGF - The coordinate number of which freedom is restrained.

Note: Repeat NBC times.

Card 10: FORMAT (8F10.0)

SIGS(I) - Yield stress in the direction of the normal to fiber for each layer.

Card 11: FORMAT (8F10.0)

SIGT(I) - Yield stress in fiber direction for each layer.

Card 12: FORMAT (8F10.0)

SIG4(I) - Yield stress in 45^{o} from fiber direction for each layer

Card 13: FORMAT (8F10.0)

TAUT(I) - Yield stress in shear for each layer

Card 14: FORMAT (8F10.0)

EPX(I) - Elastic modulus normal to fiber for each layer

Card 15: FORMAT (8F10.0)

EPY(I) - Elastic modulus in fiber direction for each layer

Note: FPX(I) = EPY(I) for isotropic case

Card 16: FORMAT (8F10.0)

GP(I) - Elastic shear modulus for each layer

Card 17: FORMAT (8F10.0)

XNU(I) - Poisson's ratio (normal to fiber) for each layer

Card 18: FORMAT (8F10.0)

YNU(I) - Poisson's ratio (in fiber direction) for each layer

Note: XNU(I) = YNU(I) for isotropic case

Card 19: FORMAT (8F10.0)

EPX(I) - Plastic modulus normal to fiber for each layer

Card 20: FORMAT (8F10.0)

EPY(I) - Plastic modulus in fiber direction for each layer

Card 21: FORMAT (8F10.0)

EP4(I) - Plastic modulus in 45° from fiber direction for each layer

Card 22: FORMAT (8F10.0)

GP(I) - Plastic shear modulus for each layer

Card 23: FORMAT (8F10.0)

ALPHA(I) - Fiber angles for each layer measured from horizontal line

Note: Repeat NELEMS times.

Card 24: FORMAT (8F10.0)

(1) TL - Relaxation time in fiber direction

(2) TT - Relaxation time in the direction of normal to fiber

(3) DSL - EPY(I) (see Card 15)

(4) DST - EPX(I) (see Card 14)

Note: Not required if IS(2) $\neq$ 0.

APPENDIX B.4.1

SP2 - SUBROUTINE ORGANIZATION CHART

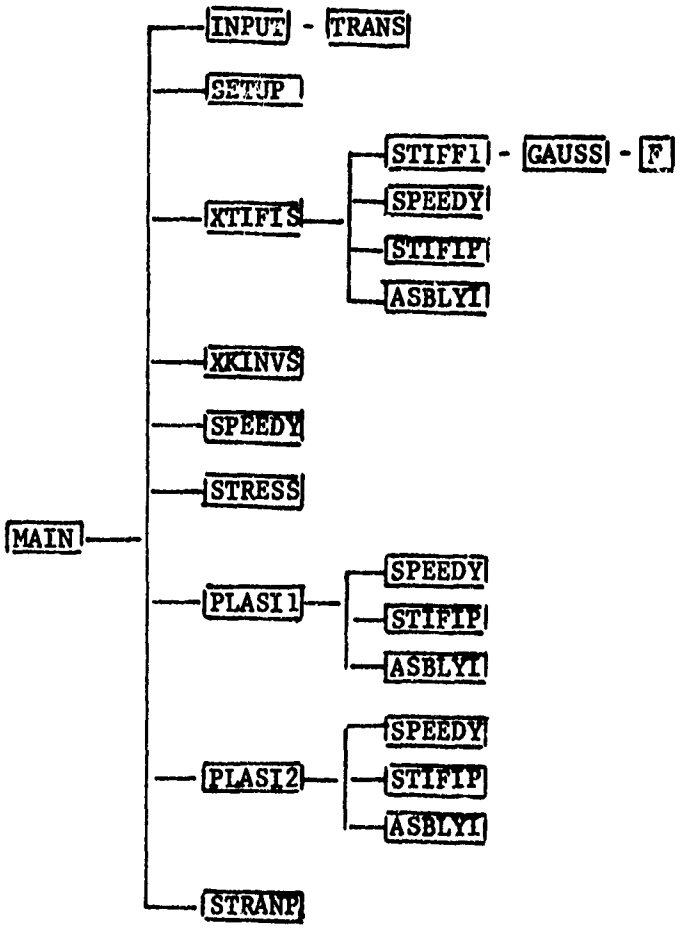

APPENDIX B.4.2

SP2 - DESCRIPTION OF SUBROUTINES

SUBROUTINE NAME	DESCRIPTION
ASBLYI	Assembles stiffness matrix.
F	Evaluates functional values used in Gaussian quadrature integration.
GAUSS	Performs Gaussian quadrature integration.
INPUT	Reads and writes input data.
PLASI1	Develops instantaneous stiffness matrix for initial yielding.
PLASI2	Develops instantaneous stiffness matrix for subsequent yielding.
SETUP	Sets up weight-function values used in quadrature integration.
SPEEDY	Performs matrix multiplication.
STIFIP	Forms element stiffness matrix for the given elasticity matrix.
STIFF1	Calculates coordinate-dependent values used in quadrature integration.
STRANP	Calculates incremental stresses, incremental equivalent stresses, and per cent error to test for convergence.
STRESS	Computes displacements and stresses under given load, and then scales the quantities to the elastic limit.
TRANS	Develops transformation matrices for both stress and strain.
XKINVS	Performs matrix inversion.
XTIFIS	Calculates local elasticity matrix, transforms this to global coordinates, and then forms global stiffness matrix.

APPENDIX B.4.3

SP2 - FLOW CHART

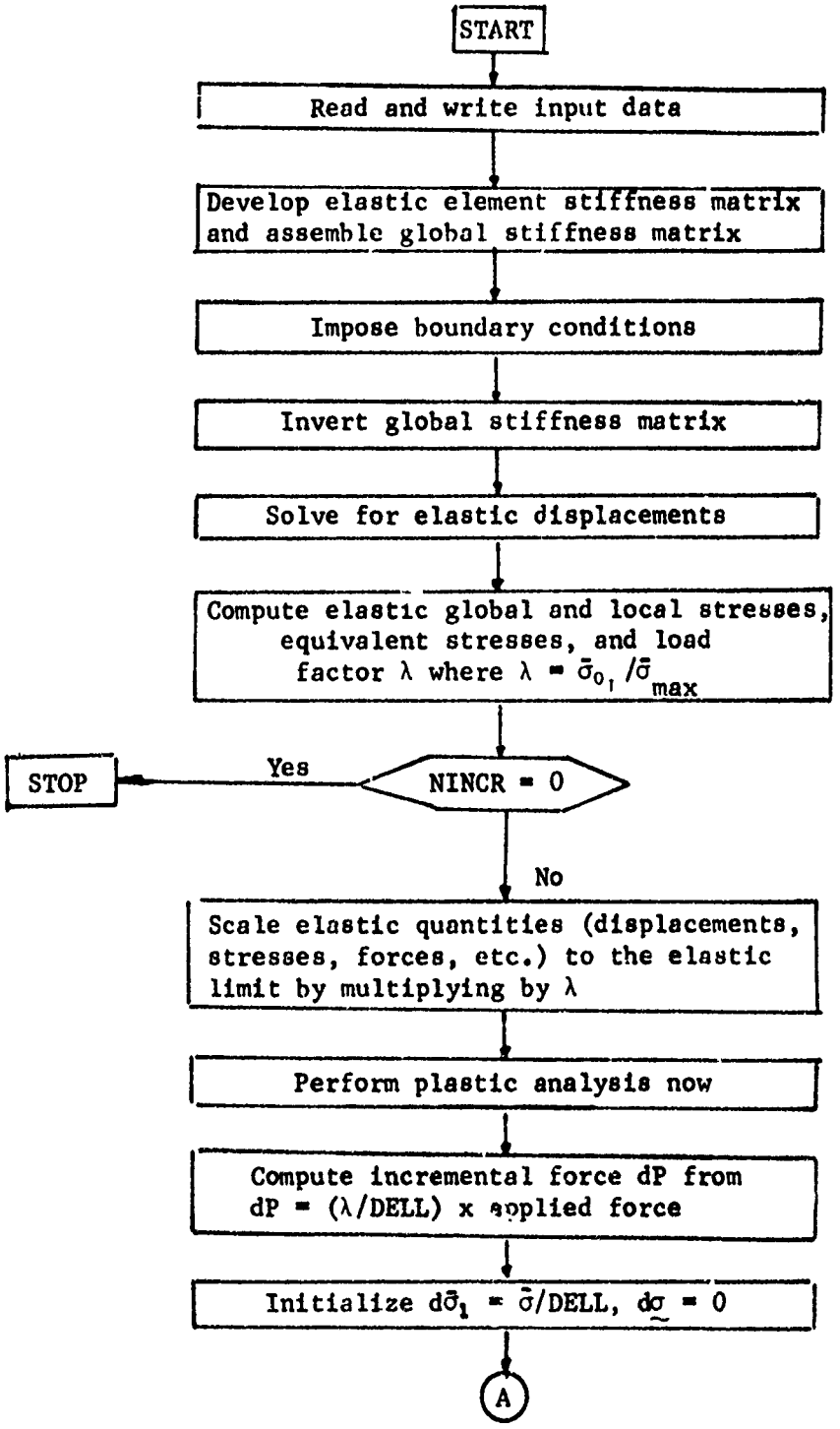

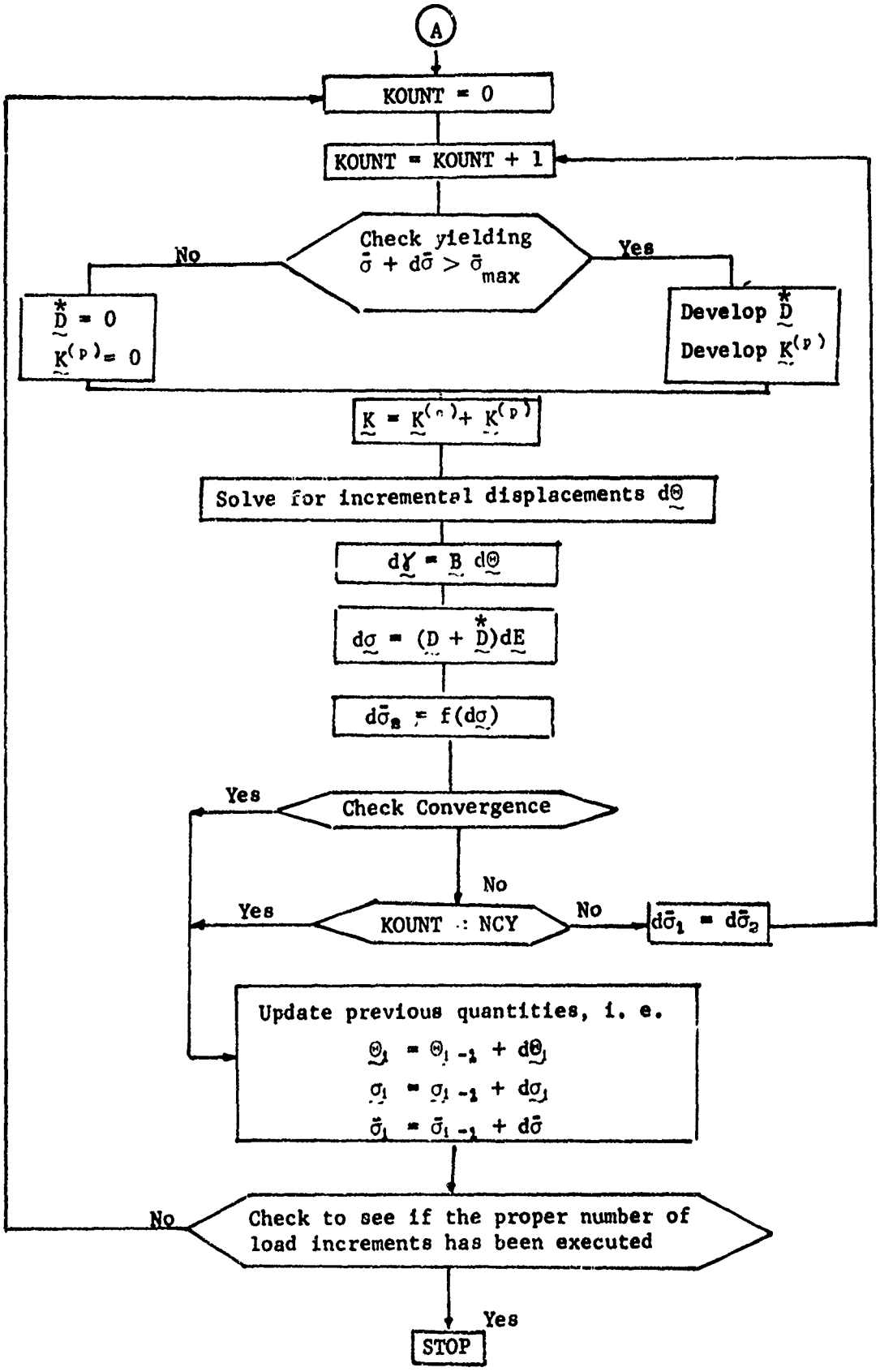
A
KOUNT = 0
KOUNT = KOUNT + 1
Check yielding
$\bar{\sigma} + d\bar{\sigma} > \bar{\sigma}_{max}$
No
Yes
$\overset{*}{D} = 0$
$K^{(p)} = 0$
Develop $\overset{*}{D}$
Develop $K^{(p)}$
$K = K^{(e)} + K^{(p)}$
Solve for incremental displacements $d\Theta$
$d\gamma = B\, d\Theta$
$d\sigma = (D + \overset{*}{D})dE$
$d\bar{\sigma}_2 = f(d\sigma)$
Yes
Check Convergence
No
Yes
KOUNT = NCY
No
$d\bar{\sigma}_1 = d\bar{\sigma}_2$
Update previous quantities, i. e.
$\Theta_i = \Theta_{i-1} + d\Theta_i$
$\sigma_i = \sigma_{i-1} + d\sigma_i$
$\bar{\sigma}_i = \bar{\sigma}_{i-1} + d\bar{\sigma}$
No
Check to see if the proper number of load increments has been executed
Yes
STOP

APPENDIX B.4.4

SP2 - DATA INPUT FORMAT

Card 1: FORMAT (20A4)

TITLE(I) Title of the problem

Card 2: FORMAT (2I5, 2F10.0)

(1) NCY - Number of iterations allowed for convergence within a load increment.

(2) NINCR - Number of load increments.

(3) PER - Allowable per cent error for convergence

(4) DELL - Fraction of elastic limit load to be applied for each load increment.

Cards 3: FORMAT (2F10.0)

(1) z - z coordinate value

(2) R - R coordinate vlaue

(Note: Provide one card for each node.

Cards 4: FORMAT (4I5)

I-J-K-L designations of nodes for a given element, in counter-clockwise order.

Note: Provide one card for each element.

Sample:

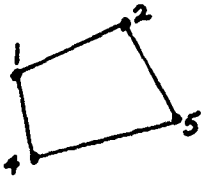

I = 4
J = 5
K = 2
L = 1

Card 5: FORMAT (I5)

NBC - Number of boundary conditions

Cards 6: FORMAT (2I5)

(1) NOD - Node number of boundary condition

(2) IDG - Degree of freedom at the node which is restrained

IDG = 1 if z displacement restrained

IDG = 2 if R displacement restrained

Card 7: FORMAT (I5)

ISAME - ISAME = 1 if all elements have same card(s) 8.

Card(s) 8: FORMAT (8F10.0)

(1) ET - Modulus of elasticity transverse to fiber

(2) EL - Modulus of elasticity along fiber

(3) GNUTL - Poisson's ratio between fiber and direction transverse to fiber

(4) GNUTT - Poisson's ratio between directions normal to fiber

(5) GTL - Shear modulus between fiber and direction transverse to fiber

(6) GT - Shear modulus between directions normal to fiber

(7) ALPH - Angle in degrees from horizontal to fiber direction within plane of the structure

(8) PHI - Angle in degrees from vertical to plane of the structure

Note: Provide one card for each element if ISAME not equal to 1.

Card 9: FORMAT (I5)

ISAME - ISAME = 1 if each element has same card(s) (10) and card(s) 11.

Card(s) 10: FORMAT (8F10.0)

(1) SOT - Yield stress in tension transverse to fiber

(2) SOL - Yield stress in tension in fiber direction

(3) TOT - Shear yield stress in tension transverse to fiber

(4) TOL - Shear yield stress in tension in fiber direction

(5) EPT - Plastic modulus normal to fiber

(6) EPL - Plastic modulus along fiber

(7) GPT - Plastic shear modulus between directions normal to fiber

(8) GPL - Plastic shear modulus between fiber and direction normal to fiber

Card(s) 11: FORMAT (8F10.0)

Same as cards 8 except for compression

Note: Provide one card(s) 10 and one card(s) 11 for each element if ISAME not equal 1.

Card 12: FORMAT (I5)

NFORCE - Number of externally applied concentrated forces

Card(s) 13: FORMAT (2I5, F10.0)

(1) NOD - Node number of applied concentrated force

(2) IDG - Degree of freedom at which force is applied

IDG = 1 if force applied in z direction

IDG = 2 if force applied in R direction

(3) FOR - Magnitude of applied force

Note: Provide one card for each applied force if NFORCE = 0 Card 13 is not needed

Card 14: FORMAT (I5, F10.0)

NPRES - Number of elements with applied pressure

PRESS - Applied pressure

Card(s) 15: FORMAT (3I5)

(1) NELP - element pressure applied to

(2) NOD1 - One node of the element having pressure

(3) NOD2 - Second node of the element having pressure

Note: Provide one card for each element having pressure. If NPRESS = 0 card(s) 15 not needed.

SAMPLE

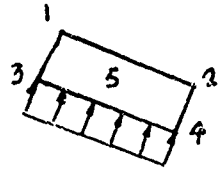

PRESS = 5.0
NELP = 5
NOD1 = 3
NOD2 = 4

APPENDIX B.5.1

SVP2 - SUBROUTINE ORGAINIZATION CHART

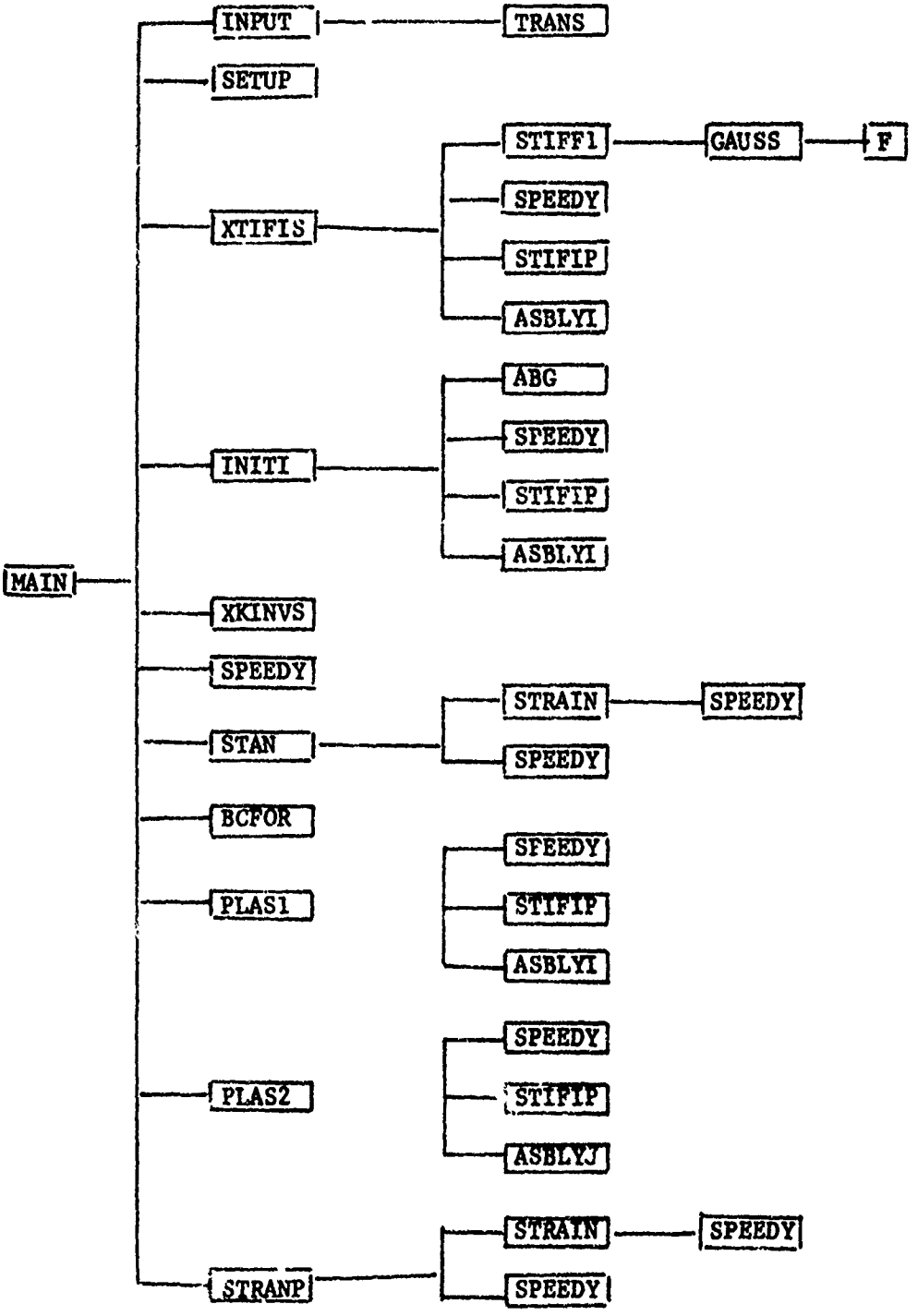

APPENDIX B.5.2

SVP2 - DESCRIPTION OF SUBROUTINES

SUBROUTINE NAME	DESCRIPTION
ABG	Calculates viscoelastic constants A, B, C
ASBLYI	Assembles stiffness matrix and damping matrix
BCFOR	Applies boundary conditions to force vectors
F	Evaluates functions used in integration
GAUSS	Performs Gaussian quadrature integration
INITI	Develops the damping matrix together with values needed in viscous stress calculations
INPUT	Reads and writes input data
PLASI1	Develops plastic stiffness matrix for initial yielding
PLASI2	Develops plastic stiffness matrix for subsequent yielding
SPEEDY	Performs matrix multiplication
SETUP	Initializes values used in Gaussian quadrature integration
STAN	Calculates elastic and viscous stresses and checks yielding. If no yielding it updates stresses, equivalent stresses, etc. If yielded it initializes incremental equivalent stress.
STIFF1	Calculates coordinate values used in the integration scheme for development of the stiffness and damping matrix
STIFIP	Forms element stiffness and damping matrix from functions evaluated in STIFF1
STRAIN	Calculates local strains from global displacements
STRANP	Calculates increment stresses, equivalent stresses and per cent error between any two iterations of a time increment

SUBROUTINE NAME	DESCRIPTION
TRANS	Forms the stress and strain transformation matrices
XKINVS	Performs matrix inversion
XTIFIS	Calculates and assembles global stiffness matrix

APPENDIX B.5.3

SVP2 - FLOW CHART

The flow chart for SVP2 is the same as that for SVP1 in Appendix B.2.3.

APPENDIX B.5.4

SVP2 - DATA INPUT FORMAT

Card 1: FORMAT (I5, F10.0)

(1) NDELT - Number of time increments

(2) DELT - Size of time increment

Card 2: FORMAT (I5, F10.0)

(1) NCY - Number of iterations allowed for convergence within a time increment if yielding has occurred.

(2) PER - Allowable per cent error for convergence

Cards 3: through Cards 15 Insert Cards 3 through Cards 15 from B.4.4.

Card(s) 16: FORMAT (4F10.0, I5)

(1) TT - Relaxation time in direction transverse to fiber

(2) TL - Relaxation time in fiber direction

(3) DT - Modulus of elasticity normal to fiber

(4) DL - Modulus of elasticity in fiber direction

(5) ISAME - Let ISAME = 1 if all elements have same properties

Note: Provide one card for each element if ISAME not equal 1.

APPENDIX B.6.1

DVP2 - SUBROUTINE ORGANIZATION CHART

The subroutine organization chart for DVP2 is the same as that for SVP2 except that MAIN calls an additional subroutine, MASS, which develops the mass matrix.

APPENDIX B.6.2

DVP2 - DESCRIPTION OF SUBROUTINES

The description of subroutines for DVP2 is the same as that for SVP2 except that subroutine MASS should be added to the list.

MASS Develops and assembles the mass matrix.

APPENDIX B.6.3

DVP2 - FLOW CHART

The flow chart for DVP2 is the same as that for DVP1 in Appendix B.3.3.

APPENDIX B.6.4

DVP2 - DATA INPUT FORMAT

Cards 1 through Card(s) 16 - Insert Card 1 through Cards 16 from SVP2 in Appendix B.5.4.

Card(s) 17: FORMAT (F10.0, I5)

(1) DEN - Weight density of the material in pounds per cubic inch.

(2) ISAME - Let ISAME = 1 if all elements have same density.

Note: Provide one card for each element if ISAME not equal to 1.